The Characterisation of the Ectodomain Shedding of the Low Density Lipoprotein receptor

A PhD thesis by

Ayesha Parker

Thesis Presented for the Degree of

DOCTOR OF PHILOSOPHY

in the Division of Medical Biochemistry, Faculty of Health Sciences

UNIVERSITY OF CAPE TOWN

April 2009

Supervisor: Professor E.D. Sturrock

Declaration

I, **Ayesha Parker**, declare that this dissertation is my own, unaided work (except where acknowledgements indicate otherwise). Neither the whole work nor part thereof has been, is being submitted for any degree or examination at any other university.

I empower the university to reproduce for the purposes of research either the whole or any part of the contents of this dissertation, in any manner whatever.

Signature of applicant: Signed by candidate

Signed on the _____day of _____, 2009

Acknowledgements

There are many people to thank and acknowledge for their part in helping, supporting and contribution towards this thesis.

Firstly, thank you to my supervisor, Prof. E.D. Sturrock who has been excellent as a mentor and supervisor, guiding me throughout the project. He has been very patient and supportive, nudging me in the right direction especially during the trying times.

To Sylva, thank you for all the technical help in the lab, emotional support and for encouraging me in so many ways.

Thank you to Zenda, for taking me under her wing and showing me the ropes. It was a pleasure and honour to learn from you.

Thank you to Sylva and Nailah for the suggestions provided while reading my thesis.

To Mike Begg, thank you for your help, valuable insight, for sacrificing time to attend meetings and for being a pleasant, patient and optimistic person.

Thank you to Dr. A.D. Marias and Bharati, for helping with the gradient gel electrophoresis and for providing the LDL samples.

Thanks to EVERYONE in the Zinc Metalloprotease Group, better known as the ACE lab!!! Without you guys I could not have done it!! Thank you to: Zenda, Sia, Pierre,

Dawn, Priscilla, Riyad, Itai, Wendy, Trudi, Jean, Tony, Nailah, Chris, Colin, Ross, Kerry, Raymond, Adele, Kate, and not forgetting the lab mascot, no-pants boy! Thank you for all the technical and emotional support and most importantly for the friendship and making the lab feel like a second home!

Thank you to the Division of Medical Biochemistry, especially to members of the Cancer lab.

Thank you to my friends!! Thank you to everyone that I see almost everyday, to those I see less often and to those I hardly see anymore! Thank you to old friends and thank you to new friends! A special mention goes to Wendy, Nailah, Saberi, Amaal, Yumna, Janis and Rashid. Thank you for everything that you guys have done for me! And Widaad, my best friend who brings out the best in me! Thank you for all the times you spent helping me in every possible way, for whatever reason, big or small.

UCT, MRC and NRF for funding provided during this project.

Thank you to my family!! To my parents, brother, all my uncles and aunts, and all my cousins, I value every moment that I spend with you. Thank you for all the love and support!

And most importantly, I thank my creator for providing me with all the amazing people mentioned here to get me through the most trying of times!!!

Contents

Abbreviations

Abz	*ortho*-aminobenzoic acid
ACE	angiotensin convering enzyme
ADAM	a distintergrin and metalloprotease
ADH	autosomal dominant hypercholesterolemia
ALCAM	activated leukocyte cell adhesion molecule
AMPS	ammonium persulphate
Apo B	apolipoprotein B
ApoER2	apolipoprotein E receptor 2
APP	amyloid precursor protein
ARH	autosomal recessivet hypercholesterolemia
BACE	β-secretase
β–ME	β-mercaptoethanol
BS3	Bis (Sulfosuccinimidyl) suberate
CAD	coronary artery disease
CHO	Chinese hamster ovary
CMV	cytomegalovirus
Cys	cysteine
DMEM	Dulbecco's modified Eagle's medium
DMSO	Dimethyl sulfoxide
DNA	deoxy ribonucleic acid
Dnp	2, 4 dinitrophenol
EGF	epidermal growth factor
ER	endoplasmic reticulum
ERK	extracellular signal-regulated kinase
FACS	fluorescence-activated cell sorting
FCS	fetal calf serum
FH	familial hypercholesterolemia
FRET	fluorescent resonance energy transfer
GFP	green fluorescent protein
GGE	gradient gel electrophoresis
GHBP	GH binding protein
GHR	growth hormone receptor
GPI	glycosyl-phosphatidylinositol
HB-EGF	heparin binding epidermal growth factor
Hepes	4-(2-hydroxyethyl)-1-piperazineethanesulfonic acid
HMG co A	3-hydroxy-3-methylglutaryl Co-ezyme A
hrGFP	humanised renilla GFP
HRP	horseradish peroxidase
HRV	human rhinovirus
ICD	intracellular domain
IFN	interferon

IL	interleukin
IP	immunoprecipitation
kbp	kilobase pairs
kDa	kilo Daltons
KL-1	kit ligand-1
KO	knock-out
LA	luria agar
LA	LDLr-type A
LB	luria broth
LC-MS	liquid chromatography mass spectrometry
LDL	low density lipoprotein
LDLr	LDL receptor
LOX-1	lectin-like oxidized LDL
LRP	LDLr-related protein
MAP	mitogen-activated protein
MCS	multiple cloning site
MMP	matrix metalloprotease
mRNA	messenger ribonucleic acid
MT-1 MMP	Membrane type 1 matrix metalloprotease
NARC-1	neural apoptosis regulated convertase
NRDc	N-arginine dibasic convertase
PAGE	poly-acrylamide gel electrophoresis
PBS	phosphate buffered saline
PC	proprotein convertase
PCR	polymerase chain reaction
PCSK9	proprotein convertase subtilisin kexin 9
PDBu	phorbol 12,13-dibutyrate
PFA	paraformaldehyde
PKC	protein kinase C
PMA	phorbol myristate acetate
PMSF	phenylmethylsulphonyl fluoride
RAP	receptor associated protein
Rf	relative mobility
ROS	reactive oxygen species
SARS-coV	severe-acute respiratory syndrome-coronavirus
SCAP	SREBP cleavage activating protein
SDS	sodium dodecyl sulphate
SILAC	stable isotope labeling with amino acids in cell culture
siRNA	small interference RNA
SP	signal peptide
SREBP	sterol-regulatory element-binding protein
SVMP	snake venom metalloprotease
TACE	TNF-α converting enzyme
TAPI	TNF-α Protease Inhibitor

TBS-T	tris-buffered saline-tween
TEMED	tetramethylethylenediamine
TGF-α	transforming growth factor-α
TNF-α	tumour necrosis factor-α
TRANCE	TNF-related activation-induced cytokine
vLDL	very LDL
VSV	vesicular stomatis viral

Abstract

The low density lipoprotein receptor (LDLr) is a 160 kDa membrane protein important in the maintenance of cholesterol levels in plasma and a member of the LDLr family of endocytic proteins. Mutated receptors contribute to high cholesterol levels in familial hypercholesterolemia (FH). A 140-kDa soluble form of the LDLr was detected in the medium of cultured mammalian cells and established to be a product of ectodomain shedding. Sheddase-mediated ectodomain release of the LDLr was stimulated by phorbol esters, a protein kinase C (PKC) activator, and sensitive to inhibition by metalloprotease inhibitors. Furthermore, the shedding of two internalisation defective receptors, namely 792-LDLr and JD-LDLr has been investigated and found to be shed more efficiently than the wt-LDLr. The tumour necrosis factor-α converting enzyme (TACE) a TNF-α sheddase, and a member of a disintergrin and metalloprotease (ADAM) family, was suggested to be involved in the shedding of LDLr. To investigate the role of TACE in LDLr shedding, TACE-deficient cell lines expressing wild-type or mutant LDLr were analysed for the ectodomain release. Constitutive levels of LDLr shedding occurred in the absence of TACE activity in mouse fibroblasts. On the other hand, stimulated shedding of wt-LDLr and 792-LDLr was dependent on TACE because when TACE is absent, no increase in shedding was observed, while the JD-LDLr could be shed by another sheddase since phorbol stimulation of the JD-LDLr release occurred in mouse fibroblasts deficient in TACE. In Chinese hamster ovary (CHO) cells, both the constitutive and phorbol-stimulated shedding of all the LDLr constructs were dependent on TACE activity. Soluble LDLr levels, sheddase activity and ADAM 10 expression were higher in the TACE-/- mouse fibroblasts than in the CHO TACE deficient cell line, thus ADAM 10 might play a role in the constitutive LDLr shedding in mouse fibroblasts. The *in vivo* formation of soluble LDLr was also explored. A soluble form of the LDLr of ~120 kDa was identified in human plasma by Western blot analysis. To determine the functional integrity of soluble LDLr, the binding of plasma LDL to a recombinant soluble LDLr was investigated. Recombinant soluble LDLr was shown to bind plasma LDL. The presence of soluble LDLr in plasma suggests that the ectodomain shedding of membrane-bound LDLr might play a role in LDL metabolism.

Chapter 1:

Literature Review

1. Introduction

Cholesterol maintenance is essential for cellular functions, in the synthesis of hormones, and for the structural integrity of plasma membranes of cells (Goldstein et al., 1985; Simons and Ikonen, 2000; Brown and Goldstein, 1986). Cholesterol, a hydrophobic molecule, is transported in an esterified form in the blood within a low density lipoprotein (LDL) particle (Brown and Goldstein, 1986). The LDL particle is made up of a large number of phospholipids and a single copy of apolipoprotein B-100 (apo B-100), surrounding the cholesterol molecule. LDL is a large particle with a molecular weight ranging from 2500 kilo Daltons (kDa) to 3500 kDa (Fisher et al., 1975). LDL binds to the LDL receptor (LDLr), which was identified as the receptor involved in cholesterol homeostasis by Goldstein and Brown, the pioneers in the field (Brown and Goldstein, 1986). The LDLr binds apo B-100 containing LDLs and apo E-containing lipoproteins [very LDLs (vLDLs) and chylomicrons]. The liver is the main site where plasma levels of cholesterol concentrations are controlled. The LDLr will be discussed further in terms of its structure, function, regulation and ectodomain release.

1.1 The LDLr

1.1.1 LDLr gene structure

The LDLr gene containing 18 exons and 17 introns, is located on chromosome 19 (Lehrman et al., 1987). The LDLr is a mosaic protein as different exons transcribe different domains. The extracellular domain is transcribed by exons 2 to 16. The transmembrane and cytoplasmic domains are transcribed by exons 16-18 (Yamamoto et al., 1984; Sudhof et al., 1985). The LDLr promoter contains a sterol regulatory element, which is sensitive to changes in cholesterol levels. The messenger ribonucleic acid (mRNA) is 5.3 kb in length (Yamamoto et al., 1984) and has a 2.5 kb untranslated region, which may serve to provide stability to the mRNA transcripts (Kong et al., 2006).

1.1.2 LDLr protein structure

The LDLr is a 160 kDa, type-I membrane protein and is 839 amino acid residues in length after the post-translational removal of the 21 amino acid signal sequence (Schneider et al., 1982; Yamamoto et al., 1984). The tertiary structure of the LDLr is divided into 5 domains. Starting from the N-terminus the first domain is a ligand binding domain, followed by an Epidermal Growth Factor (EGF) precursor homology domain, an O-glycosylated domain, a hydrophobic membrane-spanning domain, and a C-terminal cytoplasmic tail (Fig. 1.1) (Yamamoto et al., 1984).

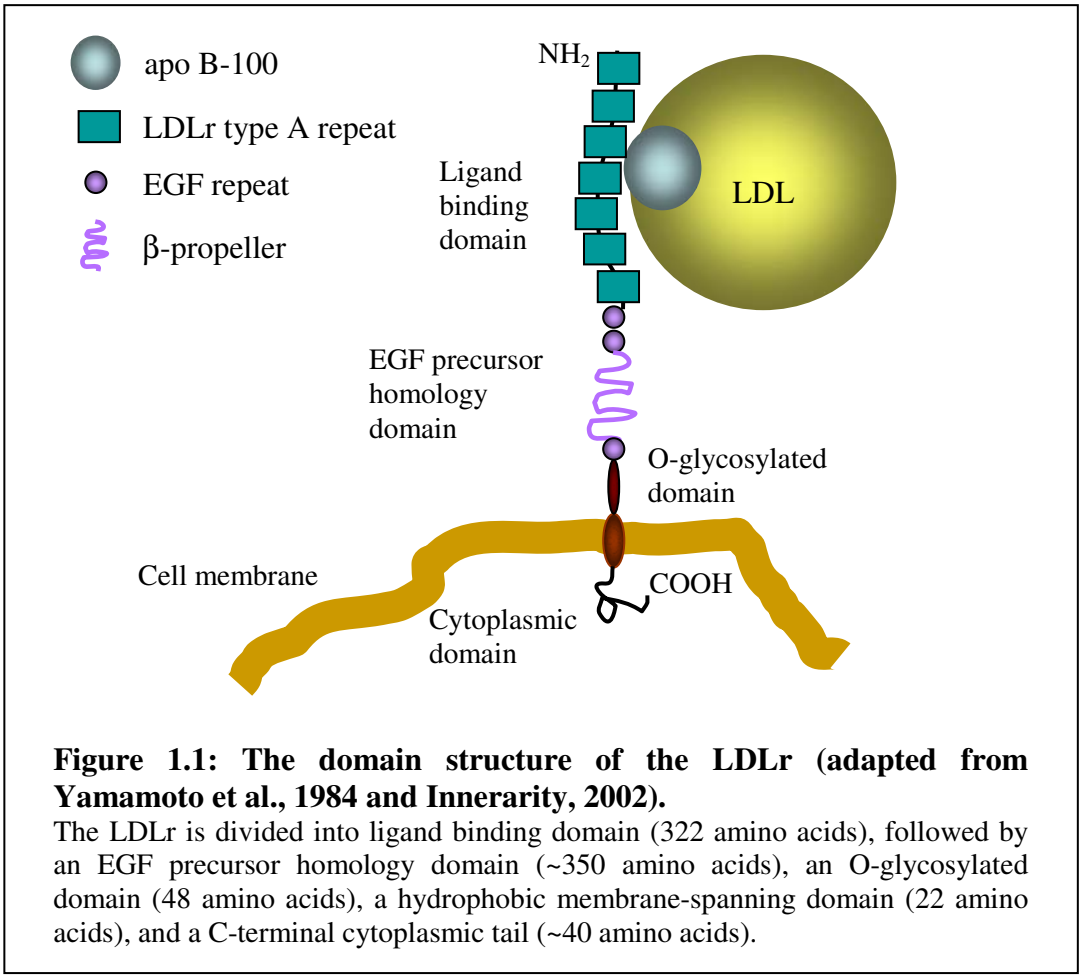

Figure 1.1: The domain structure of the LDLr (adapted from Yamamoto et al., 1984 and Innerarity, 2002).
The LDLr is divided into ligand binding domain (322 amino acids), followed by an EGF precursor homology domain (~350 amino acids), an O-glycosylated domain (48 amino acids), a hydrophobic membrane-spanning domain (22 amino acids), and a C-terminal cytoplasmic tail (~40 amino acids).

The ligand binding domain is comprised of 7 repeats, also called LDL receptor type A (LA) modules (Jeon and Blacklow, 2005). Each repeat is 40 amino acids long, and contains six cysteine residues. Each of the cysteine residues are disulphide bonded to another cysteine within the repeat in the following pattern: Cys I to Cys III, Cys II to Cys V, Cys IV to Cys VI (Bieri et al., 1998). The EGF precursor homology domain consists of two EGF cysteine-rich repeats (named EGF repeat A and B), followed by six YWTD repeats within a YWTD motif, and another cysteine-rich EGF repeat (EGF repeat C). Deletions of the EGF domain suggest that this region is important for binding to LDL, but not for Apo E. It is important however for the release of Apo E in the endosome and

recycling of the receptor (Davis et al., 1987). The YWTD motif forms a "6-bladed β-propeller domain" that is responsible for the release of the ligand in the endosome (Herz, 2001). Deletion mutants showed that Apo E and Apo B binding is not dependent on LA repeats 1 and 2 and EGF repeat B, while LA repeats 3-7 and EGF repeat A are important for Apo B binding. The only LA repeat important in the binding of apo E to the LDLr is LA repeat 5 (Russell et al., 1989; Hussain et al., 1999). The crystal structure showed that the β-propeller domain displaces the ligand at low pH and binds to repeats 4 and 5 (Innerarity, 2002). The O-glycosylated domain is rich in serine and threonine residues that are O-glycosylated and this domain is not essential for the functioning of the receptor (Davis et al., 1986; Hussain et al., 1999). The transmembrane domain is composed of hydrophobic residues. The C-terminal cytoplasmic tail of the LDLr is 40 amino acids long and has a NXPY internalisation sequence (where X is any amino acid) which is important for endocytosis (Yamamoto et al., 1984; Chen et al., 1990; Herz, 2001). The full-length, membrane bound form of the LDLr is also released as a soluble fragment, which will be discussed later in section 1.2.1.4.

1.1.3 Function of the LDLr

The primary function of the LDLr is to maintain plasma and cellular cholesterol levels by a process known as endocytosis (Goldstein et al., 1985; Brown and Goldstein, 1986). Approximately 70% of plasma LDL is cleared by hepatic LDLr through this process. Loss or inadequate function of the LDLr gives rise to inadequate LDL clearance and accumulation of LDL in the circulation resulting in a condition known as familial hypercholesterolemia (FH). Untreated FH can lead to the deposition of LDL in arteries with the concomitant formation of atherosclerotic plaques, a life-threatening condition called atherosclerosis (Brown and Goldstein, 1986; Glass and Witztum, 2001).

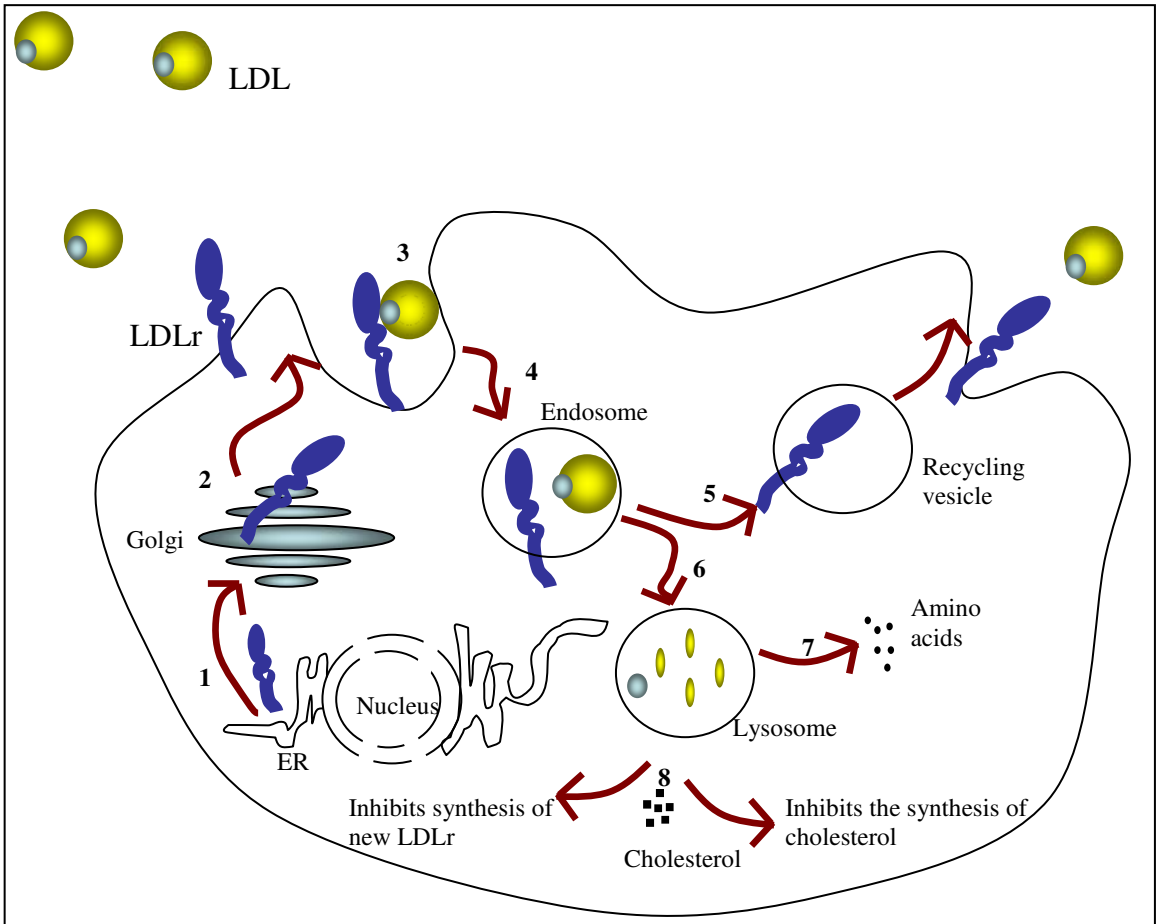

Figure 1.2: LDLr-mediated endocytosis (adapted from Brown and Goldstein 1986, and Gent and Braakman, 2004).
(1). Synthesis of the LDLr in response to low cellular cholesterol levels (2). LDLr is glycosylated and directed to the membrane (3). LDL binds to the receptor (4). The LDL is endocytosed via budding off the membrane to form a vesicle, called an endosome. A drop in pH allows for ligand release (5). LDLr is recycled to the membrane (6). The Apo B-100 portion is degraded to amino acids (7) in the lysosome (8). Increases in cholesterol concentrations inhibit the synthesis of cholesterol as well as the synthesis of the LDLr.

The LDLr is synthesised in the endoplasmic reticulum (ER) and mature LDLr is expressed at the cell surface, where circulating LDL binds to the receptor (Fig. 1.2) (Yamamoto et al., 1984; Brown and Goldstein, 1986; Gent and Braakman, 2004). The LDL-LDLr complex becomes internalised through clathrin coated pits which form vesicles by budding off from the membrane, and giving rise to the endosome. Once the endosome fuses with a lysosome, the drop in pH allows for the dissociation of the ligand-

receptor complex. The LDL particle is broken down to release cholesterol to be used in downstream events. The protein component of LDL, apo B-100 is degraded while the LDLr is recycled to the membrane. The process is controlled through a feedback mechanism which prevents overloading of cholesterol and thus maintains cellular cholesterol levels. This process is inhibited by increasing cholesterol concentrations (Yamamoto et al., 1984; Innerarity, 2002).

1.1.4 LDLr family

The LDLr family consists of the LDLr, the vLDL receptor (vLDLr), the LDLr related protein-1 (LRP)-1 a, LRP-1 b, megalin (gp330/LRP-2) (Kounnas et al., 1993), LRP-5, LRP-6, and apolipoprotein E receptor 2 (ApoER2/LRP-8) (Hussain et al., 1999; Nykjaer and Willnow, 2002; Jeon and Blacklow, 2005). Members of this family all share the same basic domain structure: a ligand binding domain, an EGF precursor homology domain, a hydrophobic membrane-spanning domain and a C-terminal cytoplasmic tail. In addition, some of the members have an O-glycosylated domain (Fig. 1.3). The receptors differ in the number of repeats within the ligand binding domain, the number of EGF repeats and the number of YWTD repeats (Hussain et al., 1999; Nykjaer and Willnow, 2002) The structure of LRP-1 is slightly different compared to the rest, as it is made up of an α- and a β-subunit which are covalently linked. A common feature amongst the LDLr family members is that they are expressed at the cell surface and undergo receptor-mediated endocytosis to transport ligands into cells. Another feature is that members of the LDLr family bind a number of unrelated ligands, in addition to their specific ligand, all of which are calcium dependent. All of the receptors are able to bind receptor associated protein (RAP), although to different levels. LDLr family members are expressed fairly widely throughout the different tissues (Hussain et al.,

1999).

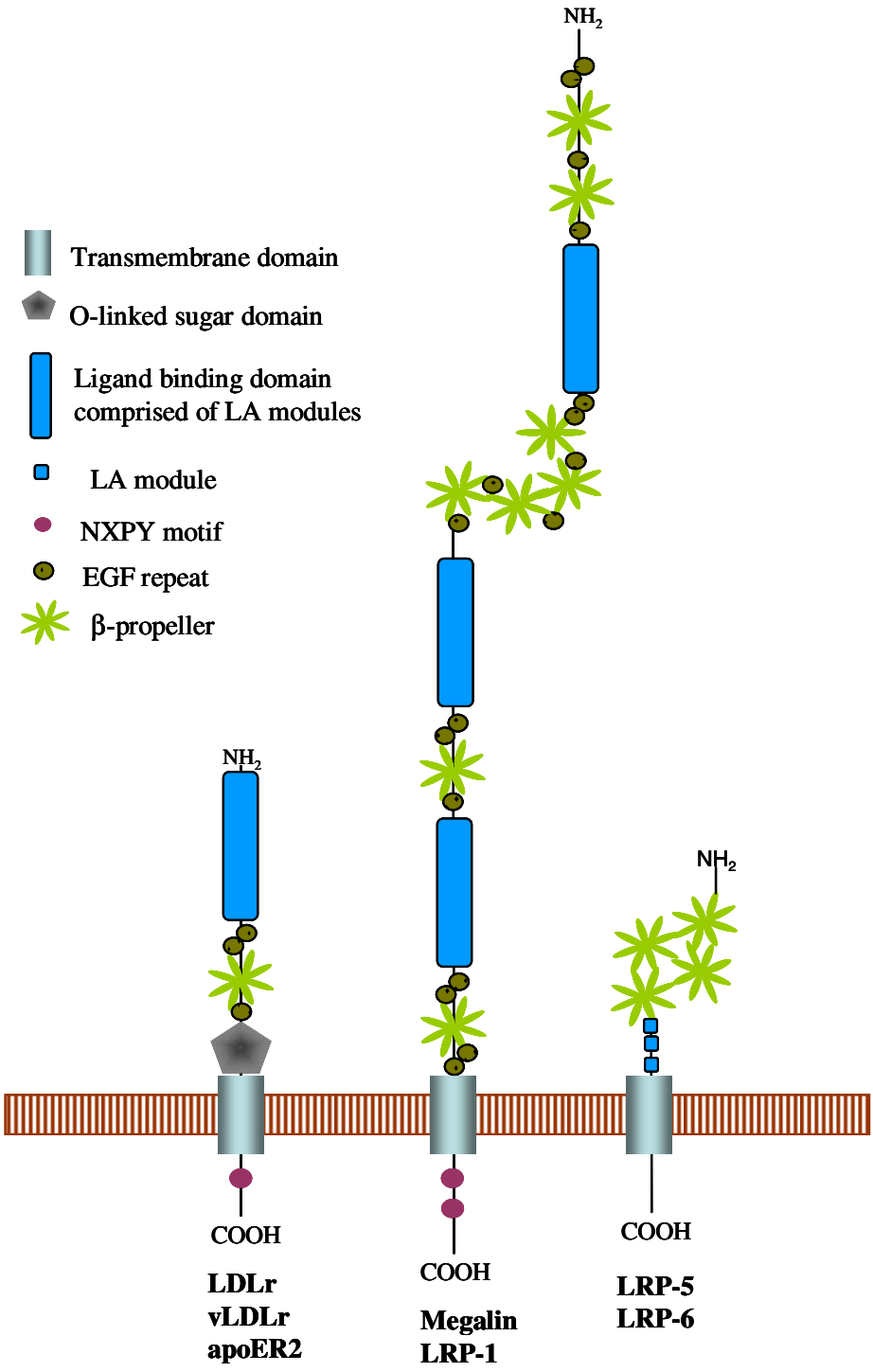

Figure 1.3: Core members of LDLr family (adapted from Gent and Braakman, 2004 and Jeon and Blacklow, 2005).
The domain structures of the LDLr family members. The LDLr, vLDLr and apoER2 share similar overall domain structures. The LRP-1 and megalin are the largest members and are comprised of more ligand binding domains. LRP-5 and LRP-6 share a similar structure.

1.1.5 LDLr regulation

The transcriptional regulation of the LDLr gene is controlled by intracellular cholesterol levels which further affect a group of proteins to activate or down-regulate the LDLr gene. In addition, the LDLr is also regulated at the post-translational level.

1.1.5.1 Sterol-regulatory element-binding proteins (SREBPs)

The LDLr is regulated at the transcriptional level by SREBPs which are important in cholesterol homeostasis and are controlled by a feedback regulation due to the accumulation of end products. SREBPs control transcriptional levels of the LDLr gene, to increase or decrease uptake of cholesterol into the cell. SREBPs also regulate genes involved in the synthesis of cholesterol (Sakai and Rawson, 2001).

The family of SREBPs are made up of SREBP-1a, SREBP 1-c and SREBP-2 (Yokoyama et al., 1993; Simons and Ikonen, 2000; Sakai and Rawson, 2001; Kong et al., 2006; Martini and Pallottini, 2007). SREBPs are membrane proteins and SREBP-2 is the main protein that is important in the regulation of cholesterol maintenance (Martini and Pallottini, 2007). SREBPs are regulated by proteolytic cleavage to produce active proteins in the ER and in the presence of cholesterol remain as inactive proteins attached to retention proteins (either Insig 1 or 2) and the chaperone protein, SREBP cleavage activating protein (SCAP). SCAP has a sterol sensory domain, so when cellular cholesterol concentrations are low the SCAP/SREBP complex is transported to the Golgi where it is cleaved consecutively by a Site-1 and Site-2 protease, releasing the N-terminal regions of SREBP which translocates to the nucleus. Binding of SREBPs to the sterol regulatory response elements within gene promoters, allows for the increase in transcription of genes that increase the levels of cholesterol synthesis such as 3-hydroxy-

3-methylglutaryl Co-enzyme A (HMG CoA) synthase and HMG CoA reductase, as well as the genes involved in cholesterol uptake such as the LDLr (Simons and Ikonen, 2000; Sakai and Rawson, 2001; Martini and Pallottini, 2007).

HMG CoA reductase is the rate-limiting enzyme in the production of cholesterol (Brown and Goldstein, 1986). Statins are inhibitors of HMG CoA reductase, which inhibits the production of cholesterol synthesis and increasing the cleavage of SREPB-2 with the concomitant increase in the production of LDLr mRNA and LDLr protein levels. Statins are used in the treatment of FH.

Estrogen, growth factors, cytokines, insulin and phorbol esters like phorbol myristate acetate (PMA), affect LDLr transcription by either increasing the binding of transcription factors to the LDLr promoter, or activating SREBPs or the activation of extracellular signal-regulated kinase (ERK) signaling cascades, all of which increase LDLr transcription (Mehta et al., 2002; Smith et al., 2004; Kong et al., 2006).

1.1.5.2 Post-translational regulation of the LDLr by proprotein convertase subtilisin kexin 9 (PCSK9)

A newly identified player in the post-translational regulation of the LDLr is the PCSK9, previously known as neural apoptosis regulated convertase 1 (NARC-1), a member of the serine protease convertase family transcribed by the NARC-1 gene (Benjannet et al., 2004). Mutations in this gene were discovered when some patients displayed high LDL levels, but had no associated mutations in either the receptor or in the ligand protein apo B-100, the two genes that are associated with FH (Haddad et al., 1999). PCSK9 was identified as the third gene which plays a role in FH (Timms et al., 2004; Dubuc et al.,

2004). Early studies indicated that PCSK9 does indeed have a role in cholesterol maintenance when this gene was identified to be regulated by sterols and further evidence showed that it was regulated by SREBP-2 and upregulated by statins (Dubuc et al., 2004).

PCSK9 is secreted from the cell and secretion requires autocatalysis, a mechanism which cleaves the prodomain from the catalytic domain, but the prodomain stays attached to the catalytic domain as a complex (Li et al., 2007a; McNutt et al., 2007, Kwon et al., 2008).

PCSK9 reduced LDLr expression in cultured lymphocytes and in rat hepatoma cells (Benjannet et al., 2004), while mice that had adenovirus-mediated expression of PCSK9 were observed to have increased plasma levels of LDL due to reduced hepatic LDLr (Maxwell and Breslow, 2004). PCSK9 had no effect on mRNA levels, while lowering surface LDLr expression in cultured human cells as well as transfected cells (Maxwell et al., 2005).

Studies on the overexpression of PCSK9 indicated that PCSK9 reduced mature LDLr protein quantities without affecting the synthesis of LDLr and was dependent on catalytically active PCSK9 (Park et al., 2004; Maxwell et al., 2005; Benjannet et al., 2006; Homer et al., 2008). PCSK9-mediated degradation of the LDLr was suggested to occur independently of the adaptor protein, the autosomal recessive hypercholesterolemia (ARH) protein (Park et al., 2004). Some proteosome, metalloprotease and aspartic or lysosomal cysteine protease inhibitors showed that these enzymes were not involved in the degradation of the LDLr (Maxwell et al., 2005). Initial experiments suggested that degradation of the LDLr occurred at the cell surface prior to internalisation (Park et al.,

2004), while later experiments indicated that degradation occured subsequent to transport from the ER in a pH dependant organelle (Maxwell et al., 2005; Holla et al., 2007). It was also shown that endocytosis of the LDLr is not needed for the receptor to be degraded by PCSK9 (Park et al., 2004; Maxwell et al., 2005; Holla et al., 2007), and PCSK9 does not degrade a recombinant secreted soluble LDLr (Holla et al., 2007), both results supporting the theory that degradation takes place in an intracellular compartment.

Exogenously added PCSK9 however, was internalised into cells and degraded the LDLr pool (Lagace et al., 2006; Holla et al., 2007) independent of clathrin-coated pit formation (Holla et al., 2007) and independent of PCSK9 catalytic activity (Li et al., 2007a; McNutt et al., 2007; Schmidt et al., 2008). The conflicting data between various groups, where some results suggest that catalytic activity is required, while others suggest that catalytic activity is not required, needs further clarification. From the literature, it seems that autocatalytically inactive PCSK9 constructs (transfected into cells or injected into mice) are defective in LDLr degradation (Park et al., 2004; Maxwell et al., 2005; Benjannet et al., 2006; Homer et al., 2008), but those used in conjunction with the prodomain (as a secreted PCSK9) have showed degradation independent of activity (Li et al., 2007a; McNutt et al., 2007; Schmidt et al., 2008). This suggests that the prodomain is important for secreted PCSK9 in the internalisation and degradation of the LDLr.

Degradation of the LDLr by secreted PCSK9 was shown to be dependent on the internalisation of the LDLr (Qian et al., 2007; Lagace et al., 2006), ARH, (in primary hepatocytes) and to some extent the LRP in mouse embryonic fibroblasts (Lagace et al., 2006). This group also showed that PCSK9 can bind the extracellular domain of the LDLr by co-immunoprecipitation and ligand blots. Experiments using parabiosis (an

experiment which involves the sharing of plasma between 2 mice), showed that secreted PCSK9 in plasma transferred from one mouse to the next parabiotic mouse was able to reduce hepatic LDLr expression in the recipient mouse (Lagace et al., 2006). Fisher et al. (2007) showed that secreted PCSK9 lowered LDL uptake by the LDLr, that its binding was detected at neutral pH, as well as at endosomal pH where the binding affinity was 150-fold higher, and that LDL reduced PCSK9 dependant LDLr degradation (Fisher et al., 2007). Because of this tight interaction at low pH, recycling to the surface is prevented and it is thought that the LDLr is rather targeted for lysosomal degradation. The region of the LDLr that binds PCSK9 to the LDLr was narrowed down to an EGF A repeat (Zhang et al., 2007; Kwon et al., 2008). It was also shown that after internalisation of PCSK9 by the LDLr, over time the LDLr was found in the early endosomes, late endosomes and lysosome. From the literature, the current understanding is that PCSK9 can act on the LDLr at two points in the LDLr lifecycle: (i) in the secretory pathway, the LDLr can be targeted for degradation, and (ii) after secretion, PCSK9 can be internalised and targets the LDLr for degradation rather than recycling, Fig. 1.4 (Horton et al., 2007; Zhang et al., 2007; Lambert et al., 2008).

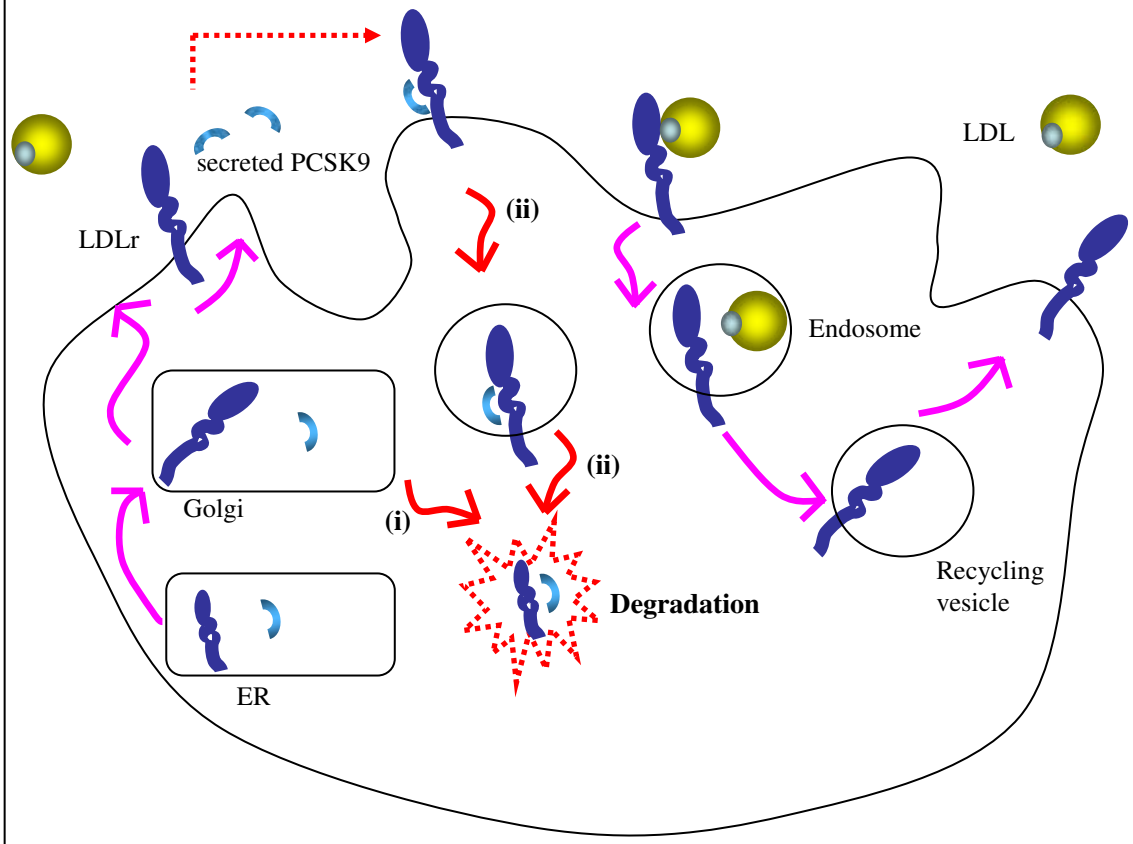

Figure 1.4: PCSK9 and LDLr degradation (adapted from Lambert et al., 2008). The normal trafficking and lifecycle of the LDLr is shown in pink. The two possible pathways for LDLr degradation is shown in red. PCSK9 may possibly act at two points in the LDLr pathway: (i) In the secretory pathway, the PCSK9 can target the LDLr for degradation, or (ii) as a secreted protein PCSK9 can be internalised and targets the LDLr for degradation rather than recycling.

1.1.6 Mutations in the LDLr

A mutation in the LDLr gene can result in the LDLr functioning sub-optimally or not at all, resulting in the inadequate clearance of plasma cholesterol. These mutations are typically called loss-of-function mutations. There are a number of mutations that can occur within the LDLr and these different mutations are classified into different groups depending on the location and effect of the mutation. The most common mutation is the

Class 1 mutation (also called null allele) which results in no LDLr production (Goldstein et al., 1985). Mutations which result in the slow release of LDLr from the ER to Golgi are called Class 2 mutations or transport-defective mutants. These mutants are smaller in molecular weight, equivalent to the immature, unglycosylated form and are not expressed at the cell surface (Li et al., 2004). Class 3 mutations are binding-defective as the LDLr is expressed on the cell surface, but does not bind LDL, and therefore does not internalise LDL. Class 4 mutants, also expressed at the cell surface, bind LDL but do not internalise it since the mutation disrupts the internalisation signal. These mutants are thus termed internalisation-defective (Lehrman et al., 1985; Davis et al., 1986). Class 5 mutants are recycling-defective, and clear plasma LDL at a slower rate than normal due to the inability of the receptor to recycle to the membrane (Miyake et al., 1989). Cholesterol maintenance in these cells is dependent on the *de novo* synthesis of LDL receptors. Patients with any of the above defects in the LDLr present with a clinical condition, known as FH (Goldstein et al., 1985; Brown and Goldstein, 1986). Patients with a heterozygous mutation have a less severe form of FH, while those with a homozygous mutation in the LDLr, present with much higher levels of cholesterol, which leads to a quicker onset in the development of atherosclerosis, coronary artery disease (CAD) and fatal heart attacks or strokes in early adult life. Heterozygous mutations are common, occurring in 1 in 500 individuals, which highlights the importance of alleviating the onset of disease in FH patients (Brown and Goldstein, 1986).

1.1.7 Autosomal Dominant Hypercholesterolemia (ADH)

In addition to mutations in the LDLr gene, mutations in other genes also contribute to hypercholesterolemia, grouped as ADH (Rader et al., 2003). These are discussed briefly, below.

1.1.7.1 Mutations in apoB-100

Mutations in the apoB-100 protein result in the disruption of binding to the LDLr, and therefore prevent the uptake of LDL particles into the cell. These mutations can be present in the binding region or outside of the binding region. These mutations can affect binding to the receptor mildly or dramatically, depending on the type of mutation and affecting plasma cholesterol levels accordingly (Vrablik et al., 2001; Rader et al., 2003).

1.1.7.2 Mutations in PCSK9

Mutations in PCSK9 can fall into two groups, either loss or gain of function. Mutations of PCSK9 can also be classified as Class 1: null, Class 2: defective in processing, Class 3: defective transport from ER, Class 4: altered stability or Class 5: altered affinity for the LDLr (Horton et al., 2007). Some gain of function mutants were shown to have higher LDLr degrading activity and thus lowered LDL uptake, which could be attributed to higher binding affinity to the LDLr (Lagace et al., 2006; Fisher et al., 2007). The loss of function mutations are of a protective type, preventing LDLr degradation and lowering LDL levels (Horton et al., 2007).

1.2 Ectodomain Shedding

Ectodomain shedding is the proteolytic release of membrane-bound proteins into the extra-cellular milieu (Fig. 1.5) (Ehlers and Riordan, 1991; Hooper et al., 1997; Peschon et al., 1998; Arribas and Borroto, 2002; Mezyk et al., 2003). The group of enzymes responsible for the release of membrane-bound protein ectodomains are termed secretases or sheddases (Hooper et al., 1997).

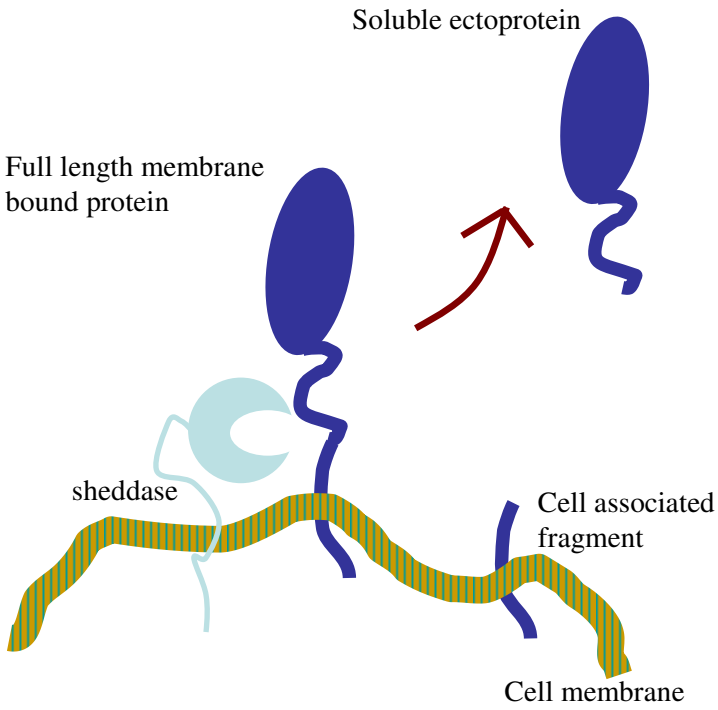

Figure 1.5: The process of ectodomain shedding (adapted from Black, 2002).
The membrane protein is solubilised through proteolysis and release of the ectoprotein by a sheddase.

Many membrane proteins are shed as part of a post-translational event that is important in cell regulation. Examples are diverse ranging from receptors, receptor ligands and cell adhesion molecules to enzymes and other proteins. Furthermore these proteins can be of

either type I or II membrane proteins, with the N-terminus facing extracellularly or intracellularly, respectively (Ehlers and Riordan, 1991; Hooper et al., 1997). A variety of functions have been attributed to ectodomain shedding, depending on the proteins involved (Peschon et al., 1998; Arribas and Borroto, 2002; Mezyk et al., 2003; Rebeck et al., 2006; Edwards et al., 2008). In the case of some cytokines, these become soluble factors that carry out functions elsewhere, either on the same cell (known as autocrine signaling) or at neighbouring cells (known as paracrine signaling). In the case of cell surface receptors or ligands involved in signaling, ectodomain release can lead to down regulation and inhibit signaling. The generation of soluble receptors could also serve to sequester ligands by binding to it (Rebeck et al., 2006). Ectodomain shedding also functions as an initial step in cell signaling, to promote the release of the intracellular domain. Shedding of some proteins such as transforming growth factor-α (TGF-α), has also been shown to be important in the development of the mammalian embryo (Peschon et al., 1998), while aberrant shedding plays a major role in some disease incidences such as the overproduction of soluble tumour necrosis factor-α (TNF-α) in arthritis and the pathological processing of amyloid precursor protein (APP) in Alzheimer's disease (Hooper et al., 1997). Shedding of most proteins is sensitive to hydroxamate based inhibitors, suggesting that the metalloproteases are the key family of enzymes responsible for this event (Arribas et al., 1996).

Most sheddases belong either to a distintergrin and metalloprotease (ADAM) or the matrix metalloprotease (MMP) family (Arribas and Borroto, 2002; Chow and Fernandez-Patron, 2007), the former contributing a major role in the shedding of proteins (Huovila et al., 2005). Since the first ADAM sheddase was isolated, 17 others of a potential of 33 were identified to have shedding activity (Chow and Fernandez-Patron, 2007). Shedding

of proteins occurs at a constitutive rate, but can be enhanced with the addition of phorbol ester, a stimulator of the protein kinase C (PKC) pathway (Arribas and Borroto, 2002) which may lead to the activation of proteases involved in shedding (Ehlers and Riordan, 1991; Black, 2002). Ongoing studies on TNF-α converting enzyme (TACE) the first sheddase to be identified (Black et al., 1997; Moss et al., 1997) and other sheddases contribute to the understanding of the requirements for ectodomain shedding for the benefit of targeting excessive or aberrant shedding.

1.2.1 Soluble counterparts of LDLr family members

A few members of the LDLr family have also been found to have soluble counterparts, some of which have either been found in mammalian cell culture, human urine and/or human plasma. These members include the LDLr (Begg et al., 2004; Molina et al., 2007), ApoER2 (Hoe and Rebeck, 2005; Rebeck et al., 2006), LRP-1 (Quinn et al., 1997), megalin (glycoprotein 330) (Kounnas et al., 1993) and vLDLr (Marlovits et al., 1998b).

1.2.1.1 Soluble LRP-1

Soluble LRP-1 was isolated from human plasma by ligand affinity purification (Quinn et al., 1997; Quinn et al., 1999). The purified soluble LRP was approximately 500 kDa (corresponding to the α-chain of LRP-1), and was detected by RAP ligand blots as well as two different antibodies specific to the α-chain of LRP. Similar methods were used to detect the 85 kDa β-chain of LRP-1. It was suggested that a fragment of the β-chain could be present, but not detected by the antibody to the C-terminus. No soluble LRP was found in cultured HepG2 cells and human fibroblasts, while it was found in cultured rat hepatocytes (Quinn et al., 1997). Further characterisation of soluble LRP showed that an antibody to the extra cellular portion of the β-chain could detect a truncated form

present in the affinity purified sample (Quinn et al., 1999). Release of soluble LRP could be inhibited by a hydroxamic acid compound, INH-3855-PI, a broad range metalloprotease inhibitor. Membrane type 1 matrix metalloprotease (MT1-MMP) is involved in the shedding of the LRP-1 (Rozanov et al., 2004). To investigate the possibility of the β-secretase (BACE) as a potential sheddase responsible for the cleavage of the extracellular domain of LRP, cells were analysed for the co-localisation and co-immunoprecipitation of BACE and LRP (von Arnim et al., 2005). In addition, the LRP was also shown to undergo γ-secretase cleavage by the release of the intracellular domain (ICD) after ectodomain release (May et al., 2003). The region of interaction was shown to be in the ICD. The presence of BACE increased shedding of LRP, while inhibitor studies and the presence of small interference RNA (siRNA) against BACE, showed a decrease in LRP shedding (von Arnim et al., 2005).

1.2.1.2 Soluble megalin

A soluble fragment of megalin was first purified from urine (Kounnas et al., 1993). Megalin was shown to undergo ectodomain shedding with subsequent regulated intracellular proteolysis and release of the ICD of the C-terminal fragment (Zou et al., 2004b; Biemesderfer, 2006). The function of ligand ectodomain shedding and release of megalin is thought to play a role in the activation of genes in the metabolism of that ligand.

1.2.1.3 Soluble ApoER2

The ectodomain release of cell surface ApoER2 was sensitive to metalloprotease inhibition and increased in the presence of ligand and in the presence of PMA (Hoe and Rebeck, 2005). In addition, like the LRP, ectodomain cleavage of the ApoER2 results in

the γ-secretase dependent release of the ICD, which may function in signaling pathways (May et al., 2003; Hoe and Rebeck, 2005; Rebeck et al., 2006).

1.2.1.4 Soluble LDLr and vLDLr

It must be highlighted that the ectodomain shedding of the LDLr is a phenomenon different to the PCSK9-mediated degradation, since degradation of the LDLr by PCSK9 was shown not to occur in fibroblasts (Horton et al., 2007) and Chinese hamster ovary (CHO) cells (Park et al., 2004; Horton et al., 2007) and soluble LDLr was not detected in medium of cells expressing PCSK9 (Maxwell et al., 2005). These data suggest that PCSK9 does not mediate release of LDLr into the external surroundings.

Soluble LDLr was shown to be produced in response to human rhinovirus (HRV) infection (Hofer et al., 1994). It was able to bind to the virus HRV-2 as demonstrated by [^{35}S] methionine-labelled virus ligand blotting and therefore prevent its uptake into the cell. Conversely, membrane-bound LDLr binds HRV-2, and internalises it. In the same study, binding of the HRV-2 is attenuated in the presence of iodinated LDL, thus further implicating the LDLr in this binding. In FH cells, however, LRP was found to be the receptor that endocytoses HRV-2 in the absence of LDLr.

Recombinant soluble LDLr (comprising the ligand binding domain) was shown to inhibit rhinovirus infection in HeLa cells by causing viral aggregates (Marlovits et al., 1998c). Further analysis using ligand blots on different lengths of recombinant, purified soluble LDLr showed that it was able to bind HRV-2 (Marlovits et al., 1998a). However, only constructs containing more than two repeats of the ligand binding domain were able to elicit anti-viral activity.

Like the LDLr, the vLDLr was also implicated to undergo shedding in response to HRV infection (Marlovits et al., 1998b). A 84 kDa band, representing the vLDLr bound to HRV-2 and antibodies against vLDLr in a calcium dependent manner (Hofer et al., 1992; Marlovits et al., 1998b).The function of soluble vLDLr formation was suggested to be important for the neutralisation of rhinovirus, thus preventing the penetration of viral RNA (Nicodemou et al., 2005).

A 28 kDa protein, identified to be a soluble LDLr N-terminal fragment by protein microsequencing and antibody studies, was shown to protect mammalian cells from vesicular stomatis viral (VSV) infection (Fischer et al., 1993). This N-terminal fragment is produced after induction by interferon (IFN), but experiments also showed that the soluble LDLr fragment added before or after viral incubation could inhibit viral titre, independent of IFN induction. It was found that inhibition does not occur through attenuation of the binding of the virus to the cell associated receptor. This indicates that the soluble LDLr fragment can act as an antiviral protein, but the mode of action is not known. The LDLr however is not the sole antiviral protein shed in response to IFN, as FH fibroblasts (LDLr null) were able to reduce viral titre by IFN induction (Fischer et al., 1993).

A truncated 140 kDa soluble form of the LDLr was found in the medium of cultured human skin fibroblasts as well as CHO cells over-expressing the receptor (Begg et al., 2004). The soluble LDLr was only able to bind antibodies directed to the N-terminal ectodomain, but not antibodies directed to the C-terminal tail, suggesting that the N-terminus had been released by ectodomain shedding. To test the possibility that the 140 kDa soluble receptor is a product of proteolysis and not gene splicing, cells were

radioactively labelled with [^{35}S] methionine and a 140 kDa band was only present in the medium and not seen in the cells, which provided further evidence that the LDLr is shed from the membrane. Moreover, the LDLr undergoes increased shedding in the presence of phorbol myristate acetate (PMA), and decreased proteolytic release in the presence of TNF-α Protease Inhibitor (TAPI), a common feature amongst shed proteins (Arribas et al., 1996). The change in size of the membrane-bound form to that of soluble receptor is also consistent with shedding occuring in the juxtamembrane stalk region of the LDLr (Begg et al., 2004).

In order to elucidate the sheddase(s) involved in the shedding of the LDLr, a range of inhibitors were tested on cells expressing LDLr (Begg et al., 2004). Compounds tested such as serine, cysteine and aspartic protease inhibitors showed no reduction in shedding. EDTA and EGTA inhibited shedding of the LDLr by 33 % and 50 %, respectively, while the inhibitor that showed the highest reduction in shedding was the hydroxamate-based inhibitor, TAPI. TAPI used at a concentration of 10 μM was capable of inhibiting LDLr shedding by 90 %. These data implicate metalloprotease activity in the ectodomain shedding of the LDLr. TACE is involved in the shedding of a number of membrane-bound proteins (which will be discussed further), and is a possible candidate in the shedding of the LDLr as a cell line deficient in TACE activity showed that conditioned medium from TACE deficient cells produced less soluble LDLr, in addition to other proteins identified, when compared to wild-type cells (Guo et al., 2002).

1.2.2 Ectodomain shedding and the glycosylation states of LDLr family members

When the LDLr was expressed in a CHO cell line deficient in O-glycosylation, it was found to be shed into the medium more rapidly than LDLr expressed in the presence of various sugars (Kozarsky et al., 1988). The vLDLr and ApoER2 occur in two forms, an O-glycosylated form and one lacking the O-glycosylated domain (Magrane et al., 1999; Rebeck et al., 2006). Studies on the function of the two forms of vLDLr showed that the presence of the O-glycosylated domain hampered shedding of the vLDLr, as constructs that did not have the O-glycosylated region were shed more rapidly from the membrane (Magrane et al., 1999). The same effect was seen when vLDLr was expressed in O-glycosylation deficient cells, and it was thought that the O-glycosylated domain, or glycans present, restricted the availability of the cleavage site residues. As with the vLDLr, it was found that increased shedding of hypoglycosylated forms of LRP and ApoER2 occurs (May et al., 2003). The role of glycosylation states in different tissues may result in different shedding rates of LRPs and possibly other members of the LDLr family as well.

1.3 TACE

Two independent groups cloned and purified TACE in 1997 and identified this enzyme as the first sheddase to cleave the cytokine, pro-TNF to mature TNF (Black et al., 1997; Moss et al., 1997). TACE is also known as ADAM 17 (Killar et al., 1999). TACE is a zinc dependent metalloprotease and is a member of the ADAMs family, which is part of the metzincin family that includes snake venom metalloproteases (SVMPs) and MMPs (Killar et al., 1999; Mezyk et al., 2003). ADAMs play a role in fertilisation, functioning of the immune systems and other processes (Mezyk et al., 2003), whereas MMPs function in the degradation of extracellular matrix proteins in addition to other proteins (Huovila et al., 2005).

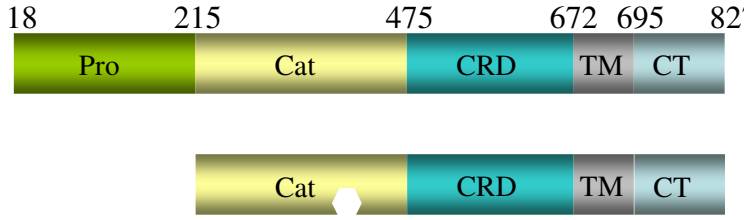

Figure 1.4 Domain structure of TACE zymoygen (upper) and mature TACE (lower) [adapted from Li et al., 2007 (b)].
Pro: prodomain, Cat: catalytic domain, CRD: cysteine-rich disintegrin domain, TM: transmembrane domain and CT: cytoplasmaic domain. The open circle represents the active site in the catalytic domain.

The structure of TACE is divided into a prodomain, a zinc-binding catalytic domain, a cysteine-rich disintegrin domain, a transmembrane domain and a cytoplasmic domain (Fig. 1.6) (Black, 2002; Li et al., 2007b). TACE is a type I membrane protein and is translated as a zymogen, as a result TACE occurs in two forms: a full length form

containing the prodomain and a mature, active form which has the prodomain removed (Schlondorff et al., 2000). The role of the disintegrin domain in TACE was not known previously, but the first evidence of its function was provided by the demonstration of an interaction of the cysteine-rich domain of TACE with that of the integrin receptor, integrin $\alpha_5\beta_1$ (Bax et al., 2004).

1.3.1 Function of TACE

TACE knock-out (KO) mice indicated that TACE and shedding are important in the development of the embryo as mice deficient in TACE died at birth and a few that survived, did not live for longer than 3 weeks (Peschon et al., 1998). These mice also had characteristics that are phenotypically similar to TGF-α KO mice, indicating that TACE was also important for the shedding of TGF-α. However, TGF-α KO mice do not die at birth indicating that TACE plays a prominent role in shedding of substrates important in development.

Soluble proteins such as cytokines and receptors released by TACE are important in the functioning of the immune system. TACE was shown to be involved in the shedding of L-selectin, interleukin (IL)-1R-II, both the TNF-α receptors [p55TNF receptor (TNFRI) and p75TNF receptor (TNFRII)], TNF-related activation-induced cytokine (TRANCE), in addition to TNF-α (Peschon et al., 1998; Lum et al., 1999; Reddy et al., 2000).

Some EGFR ligands are also dependent on TACE-mediated shedding. These include TGF-α, heparin binding EGF (HB-EGF), amphiregulin and epiregulin (Peschon et al., 1998; Sahin et al., 2004). Another substrate of TACE important in development, is the growth hormone receptor (GHR) involved in the stimulated production of GH binding

protein (GHBP) (Zhang et al., 2000). Another EGFR family member HER4, involved in the development of organs, is also dependent on TACE activity for cleavage release (Rio et al., 2000).

TACE possesses α-secretase-like activity in the cleavage of APP, while BACE cleaves at the β site in the generation of amyloid β peptide (Aβ) in Alzheimer's disease (Buxbaum et al., 1998; Asai et al., 2003; Allinson et al., 2004). Cleavage by TACE prevents the generation of the amyloidogenic peptide since it cleaves within the Aβ peptide. TACE and BACE do not compete in the proteolysis of APP under normal conditions (Kim et al., 2008). Notch-1 undergoes similar processing as APP in a TACE dependent manner (Brou et al., 2000; Delwig and Rand, 2008). Ligand dependent shedding of Notch-1 releases an intracellular domain, which translocates to the nucleus and acts as a transcription factor of genes important in development (Edwards et al., 2008).

The severe-acute respiratory syndrome-coronavirus (SARS-CoV) increased TACE activity for the release of the SARS-CoV receptor, angiotensin converting enzyme 2 (ACE) 2 (Lambert et al., 2005). The spike protein of the virus was able to induce TACE-mediated shedding of ACE 2 and TNF-α. In addition, the cytoplasmic tail of ACE 2 and the presence of TACE were needed for viral entry suggesting that signals resulting from TACE-mediated ACE 2 shedding lead to tissue damage (Haga et al., 2008).

While a number of substrates exist for TACE, it was also shown that in TACE KO cells, the absence of TACE did not affect the shedding of ACE (Sadhukhan et al., 1999), which indicated that other shedasses(s) are responsible for the ectodomain release of that protein. Mice deficient in TACE presented with normal serum levels of ACE. Using

antisense oligonucleotides, TACE as well as ADAM 10 were ruled out as sheddases responsible for the shedding of ACE (Allinson et al., 2004). In addition, recombinant ADAM 10 did not cleave an ACE peptide spanning the cleavage site of the stalk region (Lammich et al., 1999).

1.3.2 Regulation of TACE

TACE remains inactive by the co-ordination of a sulphydryl group from a cysteine present in the N-terminal prodomain to the zinc in the active site forming a "cysteine switch" (Moss et al., 1997). Cleavage by a proprotein convertase (PC) furin within the Golgi, or post-Golgi releases a mature active form which is expressed on the surface of cells (Moss et al., 1997; Schlondorff et al., 2000; Endres et al., 2003)..

While the removal of the prodomain is essential for TACE activity (Moss et al., 1997; Milla et al., 1999), the presence of the prodomain is required for transport of TACE to the membrane, as constructs without the prodomain are degraded. Studies using the purified prodomain as an inhibitor against TACE constructs, suggested that the presence of the distintegrin domain may facilitate in the furin dependent removal of the prodomain, while the cysteine present in the prodomain might prevent degradation (Gonzales et al., 2004). When a prodomain construct containing a mutation that disrupts cysteine switch formation showed the same inhibitory potential as wild-type, it was concluded that the cysteine switch is not required for inhibitory activity. To study the role of the cysteine switch in TACE further, Buckley et al., identified the amino-terminus of TACE to have inhibitory activity in the absence of the cysteine switch, as the construct used in the study increased TACE-mediated shedding of TNFR II (Buckley et al., 2005).

Despite the high sequence homology between ADAM 10 and TACE, replacing the TACE catalytic metalloprotease region with that of ADAM 10 does not result in the production of a functional construct (Reddy et al., 2000). Since a point mutation in the cysteine-rich disintegrin domain inactivated ectodomain shedding, it was suggested that this region is also important in regulating TACE (Li and Fan, 2004). Studies on the transmembrane domain of TACE showed that a secreted soluble TACE construct lacking the transmembrane was defective in cell-based shedding assays. A transmembrane-free TACE construct that was anchored to the membrane did not shed TGF-α, TNF-α and L-selectin (Li et al., 2007b). These data indicate that the transmembrane is important for anchoring TACE, in addition to other roles important for regulation.

Shedding of TNF-α, TGF-α and L-selectin at the constitutive level occurs via the p38 mitogen-activated protein (MAP) kinase pathway, while the EGF or PMA stimulated shedding occurs through the ERK-2 MAP kinase pathway (Fan and Derynck, 1999). Zhang et al., showed that reactive oxygen species (ROS) produced in response to PMA is the agent that increases TACE activity by attacking the sulphydral cysteine in the prodomain (Zhang et al., 2001).

TACE is phosphorylated in response to stimulation by PMA (Fan et al., 2003) and gastrin releasing peptide (Zhang et al., 2006). However, cleavage by TACE in a cell system occurs by membrane-anchored TACE independent of a cytoplasmic domain (Reddy et al., 2000; Doedens et al., 2003; Fan et al., 2003; Li and Fan, 2004; Edwards et al., 2008).

PMA increased cellular TACE activity on the cell surface or in a compartment, without the associated increase in TACE expression levels (Doedens et al., 2003). It was suggested that prolonged exposure to PMA leads to down regulation of mature TACE on the cell surface by the degradation of TACE, conceivably as a regulatory mechanism (Doedens and Black, 2000). Enderes et al., showed that the PMA-mediated down-regulation only affects TACE and not ADAM 10. Furin transfected into furin deficient cells was tested for degradation of TACE in response to PMA (Endres et al., 2003). No degradation of mature TACE was seen, suggesting that furin is not responsible for the PMA-mediated degradation of TACE.

Thus, the role of the cytoplasmic domain in the regulation of TACE and the mechanism by which PMA up-regulates TACE is still not clear, since data showed that TACE is phosphorylated in the cytoplasmic tail in response to PMA, while constructs lacking the cytoplasmic domain are still active and responsive to PMA stimulation (Reddy et al., 2000; Doedens et al., 2003; Edwards et al., 2008).

N-arginine dibasic convertase [Nardilysin, (NRDc)] binds to and increases TACE activity for the shedding of HB-EGF, APP and TNF-α. Addition of phorbol enhances the interaction and release of soluble HB-EGF. The catalytic activity of NRDc is not required for increased shedding of HB-EGF, APP and TNF-α by TACE. Enhancement of shedding by NRDc affects TACE-, ADAM 9- and ADAM 10-mediated shedding of APP, while it was shown not to affect TACE- and ADAM 10-mediated shedding of TNF-α (Hiraoka et al., 2008).

Under different conditions, different sheddases are responsible for the shedding of some proteins. For example, in the case of the prion protein TACE is responsible for up-regulated shedding whereas ADAM 10 is the sheddase responsible for constitutive shedding (Vincent et al., 2001). Another example is TNF-α, where TACE is the sheddase responsible for phorbol stimulated shedding, while the other ADAMs such as ADAM 9 and 10 are involved in constitutive shedding (Zheng et al., 2004). Furthermore, ADAM 9 and ADAM 10 KO experiments suggest that these are not the only sheddases responsible for constitutive shedding. TACE seems to be responsible for nearly 90 % of stimulated shedding of proteins studied, while other sheddases are important for either constitutive or stimulated shedding (Huovila et al., 2005).

1.3.3 TACE substrate specificity

The use of TACE KO systems have revealed a number of unrelated membrane-bound proteins, either of type I or II, that are dependent on TACE cleavage (Peschon et al., 1998; Reddy et al., 2000; Vincent et al., 2001; Guo et al., 2002; Mezyk et al., 2003; Huovila et al., 2005; Reiss and Saftig, 2008). Due to the apparent lack of specificity, factors that influence substrate recognition for TACE remain unclear, as TACE cleaves unrelated sequences thus resulting in different cleavage sites. Although there does not seem to be a specific recognition sequence, an Ala-Val bond seems to be preferred in some instances (Black et al., 2003). Even with different cleavage sites found for TACE substrates, there exists specificity for at least the TNF-α peptide. In this case, peptide assays showed that cleavage by TACE did not occur when the Ala was replaced with an Ile in the TNF-α peptide, while replacing it with a Val/Gly reduced cleavage by more than 90 % (Black et al., 2003). Cleavage of the peptide was reduced to 30 % when the

Val was replaced with Leu/Ile. Some of the cleavage sites of TACE substrates are highlighted in Table 1.1.

Table 1.1: Cleavage sites of peptides by TACE (adapted from Mezyk et al, 2003 and Black et al, 2003).

Protein/Peptide	**Cleavage site**
TNF-α	PLAQAV ↓ RSSS
TGF-α N-terminal peptide	PVAAA ↓ VVSHF
TGF-α C-terminal peptide	ADLLA ↓ VVAAS
Amphiregulin N-terminal peptide	SVRVEQ ↓ VVKPPQ
Amphiregulin C-terminal peptide	ERCEGEK ↓ SMKTHS
Epiregulin N-terminal peptide	NPRVAQ ↓VSITKC
TNFR-I	PQIEN ↓ VKGTE
TNF-II	APGAV ↓ HLPQP
IL-6R-α	SLPVQ ↓ DSSSV
L-selectin	QKLDK ↓ SFSMI
APP	VHHQK ↓ LVFFA

While TACE activity is implicated in a variety of substrates, the stalk peptides and their length are important factors in the cleavage of at least TNF-α and L-selectin, since stalk regions with the cleavage site present but without the adjacent sequences were not cleaved (Zheng et al., 2004, Tsakadze et al., 2006). In addition, the importance of the stalk sequence was indicated by the substitution of TACE substrate stalk sequences into non-TACE substrates allowed the ectodomain release of the non-shed proteins (Tsakadze et al., 2006).

1.3.4 Other sheddases that cleave TACE substrates

Other recombinant ADAMs such as ADAM 9 (Roghani et al., 1999) and ADAM 10 (Rosendahl et al., 1997; Hinkle et al., 2003) are able to cleave TNF-α peptides *in vitro*. ADAM 10 also cleaves a membrane form of TNF-α (Rosendahl et al., 1997) and cleaves the prion protein under constitutive conditions (Vincent et al., 2001). In the cleavage of APP, ADAM 9 and ADAM 10 also act in a α-secretase-like manner similar to TACE (Asai et al., 2003; Deuss et al., 2008). Shedding data from TACE, ADAM 9 and ADAM 10 KO cell lines suggested that the ADAMs function as a team in the cleavage of APP, and compensate for another in the absence of one ADAM. TACE KO studies indicated that the major sheddase for Notch-1 processing is ADAM 10, and that TACE KO mice do not display phenotypes associated with defects in Notch-1 signaling, suggesting a minor role for TACE in Notch processing physiologically. Additional TACE substrates that are cleaved by other sheddases are shown in Table 1.2.

Table 1.2: Table depicting different sheddases that act on TACE substrates.

Sheddase	ADAM name	TACE substrate
MS2	ADAM 8	TNF-α (Amour et al., 2002; Naus et al., 2006), APP, kit ligand 1 (KL-1) (Amour et al., 2002), TGF-α, L-selectin (Naus et al., 2006) ADAM 8 does not cleave KL-1 (Naus et al, 2006) TRANCE (Naus et al., 2006)
MDC-9/ Meltrin-γ	ADAM 9	TNF-α peptide (Roghani et al., 1999), HB-EGF (Izumi et al., 1998), APP (Asai et al., 2003), Collagen XVII, epiregulin, KL-1 (Roghani et al., 1999; Amour et al., 2002)
Kusbanian	ADAM 10	TNF-α peptide (Rosendahl et al., 1997; Hinkle et al., 2003), cellular prion protein (Vincent et al., 2001), Desmoglein-2, activated leukocyte cell adhesion molecule (ALCAM) (Bech-Serra et al., 2006), APP peptide (Lammich et al., 1999), APP (Asai et al., 2003; Allinson et al., 2004), TGF-α (Hinkle et al., 2003), HB-EGF (Lemjabbar and Basbaum, 2002), CD44, Notch, Collagen XVII [no cleavage of HB-EGF and KL-1 (Amour et al., 2002)]
Meltrin-α	ADAM 12	HB-EGF (Asakura et al., 2002), epiregulin
MDC-15	ADAM 15	TGF-α, epiregulin, amphiregulin
Meltrin-β	ADAM 19	TNF-α (Zheng et al., 2004), TNF-α peptide, TRANCE, KL-1 (Chesneau et al., 2003)
	ADAM 33	Peptides of APP, KL-1, TRANCE, TNF-α (Zou et al., 2004a)
MMP-1	N/A	TNF-α peptide (Mohan et al., 2002; Jin et al., 2002)
MMP-3	N/A	HB-EGF (Suzuki et al., 1997b)
MMP-7	N/A	TNF-α peptide (Mohan et al., 2002), TNF-α (Haro et al., 2000), HB-EGF (Yu et al., 2002)
MMP-9	N/A	TNF-α peptide (Mohan et al., 2002; Jin et al., 2002)
MMP-13	N/A	TNF-α peptide (Jin et al., 2002)

TACE is the most promiscuous of identified sheddases as it is responsible for the shedding of a larger number of unrelated proteins, including cytokines, growth factors, receptors, adhesion molecules and some other proteins when compared to other sheddases (Mezyk et al., 2003; Huovila et al., 2005; Reiss and Saftig, 2008). Redundancy between members of the ADAMs family exists, as some can take over the function when the other member is absent. This can also be seen from Table 1.2 as a number of ADAMs and some MMPs are also able to cleave TACE substrates (Chow and Fernandez-Patron, 2007). TACE cleaves many substrates, some more efficiently than others, but the role it plays in the cleavage of some proteins is not known. In conclusion, it is evident that sheddases preferentially act on a particular substrate while still being able to cleave others. In addition, there are substrates which can be cleaved by different sheddases and provides evidence that it is possible for other ADAMs to take over shedding of proteins in the absence of a particular ADAM, depending on the stimulation or tissue type or type of experiment performed (Chow and Fernandez-Patron, 2007).

Thesis outline

The aim of this thesis was to investigate the cellular machinery involved in the ectodomain release of the LDLr, which was previously shown to undergo regulation in the presence of phorbol esters and the hydroxymate inhibitor, TAPI. (Begg et al., 2004) An objective of this thesis was to sub clone the LDLr into a suitable expression vector and to mutate the LDLr from wild-type to the internalisation defective mutants, 792-LDLr or JD-LDLr (discussed in Chapter 3). These mutant receptors have been shown to be shed more efficiently than the wild-type receptor and were of interest as these mutations occur in some Familial Hypercholesterolemia cases. An initial approach in this thesis was to construct a green fluorescent protein (GFP)-tagged LDLr to assess soluble LDLr levels released into medium of cultured cells (discussed in Chapter 4). A proteomics study implicated as a TACE candidate sheddase of the LDLr (Guo et al., 2002). To determine the extent of TACE involvement as well as the possible role of other sheddases in the release of the ectodomain of the LDLr, the shedding profiles of the LDLr constructs were investigated in wild-type and TACE deficient mouse fibroblasts and wild-type and TACE deficient CHO cells (discussed in Chapter 5). In addition, LDLr shedding was assessed in the presence of a phorbol and TAPI to assess stimulated shedding and the inhibition of shedding in the absence and presence of TACE. Lastly, it was of interest to establish whether soluble LDLr was present in human plasma to show a physiological relevance of LDLr ectodomain release (discussed in Chapter 6).

Chapter 2:

Materials and Methods

2.1. Materials

2.1.1 General

The vector, pcDNA3.1 (H)- was purchased from Invitrogen. The hrGFP Vitality™ vector was obtained from Stratagene Vitality™. The pLDLr-2 vector was obtained from M. Begg (Yamamoto et al., 1984; Begg et al., 2004). Primers were purchased from Integrated DNA Technologies through Whitehead Scientific or from Inqaba Biotech Biotechnical Industries, South Africa. Pimer sequences for the GFP constructs are shown in Appendix I [Fig. I.]. Primer sequences for the site-directed mutagenesis reactions are shown in Appendix I [Fig. II.]. The restriction enzymes *Xba* I, *Hind* III, *Not* I, *Cla* I, *Bgl* II, *Kpn* I, *Bam* HI, *Eco* RI, *Nhe* I, *Aat* II, *Eco* RV, *Sma* I and the appropriate buffers were purchased from Roche. The restriction enzyme *Bfi* I and buffer were purchased from Fermentas Life Sciences. The *Pfu* polymerase, dNTP mix, and *Dpn* I and T4 DNA ligase were purchased from Promega. The transfection kit Profection® Mammalian Transfection System was purchased from Promega. Hygromycin was purchased from Sigma Aldrich Company Inc.

2.1.2 Cell lines

The wild-type and TACE KO mouse fibroblasts were obtained from R. A. Black (Amgen, USA). The CHO A7 cells were obtained from M. J. Begg (Begg et al., 2004). The CHO M2 cells were obtained from J. Arribas (Borroto et al., 2003).

Table 2.1: Table depicting the different properties of the cell lines used in this study

Cell line	Property	
	Endogenous LDLr expression	Active TACE
Wild-type mouse fibroblasts	yes	yes
TACE-/- mouse fibroblasts	yes	no
CHO A7	no	yes
CHO M2	yes	no

2.1.3 Antibodies

The rabbit polyclonal LDLr antibody (Research Diagnostics, Inc.), the goat polyclonal LDLr antibody (R & D systems), the mouse monoclonal LDLr (C7) antibody (Research Diagnostics, Inc.), the polyclonal hrGFP Vitality™ antibody (Stratagene), the anti-TACE IgG (Abcam), the anti-ADAM 9 IgG (Oncogene, Calbiochem), the ADAM 10 IgG (Oncogene, Calbiochem), the anti-rabbit IgG (Amersham Biosciences, Sweden), the anti-goat IgG (R & D systems), and the anti-mouse IgG (Amersham Biosciences, Sweden), were all purchased from the companies indicated in parenthesis.

2.2 Methods

2.2.1 Recombinant deoxyribonucleic acid (DNA) technology

2.2.1.1 Polymerase chain reaction (PCR)

PCR was performed with 1.5 units of *pfu* polymerase (Promega), 500 ng of DNA template, 0.8 µg of each primer, 200 µM dNTP mix (Promega), 1 X *pfu* buffer and water up to a final volume of 50 µl. The following parameters for PCR reactions were used: DNA was denatured at 94°C for 4 minutes for 1 cycle. This was followed by 30 cycles of amplification with a denaturing step of 1 minute at 92°C, annealing for 2 minutes at the annealing temperature, and an elongation at 72°C for 2 minutes. A final elongation for 1

cycle was carried out at 72°C for 5 minutes. The reaction was held at 4°C overnight. All the preparations for the amplifications including the addition of polymerase were done on ice and reactions were performed in the Hybaid DNASprint PCR apparatus. A 10 µl aliquot of the reaction was analysed by the addition of 1 µl of 6 X loading dye (Appendix II) and separation of products on 0.8 % (w/v) agarose or poly-acrylamide gel electrophoresis (PAGE)(12 % gel).

2.2.1.2 Agarose Gels

0.8 % (w/v) Agarose in 1X TBE (89 mM Tris base, 89 mM boric acid, 2 mM EDTA) containing ethidium bromide (0.2 mg/ml). Electrophoresis was performed at 70 volts for approximately 1 hour in 1 X TBE buffer with 0.2 mg/ml ethidium bromide. DNA bands in agarose gels were visualised by exposure to ultra violet at 260 nm and photographed.

2.2.1.3 PAGE gels

DNA was separated on PAGE (12 % gel) made up with 1 X TBE, 0.001 % ammonium persulphate (AMPS) and 10 µl Tetramethylethylenediamine (TEMED). Electrophoresis was performed at 50 volts. To visualise the DNA, gels were stained by silver staining in 0.1 % $AgNO_3$ for 10 min, followed by fixing and developing in 1.5 % NaOH and 1.5 % formaldehyde.

2.2.1.4 Restriction Enzyme Digests

The enzymes were used with compatible buffers. 10 units each of restriction enzyme, 0.5 -1 µg DNA, 2 µl buffer and sterile water up to a final volume of 20 µl were used per reaction. All the preparations, including the addition of enzymes were done on ice. All digests were incubated at 37°C for 2 hours, except for *Sma* I, which was incubated at

25°C for 1 hour, before the addition of the second enzyme and digested further for an hour. All reactions were stopped with the addition of 6 X loading dye except for *Bfi* I, where reaction was stopped with the company supplied loading dye and inactivation at 65°C for 10 minutes.

2.2.1.5 Site Directed Mutagenesis

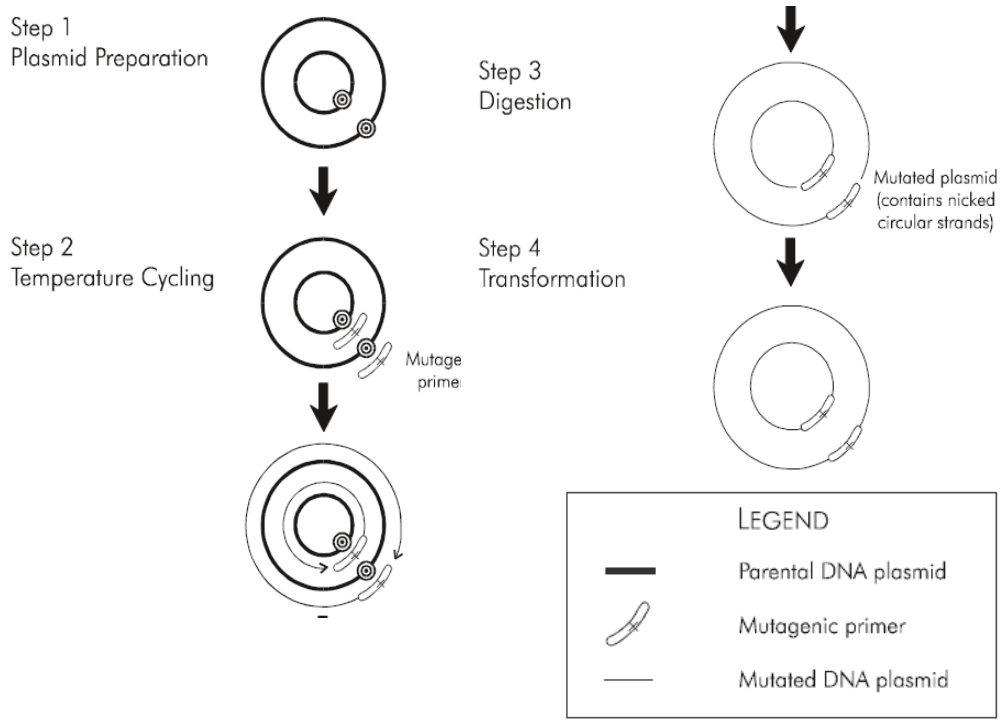

Figure 2.1: Schematic diagram representing the *Dpn* I site-directed mutagenesis approach, taken from Stratagene Quickchange™.
Step 1: Plasmid with gene of interest to be mutated.
Step 2: The plasmid is denatured and annealed with mutagenic primer containing mutation. *Pfu* DNA polymerase extends the sequence, resulting in in nicked circular strands.
Step 3: The methylated non-mutated DNA is digested with *Dpn* I.
Step 4: The DNA is transformed and *E.coli* repairs the nicks in the mutated plasmid.

The site-directed mutagenesis was adapted from the Stratagene Quickchange™ method (Fig. 2.1). Briefly, this method entails designing a set of primers that are complementary

to the sense and anti-sense of the template DNA strands and that have the mutation of interest as well as a silent mutation to introduce a restriction enzyme site [Appendix I, Fig. II.]. The restriction enzyme site was introduced so that clones could be screened for the presence of the mutation. After the mutagenesis reaction, the PCR product was digested with *Dpn* I to remove non-mutated parental DNA. The reaction was transformed into competent *E.coli* JM109 cells.

PCR was performed with 1.5 units of *Pfu* polymerase (Promega), 50 ng of DNA template, 0.8 µM of each primer, 400 µM dNTP mix (Promega), 1/10 volume of buffer (final 1 X) and water up to a final volume of 50 µl was used for the mutagenic reaction. The following parameters for PCR reactions were used: The DNA was denatured at 94°C for 5 minutes for 1 cycle. This was followed by 16 cycles of amplification with a denaturing step of 30 seconds at 92°C, annealing for 30 seconds at the annealing temperature, and an elongation step at 72°C for 16 minutes. The elongation step was 2 minutes per kilo base pairs (kbp) of DNA. A final elongation of 1 cycle long was carried out at 72°C for 20 minutes. The reaction was held at 4°C, overnight. All the preparations for the amplifications were done on ice and reactions were performed in a Hybaid DNASprint PCR apparatus. The non-mutated, template DNA was removed by digestion with *Dpn* I, for 2hrs at 37 °C. A 10 µl aliquot of the reaction was analysed by the addition of 1 µl of 6 X loading dye and separation of products on 0.8 % agarose gels.

2.2.1.6 DNA purification from agarose gels

DNA was excised from 0.8 % (w/v) agarose gels using sterile scalpel blades and was purified according to the Wizard® SV gel and PCR Clean-Up System (Promega) according to manufacturer's instructions.

2.2.1.7 DNA purification from PAGE

The desired DNA fragment was eluted in 60 µl TE (1 mM EDTA, 10 mM Trizma) at 4 ˚C, overnight.

2.2.1.8 DNA Ligation

For ligations, 10:1 pmole insert to vector ratio, 2 units of T4 DNA ligase (Promega) and 1 X ligation buffer (Promega) in a final volume of water up to 20 µl was used. The ligation reaction was incubated at 22℃ overnight and 10 µl of the reaction was used for transformation.

2.2.1.9 Production of competent *Escherichia coli* (*E. coli*)

The rubidium chloride method of making competent cells was used. *E.coli*, JM109 or DH5α were grown overnight in 5 ml Luria Broth (LB) (Appendix II). This was used as a starter culture to inoculate 100 ml LB. When an OD_{530} of approximately 0.35 was reached, the culture was poured into 2 x SS34 tubes and was placed on ice for 15 minutes. The cells were pelleted in a Beckman J2-21centrifuge at 4 000 x g for 5 minutes. The supernatant was poured off and the cells were resuspended in 10.5 ml ice-cold TFB-I (100mM RbCl, 50 mM $MnCl_2$, 30 mM potassium acetate, 10 mM $CaCl_2$, 15 % glycerol) per tube. The contents of each tube were pooled and incubated on ice for 90 minutes. Cells were centrifuged for 5 minutes under the same conditions as described earlier. The pelleted cells were resuspended in 3.5 ml TFB-II (10 mM MOPS pH 7.0, 10 mM RbCl, 75 mM $CaCl_2$, 15 % glycerol). The cell solution was divided into 100 µl aliquots and flash frozen in liquid nitrogen. The competent cells were stored at -70°C.

2.2.1.10 Transformation of DNA

Competent cells were removed from -70°C and thawed on ice for 5 minutes. The cells were transferred to sterile polypropylene tubes and plasmid DNA was added to the tubes and left on ice for 20 minutes. The cells were then subjected to heat shock at 42°C for 45 seconds and placed on ice for 2 minutes. The cells were incubated for an hour at 37°C with shaking, after the addition of 900 µl LB. The cells were centrifuged for 2 minutes at 11 000 x g. After removal of 900 µl of the supernatant, the cells were resuspended in 100 µl LB. The cells were plated out on Luria Agar (LA, Appendix II) plates containing 100 µg/ml Ampicillin. The plates were incubated at 37°C overnight.

2.2.1.11 DNA extraction from *E. coli*

2.2.1.11.1 Phenol-based quick small scale plasmid preparation

Bacterial colonies were picked and grown, shaking overnight at 37°C in 5 ml LB supplemented with 100 µg/ml ampicillin. A 1.5 ml aliquot was centrifuged at 11 000 x g for 2 minutes and the pellet was resuspended in 50 µl 1 X TE, pH 8. To the resuspended mixture, 100 µl of TE-buffered phenol and 100 µl of a mixture of isoamyl alcohol/chloroform (24:1) was added. The cells were shaken for 3 minutes at room temperature, and centrifuged at 11 000 x g for 3 minutes. The aqueous phase ~50 µl was removed and the DNA was precipitated for 30 minutes at -70°C, by the addition of 18 µl of 7.5 M Na Acetate and 140 µl of cold absolute ethanol. The precipitated DNA was centrifuged at 11 000 x g for 10 minutes. The pellets were washed with 70 % ethanol and resuspended in 25 µl TE and 1 µl RNase.

2.2.1.11.2 Large-scale plasmid preparation

Large-scale plasmid preparations were performed using the protocol supplied by the manufacturer Qiagen (GmbH, Germany). The large-scale plasmid isolation procedure was used to make stocks of the DNA. The DNA, precipitated by ethanol, was air-dried for 5 minutes and was resuspended in appropriate volumes of sterile nuclease-free water (Promega) and stored at 4°C or -20°C.

2.2.1.12 DNA quantification

For large scale plasmid preparations, DNA was diluted 1:100 and the concentration was determined using the absorbance measured at 260 and 280 nm. For the quantification of digested and purified DNA, 1 µl of the DNA sample was loaded onto an agarose gel and the quantity of the DNA was estimated by comparing it to the 500 bp band (representing 150 ng/5 µl loaded) of the 100 bp DNA ladder (Promega).

2.2.1.13 DNA sequencing

All the PCR products were sequenced for verification of correct sequence in the assembly of constructs, or for the introduction of the relevant mutations during site-directed mutagenesis. Constructs were sequenced in both directions by the DNA Sequencing Service, in the Department of Molecular and Cell Biology, University of Cape Town.

2.2.2 Cell Culture

2.2.2.1 Maintenance of cell cultures

All the tissue culture cells were grown and maintained in a humidified incubator in 5 % CO_2 at 37℃. Mouse fibroblasts and CHO A7 cell were maintained in complete growth medium [Dulbecco's modified Eagle's medium (DMEM)/Ham's F-12 supplemented with 20 mM 4-(2-hydroxyethyl)-1-piperazineethanesulfonic acid (Hepes), pH 7.5, 10 % foetal calf serum (FCS) and 10 U/ml Penicillin-10 µg/ml Streptomycin]. All growth medium that included FCS, contained FCS that was heat inactivated at 56℃ for 30 min. The CHO M2 cell line was maintained in DMEM growth medium (supplemented with 20 mM Hepes, pH 7.5 and 10 % FCS and10 U/ml Penicillin-10 µg/ml Streptomycin).
Cells were thawed quickly to inoculate a flask that contained 10 ml growth medium containing 30 % FCS. The medium was left on overnight and replaced with complete growth medium containing 10 % FCS the following day.

Medium was removed after every 2-3 days and was replaced with fresh medium till confluent. To split the cells, the medium was removed and 5 ml of trypsin-EDTA [0.5 % trypsin in phosphate buffered saline (PBS), Appendix II] was added to the cells, and incubated at 37°C for 2-3 minutes. The cells were removed from the flask and transferred into a 10 ml tube. The tube was centrifuged for 30 seconds at 2 000 x g. The supernatant was discarded and the remaining pellet was resuspended in 2 ml complete medium, and was used to inoculate flasks.

To freeze cell cultures, cells were trypsinzed and lifted as for splitting. The cells were resuspended in 2 ml 10 % Dimethyl sulfoxide (DMSO) in heat inactivated FCS and left

on ice for 20 minutes. Cells were divided into 500 µl aliquots and stored overnight at -70°C and transferred to liquid nitrogen for storage.

2.2.2.2 Transfections

All cell lines were transfected with 10-12 µg of plasmid DNA according to the Calcium Phosphate, Profection® Mammalian Transfection System protocol (Promega). The day after transfection, the medium was replaced with 400µg/ml Hygromycin-supplemented medium to select for positive colonies, and incubated until separate clones were visible. Colonies were picked using sterile swabs dipped in trypsin-EDTA, and seeded into 12 well plates. Stable clones were assessed for LDLr expression by Western blot. For transient transfections cells were transfected with 3 µg DNA in a 6 well plate. The day after transfection, cells were harvested and analysed by Western blot or analysed by fluorescent microscopy.

2.2.2.3 Fixing of cells

Cells were grown on cover slips overnight in complete growth medium, supplemented with 10 % FCS. Medium was aspirated from the cells. 500 µl of 4 % paraformaldehyde (PFA) in,250 mM Hepes, pH 7.5 was added, and incubated at room temperature for 20 minutes. The PFA was removed and the cells were washed thrice with PBS. The final PBS wash was not removed until the cover slips were placed onto slides which had a drop of MOWIOL (Aldrich) on it. The slides were left to dry for 30 minutes at room temperature. The slides were visualized under a fluorescent microscope immediately.

2.2.2.4 Fluorescent microscopy

Untransfected and GFP-transfected cells were grown on coverslips overnight in complete growth medium containing 10 % FCS and either visualized under a fluorescent microscope fitted with a GFP filter which measures the excitation wavelength between 395-440 nm (Zeiss microscope), or fixed and then visualised under the fluorescent microscope.

2.2.2.5 Shedding assay

LDLr expressing cells were plated into 6 well plates in complete growth medium containing 10 % FCS, to grow to 90 % confluency overnight. Cells were washed with PBS and medium was replaced with 1 ml Optimem (Gibco BRL Life Technologies, Inc) in the presence or absence of 1 μM phorbol 12,13-dibutyrate (PDBu) and / or 10 μM TAPI (Peptides International). Medium and cells were collected after 4 hours.

2.2.2.6 Harvesting of Cells

The medium was removed and centrifuged for 10 minutes at 11 000 x g to pellet any floating cells. The cells were scraped off on ice, in 1 ml PBS. A second ml of PBS was added to the cells in order to scrape off the remainder. The tubes were centrifuged on a bench top microcentrifuge at 11 000 x g for 2 minutes. The supernatant was discarded and the pellet was resuspended in 100 μl Triton Lysis Buffer [1 % Triton X-100, 50 mM Hepes pH 7.5, 0.5 M NaCl, 1 mM phenylmethylsulphonyl fluoride (PMSF)]. This was incubated on ice for 20 minutes after which the tubes were centrifuged for 10 minutes at 11000 x g. The harvested cells were either used immediately or stored at -20°C until needed. Medium samples were either concentrated 10-fold immediately; using Microcon

Ultracel® YM-30 centrifuge tubes (Millipore™), or stored at -20℃ and concentrated prior to loading on sodium dodecyl sulphate (SDS)-PAGE.

2.2.3 Protein Analysis

2.2.3.1 Protein quantification

The Bradford method was used to determine protein concentration (Bradford, 1976). Protein samples were diluted up to 800 µl in water and 200 µl of Bradford reagent (Bio-Rad) was added, mixed and incubated for 5 min at 22℃. The reaction was zeroed against a blank sample and read at 595 nm. Protein samples were quantified using the slope of an IgG or albumin standard curve, where applicable.

2.2.3.2 SDS-PAGE gels

SDS-PAGE gels were cast and run in a Bio-Rad PROTEAN® II gel apparatus (Laemmli, 1970). Protein samples (20 µl) were prepared by adding 5 µl 5 X SDS sample buffer (62.5 mM Tris-HCl pH 6.8, 2 % SDS, 10 % glycerol, 0.001 % Bromophenol Blue) for non-reducing conditions. For shedding experiments, equal amounts of cell lysate (~40 µg) and an equal volume of medium was used. When required, protein samples were reduced with 5 X SDS sample buffer containing 5 % β-mercaptoethanol (β-ME), and boiled for 5 min.

Protein samples were separated on SDS PAGE (7 % gel), containing running gel buffer (0.375 M Tris pH 8.8, 0.1 % SDS), 0.1 % AMPS and 7 µl TEMED made up to 10 ml with water. The 3 % stacking gel was made up of stacking gel buffer (0.125 M Tris pH 6.8, 0.1 % SDS), 0.3 % AMPS and 20 µl TEMED. The gels were run in 1 X Running Buffer (0.025 M Tris pH 8.3, 0.192 M Glycine, 0.1 % SDS) at 50 mAmp. 5 µl Prestained marker (Bio-Rad) was used.

2.2.3.3 Gradient gels

A gradient mixer that had 20 % acrylamide gel solution in the right chamber and 5 % acrylamide gel solution in the left chamber was used to mix and pour a 5-20 % gel in a gel casting apparatus. After the resolving gel was set, the stacking gel was poured and the combs were placed for well formation. For the non-denaturing PAGE, SDS was not added to protein samples and gel buffers.

2.2.3.4 Coomassie Staining of SDS gels

SDS gels were stained for a minimum of 45 minutes to 16 hours in Coomassie staining solution [50 % (v/v) methanol, 10 % (v/v) acetic acid, 0.25 % (w/v) Coomassie brilliant blue] and destained in destaining solution [25 % (v/v) ethanol, 10 % (v/v) acetic acid] until bands became prominent and the background became clear.

2.2.3.5 Western Blotting

The gels were soaked in blotting buffer (25 mM Tris pH 8.2, 200 mM Glycine, 20 % (v/v) methanol) for 10 minutes and assembled in the blotting apparatus (Bio-Rad) with the gel and the nitrocellulose membrane (Hybond-C, Amersham Biosciences) being placed into a cassette. The proteins were transferred for an hour at 100 volts, in a cooled system.

2.2.3.5.1 Probing nitrocellulose membranes with antibodies

2.2.3.5.1.1 Probing nitrocellulose membranes with LDLr antibodies

With the membrane facing protein side up, the membrane was blocked overnight in a 5 % (w/v) skimmed milk in Tris-buffered Saline-Tween (TBS-T) (0.05 M Tris pH 7.4, 0.2 M NaCl, 0.1 % Tween-20). The membrane was rinsed thrice with TBS-T. The membrane

was incubated with primary antibody at a dilution of 1:500 in 5 % (w/v) skimmed milk in TBS-T, to bind for an hour, shaking at room temperature. The antibody solution was decanted and washed with TBS-T, once for 15 minutes and thrice for 5 minutes. A 1:1000 dilution of secondary anti-rabbit/anti-goat antibody conjugated to horse radish peroxidase (HRP) (Amersham Biosciences, Sweden) in 5 % (w/v) skimmed milk in TBS-T was incubated for an hour, shaking at room temperature. The membrane was washed as before and detected in the dark room using equal amounts of detection reagents 1 and 2 (ECL Plus™ Western Blotting Detection kit, Amersham Biosciences, Sweden). This solution was left on for 1 minute and placed in cling wrap with the protein side up, exposed in the dark, to X-ray Hyperfilm™ ECL photographic film (Amersham Biosciences, Sweden) for the required time. The X-ray film was developed by placing the film in developer for 1 minute and rinsing in water. The film was then placed into fixer for a minute after which it was rinsed in water and left to dry.

2.2.3.5.1.2 Probing nitrocellulose membranes with ADAM antibodies

The same procedure was followed as for the LDLr antibodies, except for the following changes: For the primary antibody incubation of TACE, ADAM 9 and ADAM 10 antibodies, overnight incubation at 4℃ was performed. Antibody dilution of 1:500 was used for TACE and, 1:1000 were used for ADAM 9 and 10, respectively. The dilutions of primary antibodies were made in 2.5 % (w/v) skimmed milk in TBS-T. The secondary antibodies were incubated in 5 % (w/v) skimmed milk in TBS-T for an hour, shaking at room temperature.

2.2.3.6 Densitometry

Blots were scanned using GeneSnap (Vacutec) and analysed with GeneTools software to quantify protein bands.

2.2.3.7 Cross-linking of intact cells

Cells were plated out into 6 well plates and grown overnight. Medium was removed from cells and cells were washed 3 times with 1 ml PBS (pH 8.0). A final concentration of 1 mM Bis Sulfosuccinimidyl suberate (BS^3) (Pierce Biotechnology) was added and incubated at 4℃ for 30 minutes. A quenching solution (10 mM Tris) was added for 15 minutes at 22℃. Cells were harvested as described before.

2.2.3.8 Continuous fluorogenic peptide assays

1 μM TNF-α stalk substrate, 1.2 ml 2 X buffer (100 mM Tris-Cl pH7.4, 50 mM NaCl, 8 % glycerol) and water to a final volume of 2.5 ml was combined. Cell lysate (100 μg) was added after 5 minutes once a stable fluorescent reading was obtained. The stirred reaction was incubated at 37℃ and fluorescence was measured continuously at an excitation wavelength of 320 nm and emission wavelength of 420 nm on the Cary Eclipse (Varian) fluorimeter for 90 minutes.

2.2.4 Plasma studies

2.2.4.1 Collection of plasma

Informed consent was obtained from individuals who donated blood. Fasting blood was collected in EDTA tubes and centrifuged immediately for 15 minutes at 5 000 x g at 4°C. Plasma was carefully removed. Plasma samples were pooled and final concentrations of 1 mM PMSF, 1 mM Hepes, pH 7.4 and 5mM $CaCl_2$ were added to plasma. A 1:100

dilution of a cocktail mix of protease inhibitors (Calbiochem) was also added. Plasma samples were either used immediately or stored at -70°C.

2.2.4.2 Lectin Affinity purification

200 µl of lentil lectin Sepharose beads (Amersham Biosciences, Sweden) were washed 5 times with 1ml wash buffer/binding buffer [20 mM Tris-Cl pH 7.4, 0.5 NaCl] by centrifugation for 30 seconds at 11 000 x g, and removing the supernatant. An equal volume of binding buffer was added to the plasma sample, and 1ml of this was incubated for half an hour at a time. The incubation and washing steps were carried out on ice, with constant shaking. The lentil lectin Sepharose beads were washed 5 times with 1ml wash buffer, shaking on ice. The proteins were eluted with 100 µl 0.2 or 0.5 M α-D-mannopyranoside. The buffer was exchanged with water and the protein samples were concentrated using microcon (Millipore™) centrifuge tubes.

2.2.4.3 Immunoprecipitation (IP)

Plasma samples were immunoprecipitated according to the ExactaCruz (SantaCruz Biotechnology, Inc.) protocol. Briefly, the protocol entails making an IP-matrix complex for sample incubation. Plasma samples (1 ml) were pre-cleared with 45 µl 50 % protein G slurry, for 2 hours rotating at 4℃. The IP antibody-IP matrix complex was made using 50 µl of IP matrix and incubating it with 2.5 µg C7 anti-LDLr (Research Diagnostics, Inc.) for 2 hours rotating at 4℃. The pelleted IP antibody-IP matrix was washed twice with PBS and 1 ml of pre-cleared plasma sample was added and rotated overnight at 4℃. The precipitate was washed 3 times with PBS, and 40 µl 2 X sample buffer was added and boiled for 5 minutes, prior to loading onto SDS-PAGE (7 % gel).

2.2.4.4 Removal of high abundance proteins from plasma using ProteoMiner protein enrichment kit (Bio-Rad) (Guerrier et al., 2006)

The ProteoMiner protein enrichment (Bio-Rad) protocol was followed. Briefly, the column was prepared by washing with wash buffer. Plasma (1 ml) was added to the column and incubated at room temperature, rotating for 2 hours. After removal of plasma by centrifugation, the column was washed 3 times with 1 ml of wash buffer. Before elution, the column was washed with 1 ml of water. To elute proteins, 100 µl of elution buffer was added to column and incubated rotating at room temperature for 15 minutes. After incubation the column was centrifuged into a new tube. This step was repeated twice and the eluant was pooled. To confirm successful enrichment, fractions were analysed on SDS-PAGE (7 % gel) and stained by Coomassie.

2.2.4.5 One-Step Western™

To reduce non-specific binding of the secondary antibody for some of the plasma experiments, the One-Step Western™ (GenScript) method was used. A mixture-1 was prepared using 12.5 µl (~1.25 µg) of polyclonal anti-LDLr with 50 µl WB-1, and incubated for 40 minutes at room temperature. Pretreat A was mixed with Pretreat B. The membrane was incubated in 5 ml of the Pretreat mixture for 5 minutes, on a shaker. The membrane was rinsed twice in 5 ml 1 X wash solution. Mixture-1 was mixed into 5 ml of WB solution. The membrane was incubated in this mixture for 40 minutes on a shaker, at room temperature. The membrane was rinsed in 1 X wash solution, and then washed with 5ml of wash solution, thrice for 10 minutes, on a shaker. For detection, the membrane was incubated for 1 minute with the LumiSensor™ Chemiluminescent HRP Substrate provided in the kit. The membrane was exposed to X-ray film accordingly. The X-ray film was developed by placing the film in developer for 1 minute and rinsing in water.

The film was then placed into fixer for a minute after which it was rinsed in water and left to dry.

Chapter 3:

Cloning and Mutagenesis of the LDLr

3.1 Introduction

This chapter discusses the sub cloning and site-directed mutagenesis of the LDLr. pLDLr2 encodes the wild-type human LDL receptor (Yamamoto et al., 1984). For mammalian expression, the LDLr sequence was sub cloned into the expression vector pcDNA3.1 (H)-. This vector was chosen since it had compatible restriction enzyme sites as well as for the Hygromycin selection marker that the vector provided for transfected cells, as the mouse fibroblasts used in this project were resistant to Neomycin, a common antibiotic marker found on other mammalian expression vectors.

3.1.1 Construction of the LDLr expression vector

The sub cloning strategy involved the removal of the LDLr insert from pBR322 by *Xba* I and *Sma* I [Fig.3.1 (a).]. The vector pcDNA3.1 (H)-, was digested with *Xba* I and *EcoR* V to create compatible sites for ligation [Fig.3.1 (b).]. Both *Sma* I and *EcoR* V are blunt end cutters and therefore the blunt ends could re-ligate. Upon re-ligation, though, the restriction enzyme site was lost and the presence of the insert was confirmed by digestion with *Xba* I and *Hind* III [Fig.3.1 (c).].

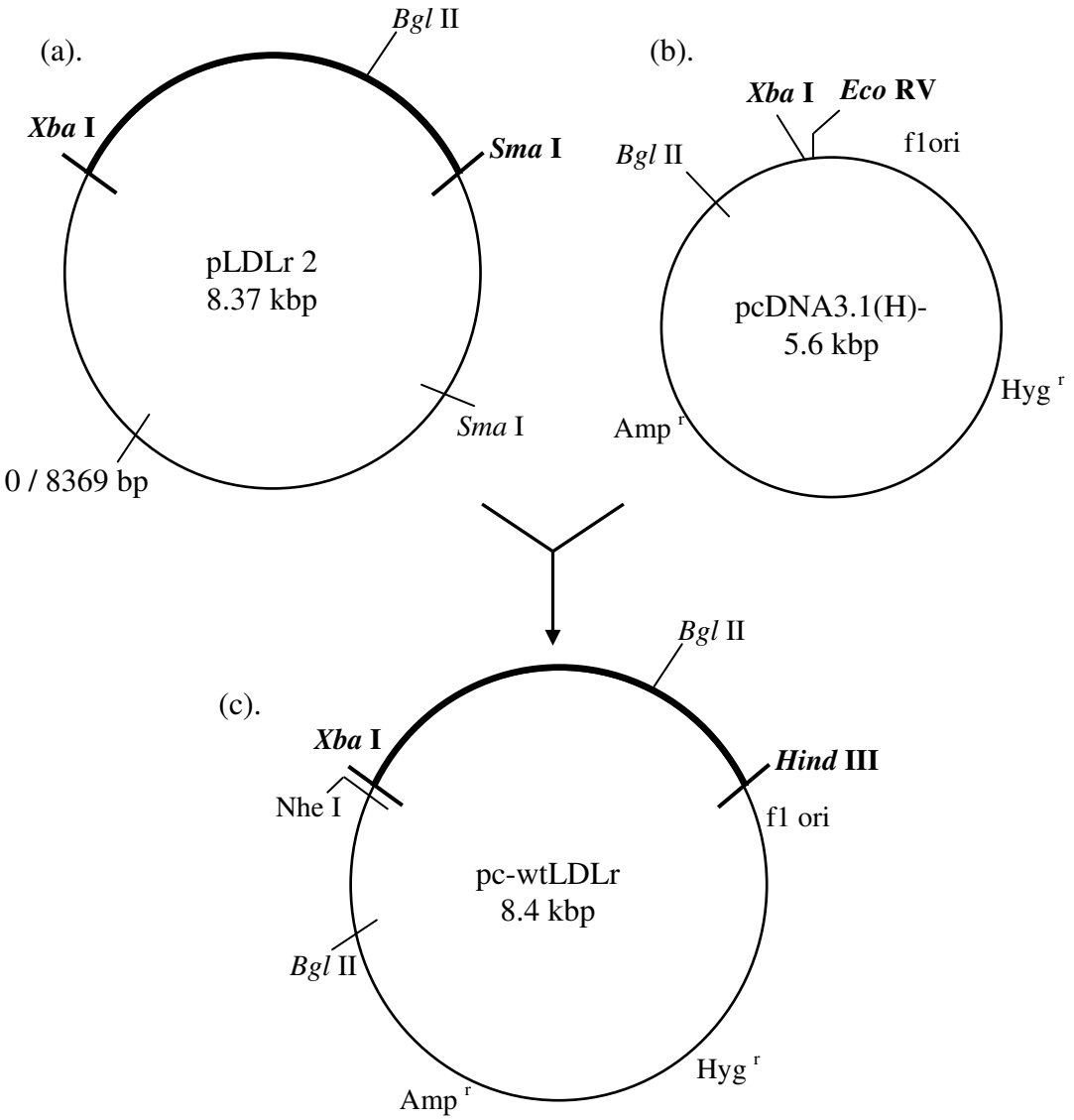

Figure 3.1: A flow diagram depicting the sub cloning pc-wt-LDLr.
The LDLr insert was digested from the original vector with *Xba* I and *Sma* I (a) and sub cloned into pcDNA3.1(H)- (b) to give a final construct called pc-wt-LDLr (c).

3.1.2 Site-directed mutagenesis of the LDLr

The LDLr was mutated to either the 792-LDLr or the JD-LDLr (Fig 3.2). These mutations occur in some patients presenting with FH and they have been shown in a previous study to be of interest since they are shed more efficiently than the wild-type counterpart (Begg et al., 2004). Both receptors are internalisation defective in that the

792 construct has a premature stop codon at position 792, resulting in a truncated receptor with a shortened cytoplasmic tail (Lehrman et al., 1985; Davis et al., 1986), while the JD construct is a full length construct with a tyrosine to cysteine substitution at position 807, hence disrupting the internalisation signal (Davis et al., 1986).

Figure 3.2: Schematic representation of the LDLr constructs (adapted from Begg et al., 2004).
The wt-LDLr was mutated to either the 792-LDLr, containing a stop codon at position 792, or the JD-LDLr, containing a cysteine (Cys) residue in place of tyrosine (Tyr) at position 807.

The site-directed mutagenesis was adapted from the Stratagene Quickchange™ method. For the 792-LDLr construct, the primer contained a silent mutation that created an *Aat* II site (Appendix I, Fig. II.). For the JD-LDLr construct, the primer contained a silent mutation that created a *Bfi* I site (Appendix I, Fig. II.). The restriction enzyme site was introduced so that clones could be screened for the presence of the mutation. After the mutagenesis reaction, the PCR product was digested with *Dpn* I. The reaction was

transformed into competent *E.coli* JM109 cells. Bacterial colonies were picked and screened for the presence of the mutation by restriction enzyme digestion. The DNA was sequenced to confirm presence of introduction of relevant mutations.

3.2 Results

3.2.1 Sub cloning of the LDLr into pcDNA3.1(H)-

The LDLr was sub cloned from pLDLR2 (Yamamoto et al., 1984; Begg et al., 2004). The LDLr sequence was digested and ligated into pcDNA3.1(H)-. The ligation reaction was transformed into competent *E.coli* JM109 cells. Ampicillin resistant clones were analysed by small scale plasmid preparation and restriction enzyme digests. The identified positive clones were grown and the plasmid DNA was extracted. The DNA was restriction enzyme digested to confirm the correct sequence.

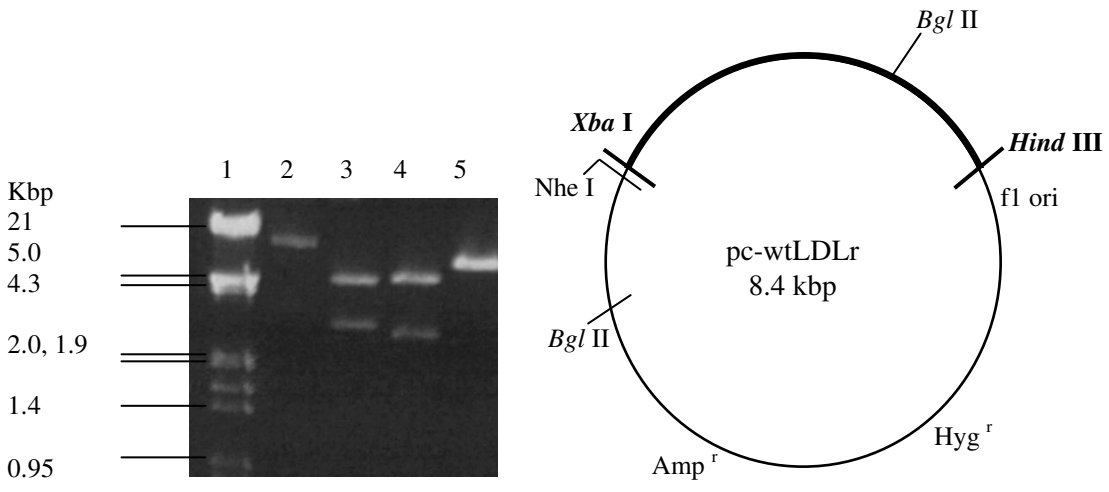

Figure 3.3: Confirmation of pc-wtLDLr by restriction enzyme digest.
Lane 1: λ DNA digested with *EcoR* I and *Hind* III. Lane 2: undigested pc-wt-LDLr. Lane 3: DNA digested with *Xba* I and *Hind* III. Lane 4: DNA digested with *Bgl* II. Lane 5: DNA linearised with *Nhe* I.

In Figure 3.3, lane 2, undigested DNA was loaded as a control. Lane 3 depicted the presence of the 2.8 kbp LDLr insert and the 5.6 kbp pcDNA3.1 (H)- vector. Lane 4 showed the product of a digest with *Bgl* II, which resulted in a 2.7 kbp fragment as well as a 5.7 kbp fragment as a *Bgl* II site occured once in the LDLr insert and once in the vector. Lane 5 showed a Nhe I digest, resulting in an 8.4 kbp linearised plasmid.

3.2.2 Site-directed mutagenesis of the LDLr

Site-directed mutagenesis was used to convert wt-LDLr template into a 792-LDLr or JD-LDLr construct. The PCR product was *Dpn* I digested and transformed into *E.coli*. Ampicillin resistant colonies were subjected to small scale plasmid preparation and these were screened with relevant enzymes for the introduction of silent mutations. The positive clones were sequenced to confirm the introduction of relevant mutations.

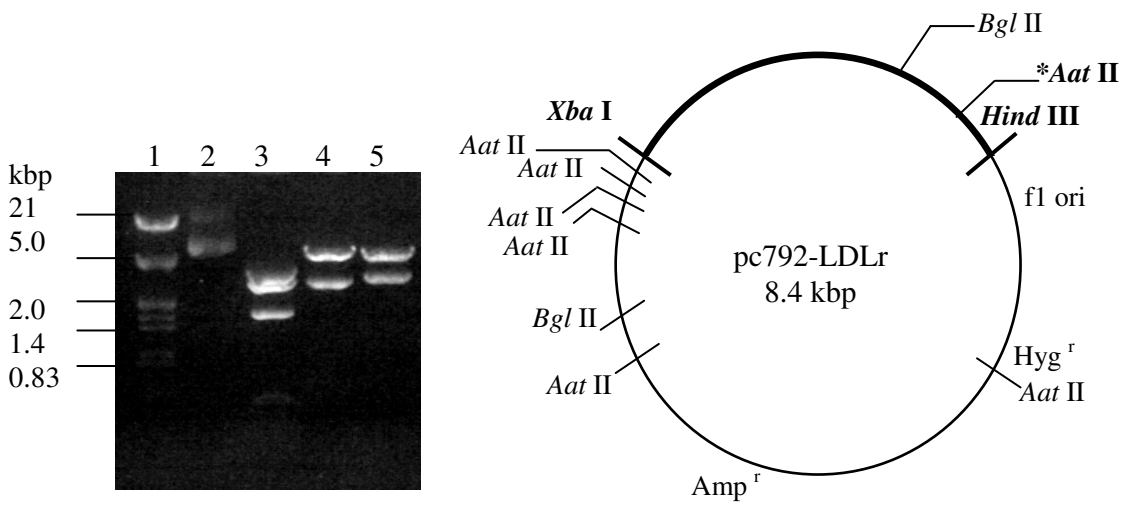

Figure 3.4: Confirmation of pc792-LDLr by restriction enzyme digest.
Lane 1: λ DNA digested with *EcoR* I and *Hind* III. Lane 2: undigested pc792-LDLr. Lane 3: DNA digested with *Aat* II. Lane 4: DNA digested with *Bgl* II. Lane 5: DNA digested with *Xba* I and *Hind* III.

Restriction enzyme digests of the pc792-LDLr were shown in Figure 3.4. In lane 5 a digest with *Xba* I and *Hind* III was seen. These two enzymes were used to confirm the presence of the LDLr insert. The digest released the 792-LDLr insert (2.8 kbp) from the vector (5.6 kbp). In lane 4, the digest with *Bgl* II indicated the formation of two bands, a 2.7 kbp fragment as well as a 5.7 kbp fragment. *Bgl* II cuts once in the LDLr insert and once in the vector. The *Aat* II digest (lane 3) showed bands of 3.45, 2.5, and 1.7 kbp and smaller bands that could not be detected since they were too small. The digest showed that the mutation had been incorporated, since in the absence of the mutation the expected band sizes were 3.45 and 4.27 kbp, while in the presence of the mutation the 4.27 kbp band was split into the 2.5 and 1.7 kbp bands, due to the additional *Aat* II site.

The presence of the mutation was subsequently also confirmed through sequencing.

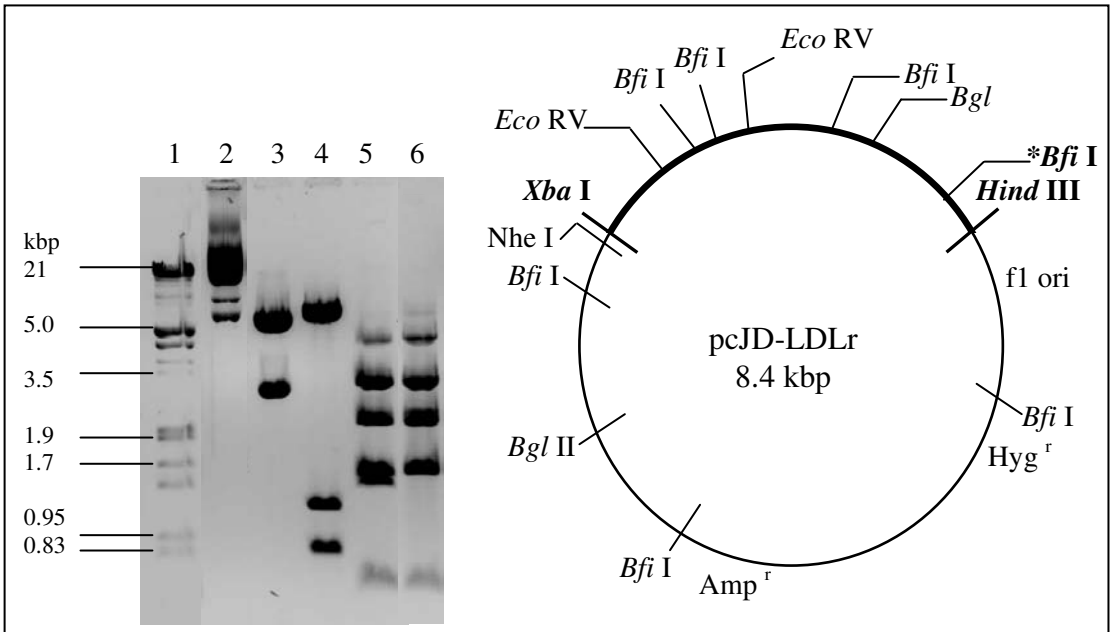

Figure 3.5: Confirmation of pcJD-LDLr by restriction enzyme digest.
Lane 1: λ DNA digested with *EcoR* I and *Hind* III. Lane 2: undigested pcJD-LDLr. Lane 3: DNA digested with *Bgl* II. Lane 4: DNA digested with *Nhe* I and *Eco* RV. Lane 5: DNA digested with *Bfi* I. Lane 6: pc-wt-LDLr digested with *Bfi* I.

Figure 3.5 showed the restriction digest of pcJD-LDLr. Lane 2 showed the undigested forms of the DNA. Lane 3 was digested with *Bgl* II, which released a 2.7 kbp band and a 5.7 kbp band. The digest with *Nhe* I and *Eco* RV displayed bands of 6.5, 1.1 and 0.8 kbp sizes (lane 4). In lane 5 the DNA was digested with *Bfi* I, and bands of 2.7, 2.0, 1.4, 1.2 and 0.6 kbp as well as a band of 4.1 kbp band was seen. The 4.1 kbp band (in lanes 5 and 6) was due to the partial digest as that band was digested further into the 2.7 and 1.4 kbp bands. Lane 6 had pc-wt-LDLr digested with *Bfi* I as a control, to compare to the mutated construct in lane 5, where the appearance of the 1.2 kbp band was seen. There were two 1.4 kbp bands, and the one 1.4 kbp band was split into a 1.2 kbp and 200 bp band if the mutation was present, as seen in lane 5.

In addition, the DNA construct was also sequenced for the introduction of the correct mutation.

3.3 Discussion

The LDLr was subcloned successfully from pLDLr2 into pcDNA3.1 (H)-, as the restriction enzyme digest confirmed the presence of the insert. Additional digests showed bands of expected base pair sizes.

The constructs that were made by site-directed mutagenesis, were analysed by restriction enzyme digests and showed correct banding patterns. In addition, nucleotide sequencing confirmed the presence of desired mutations. All constructs gave bands of calculated size and no additional mutations were introduced during mutagenesis reactions.

Chapter 4:

The use of GFP for the localisation of the LDLr

4.1 Introduction

In order to study LDLr ectodomain release, the receptor was tagged with the GFP to detect LDLr expression and assay ectodomain release. The GFP has been proven to be a useful tool in the visualisation of protein expression, trafficking and interactions between other proteins by means of fluorescent microscopy (Kaether and Gerdes, 1995; Ogawa et al., 1995), fluorescence-activated cell sorting (FACS) (Zeyda et al., 1999), or fluorescent resonance energy transfer (FRET) (Pollok and Heim, 1999). The construct used in this project was a GFP sequence that was codon optimised for human expression, called humanised *Renilla reniformis* (*R. reniformis*) or hrGFP, as it was isolated from the anthazoan *R. reniformis*. The hrGFP is less toxic than the *Aequorea victoria* GFP counterpart, allowing for the establishment of stable cell lines expressing GFP (Kirsch et al., 2003).

The C7 monoclonal antibody to the LDLr binds cellular LDLr in binding studies (Russel et al., 1989) and binds to cell lysate of LDLr expressing cells in a Western blot, under non-reducing conditions (data not shown). The LDLr is a cystein-rich protein and therefore the C7 monoclonal antibody, which is directed to the ligand binding domain, does not recognise the reduced form of the receptor. In addition, the C7 antibody does not recognise the non-reduced soluble LDLr from medium by standard Western blotting conditions. The soluble LDLr was previously detected by [^{35}S] methionine labelling of cells combined with the IP with the C7 antibody and autoradiography (Begg et al., 2004).

Soluble LDLr from medium also bound a C7 antibody column. The C7 antibody seemed to recognise the soluble LDLr during IP, but not in a Western blot after it had been transferred to nitrocellulose. The current theory is that the epitope on the soluble LDLr to the C7 antibody might be masked after transfer. This approach was not used since it required lots of optimisation and it would not have been feasible to assess stable clones expressing LDLr in this way.

The rationale for making a GFP-LDLr fusion protein in this project was that expressing clones transfected with tagged constructs could be visualized easily by fluorescent microscopy. In addition, intracellularly-tagged GFP proteins could be visualised through the secretory pathway (Kaether and Gerdes, 1995) and the GFP-tagged proteins that were secreted into the medium could be assessed by fluorimetry (Wacker et al., 1997). In the case of the LDLr, since it is a membrane protein and subsequently shed, the receptor had to be tagged on the extracellular N-terminus so that soluble LDLr released into the medium could be measured by fluorimetry in a similar way as the approach used for secreted constructs (Wacker et al., 1997).

The first part of this chapter describes the construction of two GFP vectors, both containing signal peptide (SP) sequence at the start of GFP sequence. The second part focuses on the expression of these constructs in mammalian cells.

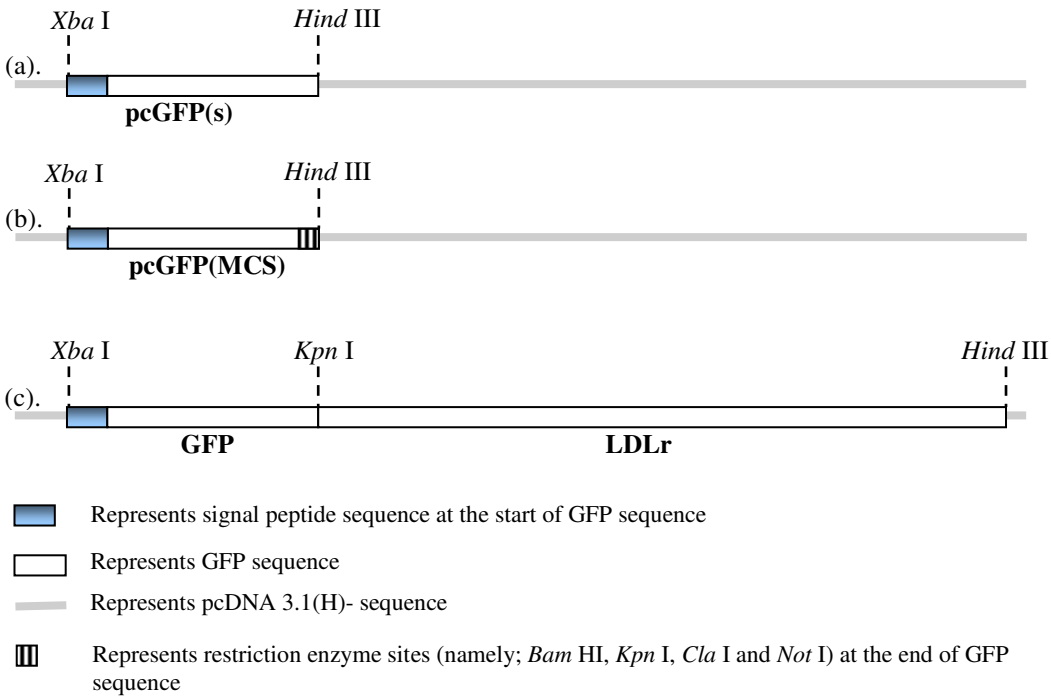

Figure 4.1: A schematic representation of the vector constructs.
(a). pcGFP(s) cloned via *Xba* I and *Hind* III into pcDNA 3.1(H)-. This was used as a control in subsequent experiments. (b). pcGFP(MCS) was cloned via *Xba* I and *Hind* III. (c). The LDLr was cloned into pcGFP(MCS) via *Kpn* I and *Hind* III. This is the experimental vector.

The one GFP vector [named pcGFP(s)] has a stop condon at the end of GFP sequence [Fig. 4.1 (a)], to serve as a control for downstream experiments, while the second GFP vector [named pcGFP(MCS), Fig. 4.1 (b)] has an open reading frame for the introduction the LDLr sequence [Fig. 4.1 (c).].

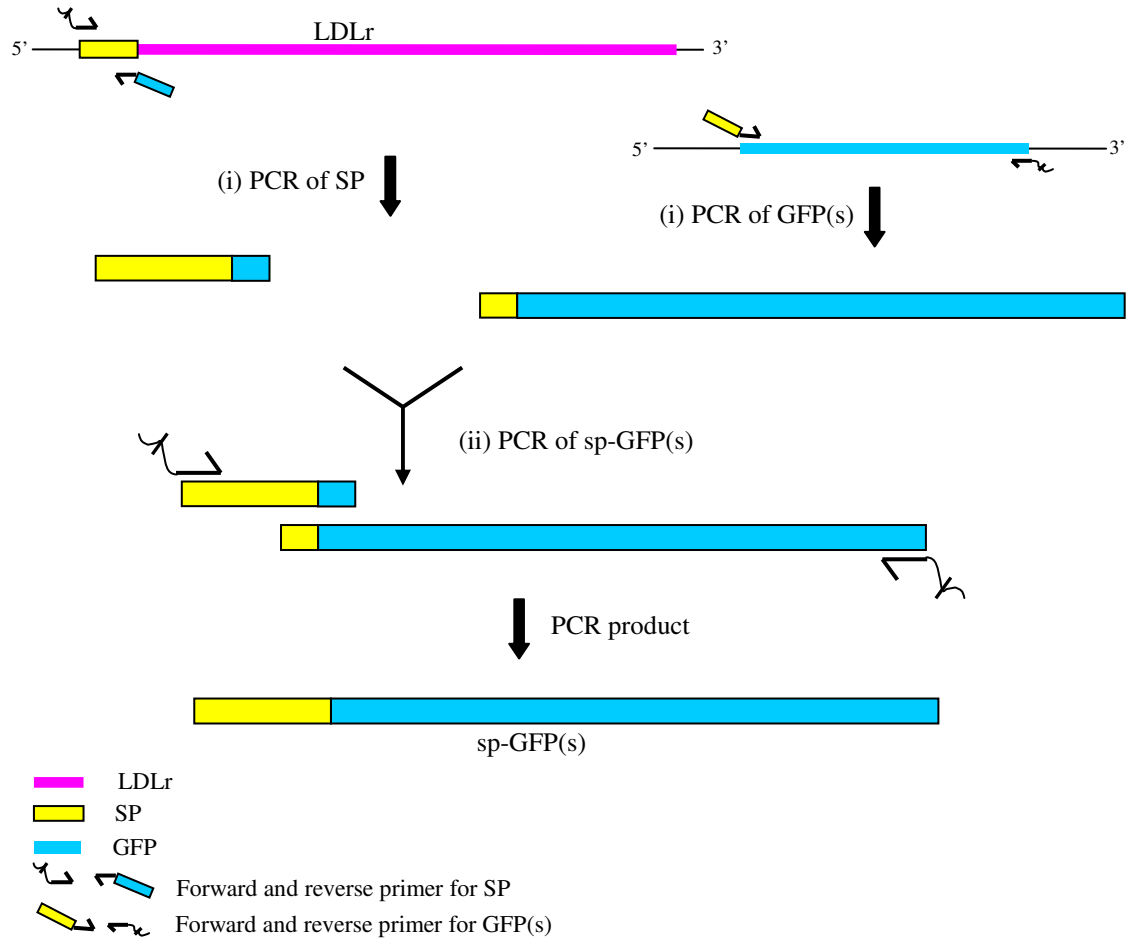

Figure 4.2: Overlap PCR for the construction of sp-GFP(s).
(i). The SP and GFP were amplified and purified. (ii). The PCR products acted as a template for the next PCR, using the two flanking primers, to fuse the two products. **The sp-GFP(MCS) was constructed in the same way.**

The approach used in the construction of GFP vectors included PCR and cloning. For the construction of GFP, the overlap PCR method was used so that the SP of the LDLr could be incorporated into the start of the GFP sequence. This method entails a two step approach: firstly the SP is amplified and the GFP sequence is amplified separately [Fig. 4.2 (i)], followed by a final PCR step that incorporates the SP and GFP sequence [Fig. 4.2 (ii)].

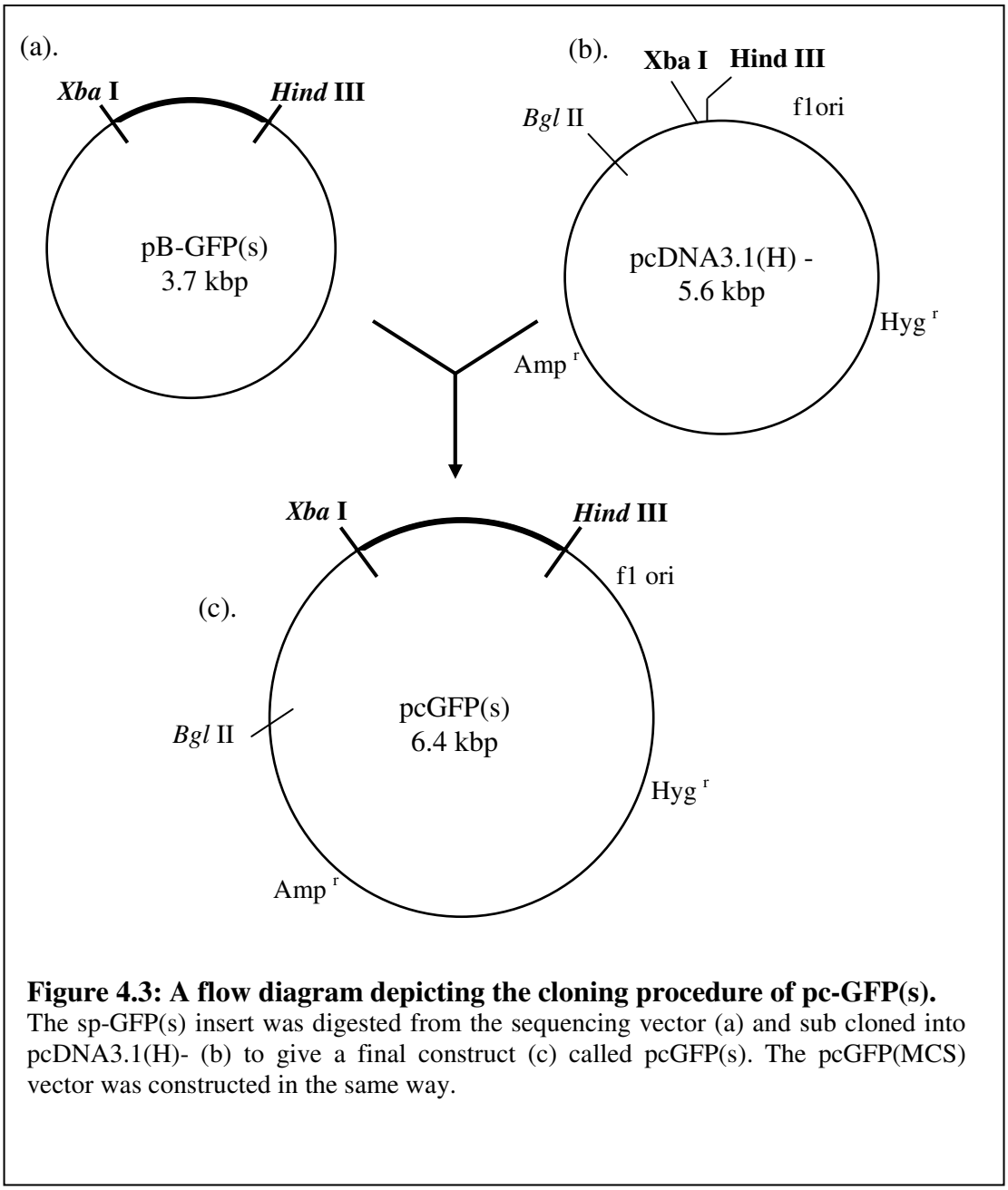

Figure 4.3: A flow diagram depicting the cloning procedure of pc-GFP(s). The sp-GFP(s) insert was digested from the sequencing vector (a) and sub cloned into pcDNA3.1(H)- (b) to give a final construct (c) called pcGFP(s). The pcGFP(MCS) vector was constructed in the same way.

The GFP amplification products were digested, cloned and sequenced in pBS-K [Fig. 4.3 (a).]. When sequencing was confirmed the insert was sub cloned into pcDNA3.1(H)- [Fig. 4.3 (c).].

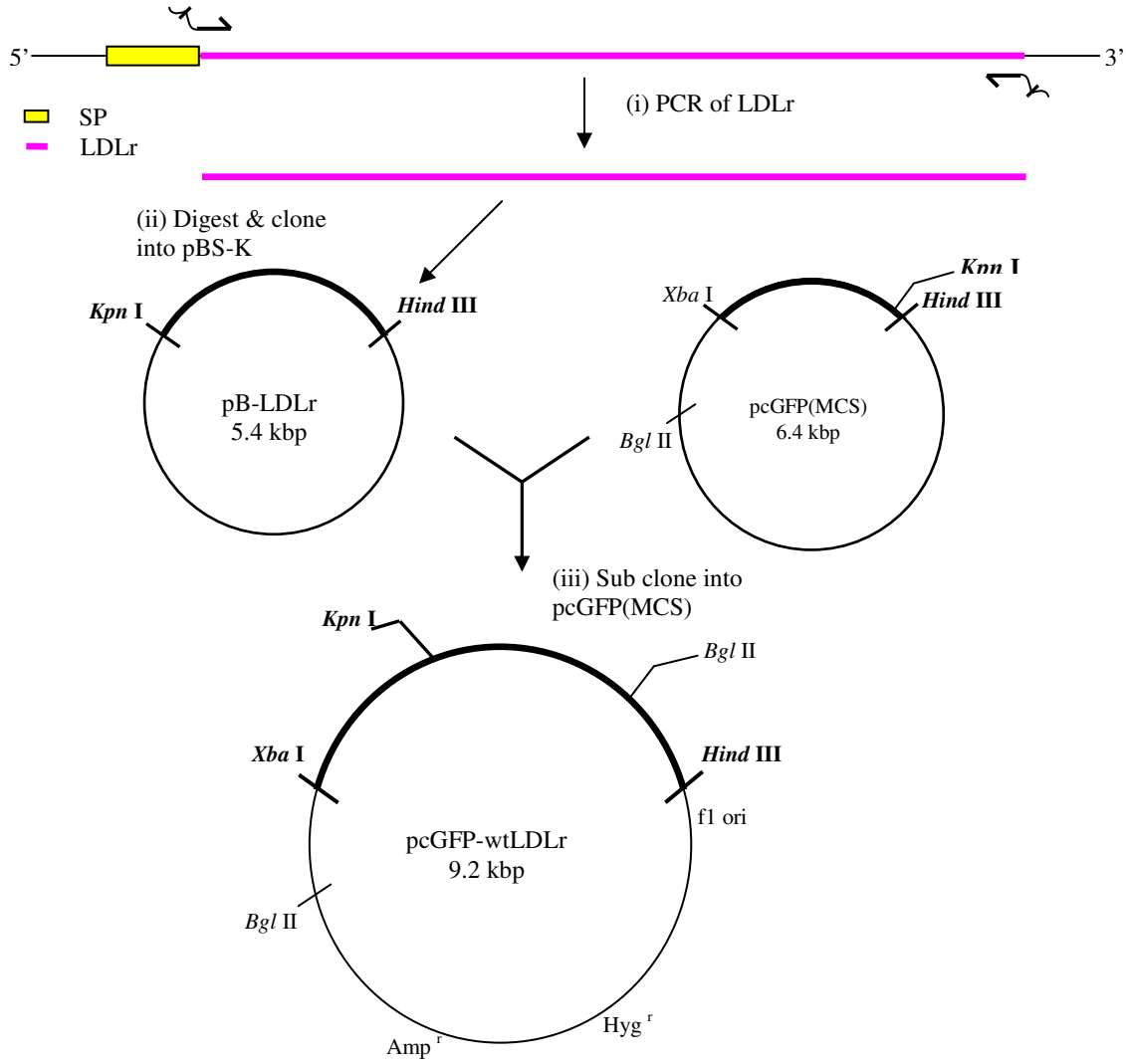

Figure 4.4: A flow diagram depicting the construction of pcGFP-wt-LDLr. (i). The LDLr was amplified. (ii). The PCR product was digested and cloned into pBS-K for sequencing. (iii). On confirmation of the correct sequence, the LDLr was cloned into pcGFP(MCS), via *Kpn* I and *Hind* III.

For the construction of GFP-LDLr, the LDLr was amplified by PCR, digested, gel purified and cloned into pBS-K vector for sequencing and subsequent cloning [Fig. 4.4 (i-ii)]. Due to the large size of the LDLr, it had to be digested into 3 fragments and

cloned into pBS-K, for sequencing. Upon confirmation of correct sequence, the LDLr was sub cloned into the pcGFP(MCS) vector [Fig. 4.4 (iii)], to generate pcGFP-wt-LDLr.

4.2. Results

4.2.1 Cloning of the GFP constructs

Since the LDLr is a transmembrane protein and expressed at the cell surface, it contains a SP sequence at the 5' end (Yamamoto et al., 1984). In the construction of the GFP vectors a SP needed to be incorporated at the 5' end for the correct processing of the translated GFP and GFP fusion protein. The overlap PCR method was used to create a fusion of SP and GFP sequences. The reverse primer of the SP contained GFP sequence at the 3' end. The LDLr sequence which was in pcDNA3.1(H)- was used as template DNA for the amplification of the SP and LDLr sequence. GFP sequence was amplified from the phrGFP vector. Two GFP constructs were made, one containing a stop codon at the end of the GFP sequence [Fig. 4.1 (a).], as a control for further experiments, and a second GFP construct containing an open reading frame and restriction enzyme sequence coding for a multiple cloning site (MCS) [Fig. 4.1 (b).]. The GFP construct containing the stop codon was termed GFP(s), while the GFP containing an open reading frame was termed GFP(MCS).

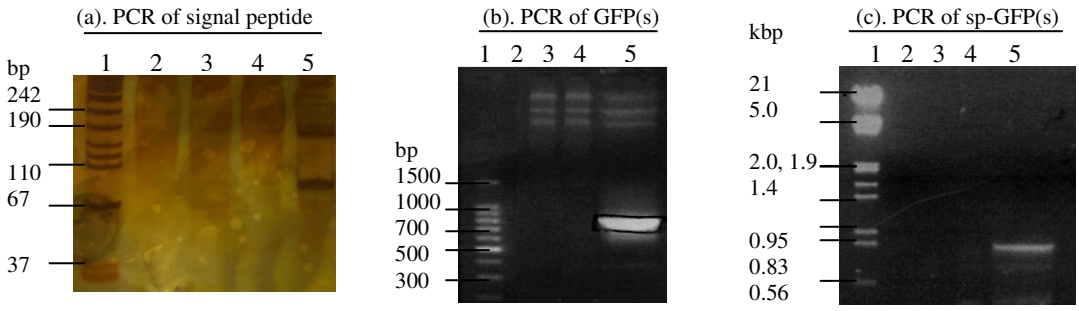

Figure 4.5: Construction of sp-GFP(s).
Lane 1: DNA ladder markers. Lane 2: no DNA, control. Lane 3: PCR with forward primer only. Lane 4: PCR with reverse primer only. Lane 5: PCR with both primers in PCR.

In Fig. 4.5 (a), the SP DNA sequence was amplified with a reverse primer that resulted in a SP construct that had GFP sequence at the 3' end. The products were separated on a 12 % polyacrylamide gel. There were no products of 80 bp seen in the controls (lanes 2-4). The 80 bp signal peptide PCR product (lane 5), was excised from the gel and the DNA was resuspended in TE overnight.

The GFP(s) was amplified with a forward primer that included SP sequence, and a reverse primer that included a stop codon at the end of the 720 bp GFP sequence [Fig. 4.5 (b).]. The PCR controls were shown in lanes 3-5 in Fig. 4.5 (b), and showed nonspecific amplification of template DNA as seen at the top of the lanes. The 720 bp product [Fig. 4.5 (b), lane 5] was excised from the gel and the DNA was gel purified. For the generation of the sp-GFP construct the template for the PCR, consisted of TE-resuspended SP and the purified GFP(s) product and the primers used here were the forward primer of the SP and the reverse primer of GFP in order to obtain what is called 'a zipper reaction' which resulted in a combined DNA sequence of 800 bp [see Fig. 4.2 (ii)]. The product of this reaction was seen in Fig. 4.5 (c) lane 5, in addition to some

minor nonspecific amplification that resulted in truncated products. The desired band was excised from the gel, the DNA was purified and digested with compatible enzymes.

The digested DNA was ligated into digested pBS-K overnight. The ligation reaction was transformed into competent *E.coli* cells. Transformed colonies were selected by resistance to Ampicillin, as the vector has an Ampicillin resistance gene. Colonies were screened for positive clones by small scale plasmid isolation and restriction enzyme digestion. The positive clones were identified and DNA was isolated by plasmid preparation. The DNA was sequenced to confirm correct GFP sequence and to ensure that no mutations were introduced.

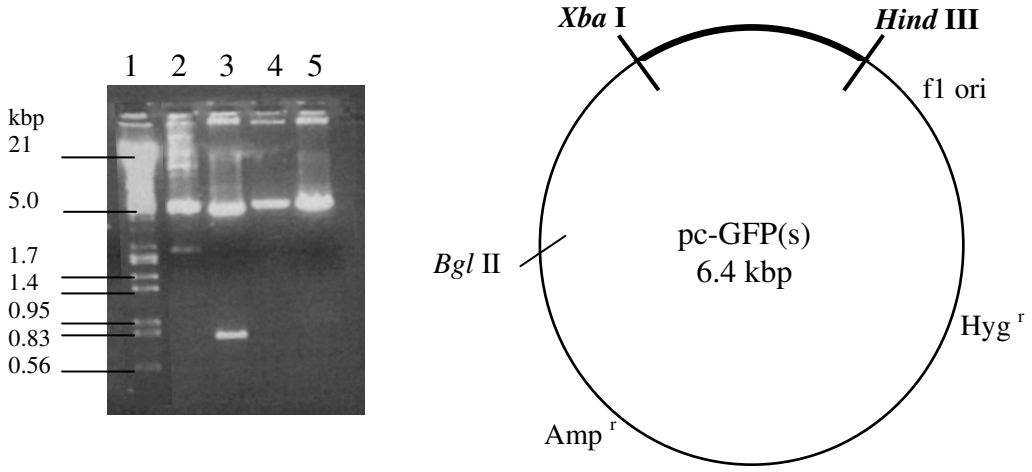

Figure 4.6: Confirmation of pcGFP(s) by restriction enzyme digest.
Lane 1: λ. (*EcoR* I/*Hind* III) marker. Lane 2: undigested pcGFP(s). Lane 3: pcGFP(s) digested with *Xba* I and *Hind* III. Lane 4: pcDNA-GFP(s) digested with *Xba* I and *Bam* HI. Lane 5: pcGFP(s), linearised with *Bgl* II.

The GFP(s) was then sub cloned into pcDNA3.1(H)-. A restriction digest with *Xba* I and *Hind* III confirmed the presence of the 800 bp insert (Fig. 4.6, lane 3). In lane 4 the DNA was digested with *Xba* I and *Bam* H I. An *Xba* I site existed in the MCS, but the *Bam* HI

site was removed during the digestion of pcDNA3.1(H)-, and hence a linearised 6.4 kbp band was seen. Lane 5 showed DNA digested with *Bgl* II, which linearised the vector outside the MCS. All the bands were of expected size, but the agarose gel was not run long enough to see better separation between the linearised 6.4 kbp band of lanes 4 and 5 and that of the pcDNA3.1(H)- vector band in lane 3.

The sp-GFP(MCS) was constructed in the same way as the sp-GFP(s). The 740 bp sp-GFP PCR product [Fig. 4.7 (b) lane 5] was purified and amplified together with signal peptide DNA [Fig. 4.7 (a) lane 5], to generate a 820 bp product [Fig. 4.7 (c), lane 5].

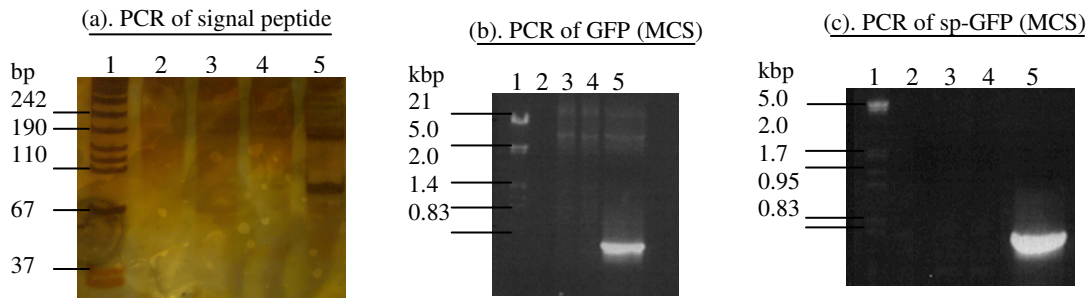

Figure 4.7: Construction of sp-GFP(MCS).
Lane 1: DNA ladder markers. Lane 2: no DNA, control. Lane 3: PCR with forward primer only. Lane 4: PCR with reverse primer only. Lane 5: PCR with both primers.

There was some nonspecific amplification of the template DNA, seen in lanes 2-5 of Fig. 4.7 (b), and there were no products of 80 bp seen in the controls of the amplification of the SP [Fig. 4.7 (a), lanes 2-4]. No nonspecific amplification of sp-GFP(MCS) was seen in the control lanes 2-4 in Fig. 4.7 (b). The sp-GFP(MCS) [Fig. 4.7 (c), lane 5] product was purified, digested and ligated into pBS-K. The ligation reaction was transformed into competent *E.coli* cells. The ampicillin resistant colonies were screened by small scale plasmid isolation and restriction enzyme digests to identify positive clones. The DNA

was sequenced to confirm the sp-GFP(MCS) sequence. The sp-GFP(MCS) was sub cloned into pcDNA3.1(H)-.

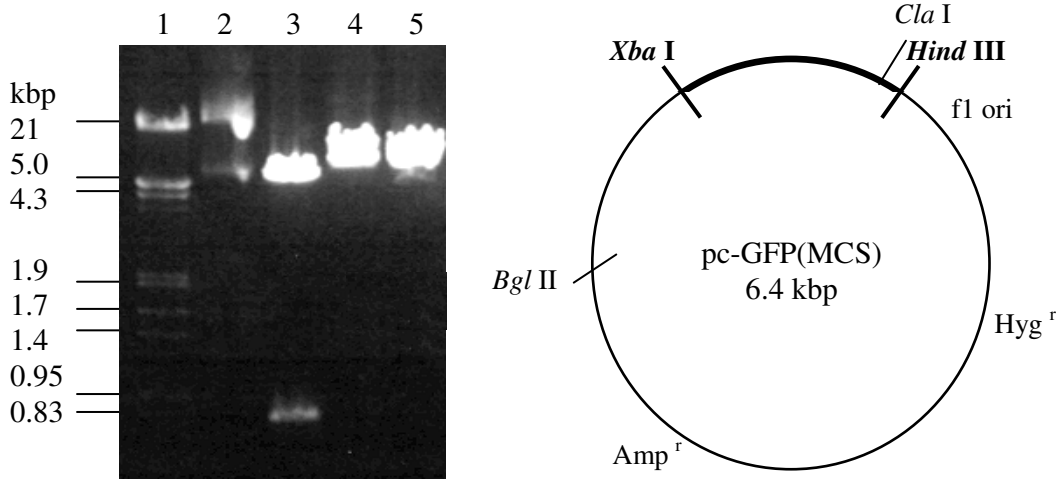

Figure 4.8: Confirmation of pcGFP(MCS) by restriction enzyme digest.
Lane 1: λ. (*EcoR* I/*Hind* III) marker. Lane 2: undigested pcGFP(MCS). Lane 3: pcGFP(s) digested with *Xba* I and *Hind* III. Lane 4: pcGFP(MCS) digested with *Cla* I. Lane 5: pcGFP(MCS) linearised with *Bgl* II.

A restriction digest with *Xba* I and *Hind* III confirmed the presence of the 820 bp insert (Fig. 4.8, lane 3). In lane 4 DNA was digested with *Cla* I, as a restriction enzyme site occured in the MCS at the end of the GFP sequence. Lane 5 showed DNA digested with *Bgl* II, which linearised the vector outside of the MCS. This vector was used later for the introduction of the LDLr sequence. All the digests in Fig. 4.8 had bands of predicted size.

The LDLr was amplified from the template, pc-wtLDLr, so that the LDLr construct obtained did not contain the SP sequence. Primers that contained restriction enzyme sites were used to introduce unique restriction enzyme sites at the 5' and the 3' end of the

sequence. These allowed for compatible cloning sites for sequencing and subsequent ligation into the expression vector.

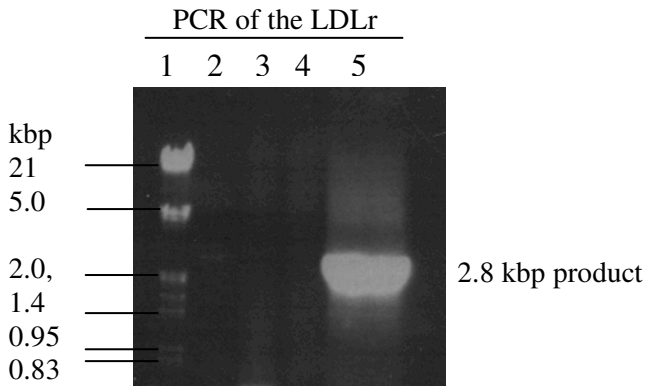

Figure 4.9: Amplification of the LDLr.
Lane 1: λ (*EcoR* I/*Hind* III) marker. Lane 2: PCR control using no DNA template. Lane 3: DNA that has been amplified with forward primer only. Lane 4: template DNA that has been amplified with reverse primer only. Lane 5: Both primers in the PCR.

In Figure 4.9, the LDLr PCR product can be seen as a 2.8 kbp band in lane 5. The controls for the PCR do not show any nonspecific amplification of products. The DNA was digested with *Kpn* I and *Hind* III and cloned into pBS-K for sequencing. The LDLr DNA was then sub cloned into pcGFP(MCS).

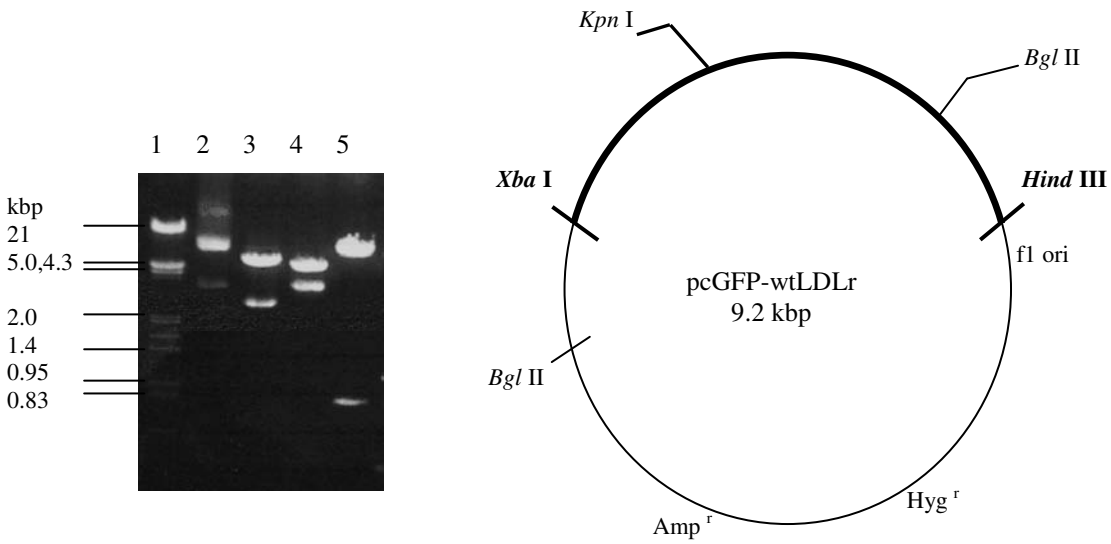

Figure 4.10: Confirmation of pcGFP-LDLr by restriction enzyme digest.
Lane 1: λ (*EcoR* I/*Hind* III) marker. Lane 2: undigested pcGFP-wt-LDLr. Lane 3: pcGFP-LDLr digested with *Kpn* I and *Hind* III. Lane 4: pcGFP-wt-LDLr digested with *Bgl* II. Lane 5: pcGFP-wt-LDLr digested with *Xba* I and *Kpn* I.

In Figure 4.10, the restriction enzyme digest with *Kpn* I and *Hind* III of pcGFP-LDLr resulted in a 2.8 kbp LDLr band and a 6.4 kbp pcGFP(MCS) vector band (Fig. 4.10, lane 3). A digest with *Bgl* II only (lane 4), revealed a band of 5.5 and 3.4 kbp, since this enzyme occurred once in the vector and once in the LDLr sequence. Lane 5 showed a digest with *Xba* I and *Kpn* I, which resulted in an 8.4 kbp band and the release of the 820 bp GFP band.

All constructs that were made by PCR, were analysed by nucleotide sequencing and restriction enzyme digests were used to determine correct banding pattern. All constructs gave correct banding patterns and no unwarranted mutations were introduced during PCR. Ultimately, a GFP-LDLr fusion construct was produced as determined by restriction enzyme digest and sequencing.

4.2.2 Expression of the GFP constructs in mammalian cells

To test the hypothesis that TACE was involved in the shedding of the LDLr, GFP-LDLr shedding in TACE activity KO (TACE-/-) mouse fibroblasts was compared to the shedding of that in wild-type mouse fibroblasts (TACE+/+). In order to assess the cleavage secretion of GFP-LDLr; wild-type and TACE-/- mouse fibroblasts were transfected with the GFP and GFP-LDLr constructs. However, these constructs could not be stably expressed for a number of reasons, discussed later.

In order to establish whether the constructs were functional; GFP and GFP-LDLr constructs were transiently expressed in CHO cells. Expression of the constructs was analysed using fluorescent microscopy and Western blotting.

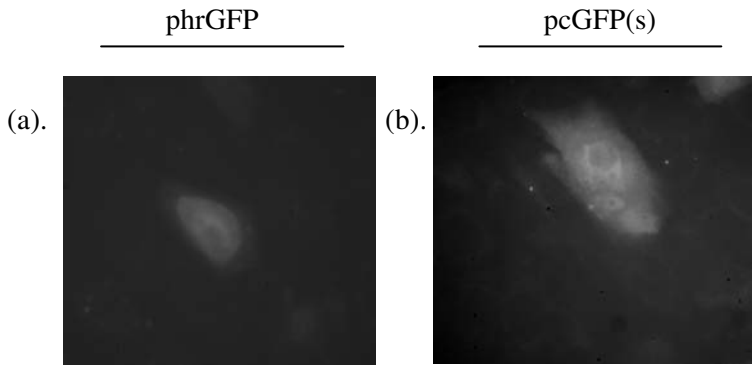

Figure 4.11: GFP expression in CHO cells.
(a). CHO cells transfected the GFP vector, phrGFP. (b). CHO cells transfected with the sp-GFP(s) construct in pcDNA3.1 (H)-, named, pcGFP(s). 24 hours after transfection cells were fixed and visualised by fluorescent microscopy under 40 x magnification. The cells presented here are representative cells.

Fluorescence was observed in CHO cells transfected with the phrGFP construct, the positive control for the experiment as well as the GFP(s) construct (Fig.4. 11). The cells were not counted, but a few slides per transfection were analysed for the experiments.

The sp-GFP(s) construct was expected to be secreted, since it contained a signal peptide at the start of the GFP sequence, but does not have a transmembrane domain. The fluorescence seen in Figure 4.11 (b) was likely due to newly synthesized GFP that has not been secreted from the cell. The GFP-LDLr showed negligible fluorescence (data not shown) that was similar to the background fluorescence of the mock transfected cells.

In addition to detection of GFP fluorescence in transfected cells, expression of GFP constructs was assessed by Western blotting using GFP and LDLr antibodies. The samples were separated under non-reducing conditions, since the polyclonal LDLr antibody obtained detected the non-reduced form more effectively than the reduced form as the LDLr is a cysteine-rich protein.

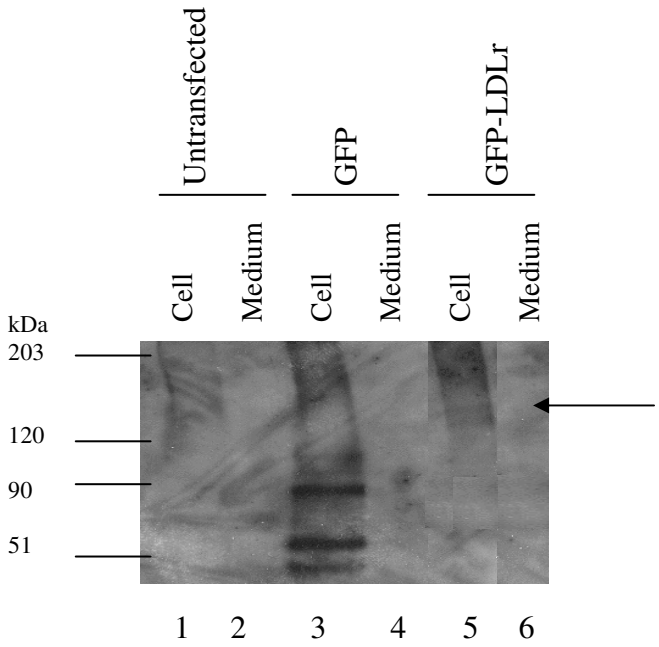

Figure 4.12: Western blot showing GFP and GFP-LDLr expression in CHO cell lysate and medium samples using the anti-GFP antibody.
Lane 1: Untransfected cells. Lane 2: medium from untransfected cells. Lane 3: pcGFP(s) transfected cells. Lane 4: medium from pcGFP(s) transfected cells. Lane 5: Lane: pcGFP-LDLr transfected cells. Lane 6: medium from GFP-LDLr transfected cells. To assay for soluble receptors, medium was replaced with serum-free medium and harvested after 4 hours. Medium was concentrated 5X and 20 µl was used. ~40 µg of non-reduced cell lysate samples were separated by SDS-PAGE (10 % gel) detected with a GFP antibody by Western blotting. The arrow indicates GFP-LDLr in lane 5. The experiment was performed 3 times.

In the untransfected cells and medium samples that served as controls for the experiment, no GFP was detected [Fig. 4.12 (lanes 1 and 2)]. In the GFP transfected cells, GFP was detected as a "monomer (~30 kDa), dimer (~60 kDa) (Tsien, 1998) and trimer (90 kDa)" in the cell lysate sample (lane 3), indicating that the bands seen here are specific to GFP as these bands were not seen in the controls. However, in lane 4 no significant amo unt of secreted GFP was detected in the medium. The expression level of GFP-LDLr was less than GFP alone, seen as an extremely faint band of ~160 kDa, indicated by the arrow [additive of the GFP (~30 kDa) and LDLr size, ~130 kDa, under non-reduced conditions (Daniel et al., 1983)] in cell lysate in lane 5. After 4 hours, no GFP-LDLr was detected in the medium sample, lane 6.

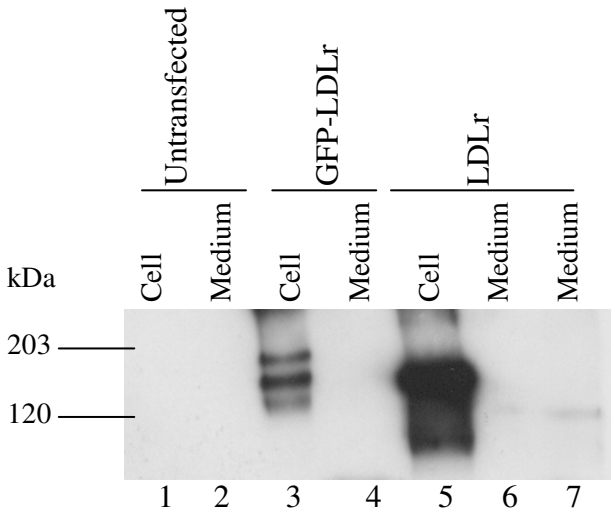

Figure 4.13: Western blot showing GFP-LDLr and wt-LDLr expression in CHO cell lysate and medium using a rabbit polyclonal anti-LDLr anti-serum. Lane 1: Untransfected cells. Lane 2: 5X concentrated medium. Lane 3: pcGFP-LDLr transfected cells. Lane 4: 5X concentrated medium from pcGFP-LDLr transfected cells. Lane 5: Lane: LDLr transfected cells. Lane 6: 5X concentrated medium from pc-wt-LDLr transfected cells harvested after 4 hours. Lane 7: 5X concentrated medium from pc-wt-LDLr transfected cells harvested after 16 hours. To assay for soluble receptors, medium was replaced with serum-free medium and harvested after 4 hours. Non-reduced samples were separated on SDS-PAGE (7 % gel), transferred to nitrocellulose and detected with a rabbit polyclonal anti-LDLr.

To complement the data seen in Fig. 4.12, Western blot analysis using a rabbit polyclonal antibody to the LDLr was tested against the GFP-LDLr construct. The antibody to the LDLr did not detect the presence of the receptor in untransfected cells and medium and no nonspecific interaction was obtained [Fig. 4.13 (lanes 1 and 2)]. In lane 3, GFP-LDLr transfected cells displayed 3 bands, one that corresponded to the GFP-LDLr construct (~160 kDa), another which corresponded to the LDLr as compared to the size (130 kDa) of the band seen in the positive control (lane 5) for the experiment, and a low intensity component that corresponded to immature GFP-LDLr (~120 kDa). Again, the bands seen in lane 3 were not seen in the negative control (lane 1), indicating that the antibody was

specific to the GFP-LDLr transfected into these cells. No GFP-LDLr was detected in the medium, lane 4. Soluble LDLr was detected in both lanes 6 and 7, which were medium samples harvested from LDLr expressing cells, after 4 hours and 16 hours, respectively. The reason for detecting soluble LDLr in lanes 6 and 7, and not any soluble LDLr of GFP-LDLr in lane 4, could be due to higher levels of LDLr expression in lane 5 compared to GFP-LDLr or LDLr expression in lane 3.

Using the GFP antibody, only one faint band was seen for the GFP-LDLr construct in Figure 4.12, lane 5, since it only detected the GFP on the GFP-tagged receptor. The LDLr antibody on the other hand seemed to be more sensitive than the GFP antibody since it detected 3 bands for the same construct under the same conditions (Fig.4.13, lane 3). In addition, this indicated that the protein corresponding to the LDLr size did not have GFP associated with that construct. Possible origins for these bands are discussed in section 4.3. From Figure 4.13, it was evident that the epitope for the LDLr antibody was not masked in the GFP-LDLr construct. As with the fluorescent microscopy data, it was seen that the expression levels of GFP-LDLr was much lower when compared to GFP or LDLr expression levels.

4.3. Discussion

Two GFP vectors were made by PCR and cloning. Since the stable expression of GFP was unsuccessful in mouse fibroblasts, the expression of GFP and GFP-LDLr vector constructs were assessed in CHO cells.

Transient expression of GFP in mammalian cells is performed routinely, while the stable expression of GFP is more problematic. Producing stable mouse fibroblast cell lines expressing GFP(s) or GFP-LDLr were not successful. This could be due to any or a combination of the following factors: (i) toxicity of the GFP constructs, (ii) loss of expression/overgrowing of non-expressing cells or, (iii) stability of GFP constructs (Zeyda et al., 1999). It was also reported that even after cells were sorted by FACS analysis so that a 100 percent of cells expressed GFP, a loss of GFP expression was observed (Zeyda et al., 1999). Researchers who used the hrGFP construct in Hela cells, showed hrGFP expression peaked at 4 days, after which a continual loss in GFP expression occurred while the cells were under antibiotic selective pressure (Kirsch et al., 2003). PCR of non-fluorescent, resistant clones showed the presence of the GFP gene in the genome of transfected cells, but Western blots indicated that GFP was not produced at the protein level. In addition it was found that for the hrGFP construct, expression decreased over time from a population of positive cells, as well as that the GFP linked to the cytomegalovirus (CMV) promoter displayed lower fluorescence intensity compared to another promoter that emitted a stronger fluorescence signal (Zeng et al., 2003).

Similarly, the author also found that while a percentage of TACE-/- mouse fibroblasts were fluorescent (as shown by fluorescent microscopy) a couple of days after transfection, none of the selected resistant clones when checked after ~2 weeks, expressed GFP (data not shown).

In addition, all PCR products were sequenced and restriction digests of the DNA constructs all gave the predicted fragment sizes, validating the integrity of the constructs.

To determine if the constructs were transiently expressed in CHO cells, transfected cells were analysed by fluorescent microscopy and Western blot.

From the experiments performed (Figures 4.11, 4.12 and 4.13), it could be concluded that not only was the GFP-LDLr difficult to express as it seemed to be expressed at low levels, it also appeared to be expressed as two proteins. Using the polyclonal antibody to the LDLr, it showed that the construct was expressed as two proteins, an LDLr and a GFP-LDLr fusion protein. It is also not clear from the Western blot data whether the GFP-LDLr was released by ectodomain cleavage, into the medium.

In tobacco plant cells, an ER-targeted GFP-fusion protein was shown to degrade in the following manner where the GFP fusion protein was degraded into a smaller protein corresponding to GFP alone (Persson et al., 2002). This is a similar trend that the author observed in Figure 4.13, lane 3, where the GFP is 'removed' or cleaved from the GFP-LDLr construct. It may be possible that the GFP part of the GFP-LDLr fusion protein was not that stable and became cleaved and/or degraded in the ER.

It was possible that proper folding of the GFP-LDLr construct was compromised since a 30 kDa GFP protein tagged onto the extracellular side of a large receptor might have made the overall construct floppy and unstable, not allowing for the proper folding and fluorophore formation of GFP, and hence no fluorescence was seen. Researchers have tagged GFP to an LDLr before, but this construct was tagged on the intracellular side of the receptor, making it a more stable construct (Holst et al., 2001).

In this study, the GFP constructs were not investigated further, since a commercial rabbit polyclonal antibody to the LDLr could detect soluble LDLr from medium when used in Western blots (Fig.4.13, lanes 6 and 7). This method of detecting LDLr ectodomain release was preferred and used in further experiments to investigate the role of TACE in the ectodomain release of the LDLr.

Chapter 5:

The ectodomain shedding of the LDL receptor

5.1 Introduction

A number of unrelated proteins, including members of the LDLr family undergo cleavage near the cell surface to release the ectodomain into the surroundings (Rebeck et al., 2006; Edwards et al., 2008). Constitutive levels of ectodomain release of proteins can be upregulated by the addition of phorbol esters and inhibition in the presence of TAPI implicates metalloprotease activity, mainly due to members of the ADAMs family.

LDLr shedding was previously shown to be upregulated by phorbol esters in CHO cells (Begg et al., 2004). Certain candidate sheddases of the LDLr were eliminated by investigating the effect of inhibitors on its shedding. Furthermore, a metalloprotease was implicated to be responsible for the ectodomain release of the LDLr, as the shedding was shown to be sensitive to a hydroxamate inhibitor. TACE is an extensively studied metalloprotease that has many substrates (Huovila et al., 2005; Edwards et al., 2008), and was thought to play a role in LDLr ectodomain release since data from a proteomics study showed that TACE KO cells produced less soluble LDLr than the wild-type cells (Guo et al., 2002).

The aim of this chapter was to further investigate the role of TACE in LDLr shedding. Therefore, wild-type (named TACE+/+ hereafter) and TACE knockout (named TACE-/- hereafter) mouse fibroblasts expressing LDLr constructs were analysed for ectodomain

release. The rationale for including the 792-LDLr and JD-LDLr constructs in this chapter was to identify the role TACE plays in the shedding of these constructs. These internalisation mutant LDLr constructs were investigated previously and showed higher levels of shedding when compared to the wild-type, which suggested that the shedding of the LDLr was not dependent on endocytosis or that the mutant LDLr was possibly shed by a different sheddase to the wild-type LDLr (Begg et al., 2004). The TACE-/- mouse fibroblasts are deficient in TACE activity since the mature TACE expressed in these cells lacks the zinc binding motif in the catalytic site (Black et al., 1997; Peschon et al., 1998). Cells were also tested in the presence of PDBu, a phorbol ester, and a stimulator of shedding, to determine the role of TACE in the shedding of LDL receptors in response to up-regulation by phorbol ester treatment in the absence or presence of TACE. The effect of metalloprotease inhibition in the presence of phorbol was also tested to determine the role of hydroxymate sensitive metalloproteases in the stimulated shedding of the LDLr in the absence or presence of TACE. All cell lines were stably transfected with the LDLr, 792- or JD-LDLr constructs in the pcDNA 3.1(H)- vector, unless stated otherwise.

5.2 Results

5.2.1 Shedding of the LDLr constructs in TACE-/- mouse fibroblasts

TACE-/- mouse fibroblasts expressing LDLr constructs were assessed for the proteolytic release of their ectodomains in the presence or absence of PDBu and TAPI. Cell lysate and medium proteins were separated on SDS-PAGE (7 % gel) under non-reducing conditions and analysed by Western blotting. The rabbit polyclonal antibody to the LDLr was chosen and used for the detection of cell associated LDLr and soluble LDLr since this antibody could detect soluble LDLr in medium. The LDLr has a high cysteine

content and therefore the epitope to the LDLr antibody would be better preserved if samples were separated via SDS-PAGE under non-reducing conditions, as suggested by the suppliers.

The apparent molecular weight of the LDLr under reducing conditions is ~160 kDa (Schneider et al., 1982). In the absence of reducing agents, the apparent molecular weight of the LDLr is ~130 kDa (Daniel et al., 1983). Since the LDLr is a cysteine-rich protein, reduction of the disulphide bonds allows the receptor to unfold and mobility on SDS-PAGE is slowed. Similarly, the reported value for the soluble LDLr is 140 kDa under reducing conditions (Begg et al., 2004).

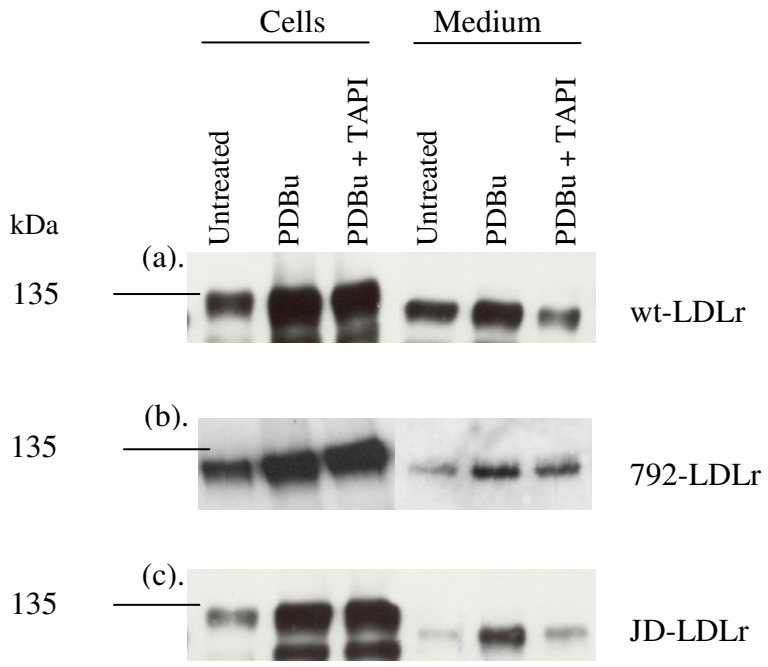

Figure 5.1: Western blots showing LDLr expression in TACE -/- mouse fibroblasts.
TACE-/- mouse fibroblasts expressing wt-LDLr (a), 792-LDLr (b) or JD-LDLr (c), were incubated with Optimem for 4 hours at 37°C, in the presence or absence of 1 μM PDBu or 1 μM PDBu + 10 μM TAPI. Cell lysate and medium proteins were analysed under non-reducing conditions by Western blotting. These Westerns are representative blots.

Full length (~130 kDa) and soluble (~110 kDa) forms of the LDLr were detected in the cell lysates and medium samples of TACE-/- mouse fibroblasts expressing the LDLr constructs (Fig. 5.1). The LDLr bands detected in the cell lysate were similar in size as reported in the literature. The soluble LDLr in the media was ~20 kDa less than the full length LDLr (as reported previously) (Begg et al., 2004). Both the membrane and soluble forms of the LDLr were up-regulated in response to PDBu. Untransfected cells were not shown as a control, as the antibody does not detect LDLr in this cell line (data not shown) as well as the CHO cell line (see Figure 4.13, lanes 1-2).

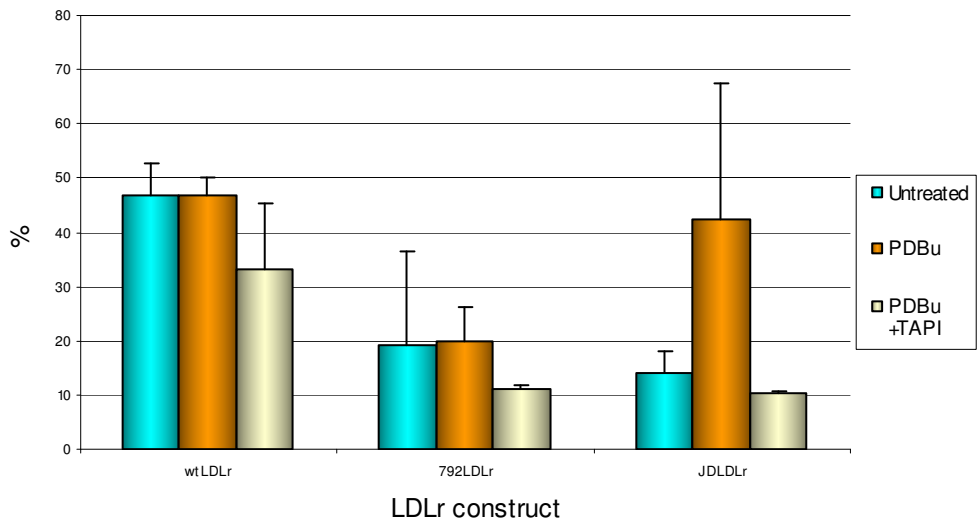

Figure 5.2: Soluble LDLr production in TACE-/- mouse fibroblasts.
X-ray films of Western blots were scanned and analysed by densitometry using the GeneSnap and GeneTools, respectively. % soluble LDLr is expressed as a % of total LDLr (cell associated and medium). Results are the average of 2 independent experiments. The error bars indicate the range.

The shedding of the LDLr in TACE-/- mouse fibroblasts was quantified using densitometric scanning (Fig. 5.2). A constitutive level of ectodomain release of the wt-LDLr, 792-LDLr and JD-LDLr constructs occurred in TACE-/- mouse fibroblasts (Figures 5.1 and 5.2). Levels of the wt-LDLr shedding were higher than the mutant receptors under these unstimulated conditions. In Figure 5.1, medium samples in the presence of PDBu, showed an increase in soluble LDLr levels over untreated conditions. However, when expressed as a % of total LDLr, the values were normalised (Fig.5.2), since an increase in the cell expression of LDLr in the presence of PDBu also occurred (Fig.5.1). In the presence of phorbol, shedding levels of the wt-LDLr and 792-LDLr did not increase as compared to unstimulated conditions, while the JD-LDLr shedding was stimulated ~3-fold by phorbol. TAPI decreases shedding of wt-LDLr and 792-LDLr as compared to untreated conditions by 1.7 and 2-fold, respectively, indicating and that the TAPI was inhibiting constitutive activity. This further supports that PDBu stimulated shedding of the wt-LDLr and 792-LDLr was TACE dependent, since in the absence of TACE, no increase in phorbol-stimulated shedding was observed. In the presence of TAPI, the phorbol-stimulated shedding of the JD-LDLr construct was decreased to constitutive levels. It can be concluded that in the absence of TACE, the constitutive level of shedding observed in mouse fibroblasts is due to another secretase or other secretases present in this cell line.

To verify the role TACE has in the nonstimulated and stimulated levels of soluble LDLr production, levels of soluble LDLr in TACE deficient cells needed to be compared to levels in TACE+/+ mouse fibroblasts.

Using the calcium phosphate as a transfection method, numerous attempts to introduce stable LDLr over-expression into TACE+/+ mouse fibroblasts were unsuccessful. In these instances, resistant colonies were selected with Hygromycin, picked and propagated only to show no LDLr expression as assessed by Western blot. Other transfection methods, which yielded higher transfection efficiencies, such as transfection with Fugene or electroporation, also showed no LDLr expression in TACE+/+ mouse fibroblasts.

A different strain of wild-type mouse fibroblasts was later used for the transfection of LDLr DNA. However, several attempts at expressing LDLr using either calcium phosphate or Fugene methods for transfection were unsuccessful.

To circumvent this problem, the author opted to use the episomal vector BCMGSNeo (Karasuyama et al., 1990; Suzuki et al., 1997a). This vector confers Neomycin resistance to transfected cells and the vector does not incorporate into the cell's genome, thus increasing the chances of improving transfection efficiency.

The LDLr constructs were subcloned into BCMGSNeo and transfected into TACE+/+ mouse fibroblasts. The mouse fibroblasts were transfected using calcium phosphate but did not produce any clones, when selected with 0.8 mg/ml Geneticin.

A third source of TACE+/+ mouse fibroblasts yielded the same results when transfected, i.e. the cells died and no clones were formed during selection. More stable transfections were attempted, reducing the concentration of Geneticin to 0.35 mg/ml in the medium.

This time, after a week of selective medium the mouse fibroblasts formed clones but when picked, they did not grow.

To provide evidence that the LDLr construct in the BCMGSNeo vector could be expressed in mammalian cells, CHO cells were stably transfected with the LDLr in BCMGSNeo and assessed by Western blotting.

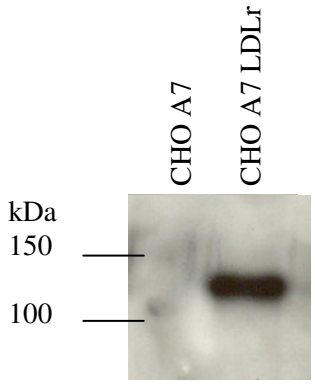

Figure 5.3: Western blot showing LDLr expression in a CHO A7 clone.
CHO A7 cells were stably transfected with BCMGSNeo-LDLr. ~30 µg cell lysate of untransfected CHO A7. A CHO A7 clone was loaded on a SDS-PAGE (7% gel) and assessed for LDLr expression under non-reducing conditions.

CHO cells transfected with the LDLr constructs in the BCMGSNeo vector, produced resistant clones which stably expressed LDLr as assessed by Western blot (Fig. 5.3). The LDLr expressed here is of the same molecular weight as seen before in TACE-/- mouse fibroblasts (Fig. 5.1).

GFP was used to determine if TACE+/+ mouse fibroblasts could be transfected with another construct. To compare transfection efficiencies of mouse fibroblasts, TACE-/- and TACE+/+ mouse fibroblasts cells were transiently transfected with GFP (Fig. 5.4).

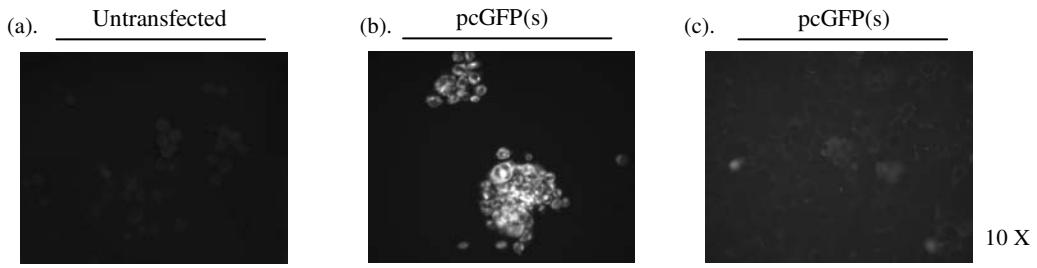

Figure 5.4: GFP expression in TACE-/- and TACE+/+ mouse fibroblasts.
(a). Untransfected TACE-/- mouse fibroblasts. (b). TACE-/- mouse fibroblasts. (c). TACE+/+ mouse fibroblasts. Cells were transfected with pcGFP(s) by the calcium phosphate method. 72 hours after transfection, non-fixed cells were visualised by fluorescent microscopy.

A number of TACE-/- mouse fibroblasts, seen as clusters of cells in Figure 5.4 (b), showed GFP expression while the TACE+/+ mouse fibroblasts failed to express GFP under the same conditions [Fig. 5.4 (c).]. This suggested that the transfection efficiency of TACE+/+ was lower than the TACE-/- counterparts. From all the transfection experiments, it was evident that expression of both the LDLr and GFP was problematic in TACE+/+ mouse fibroblasts.

After numerous unsuccessful attempts to transfect LDLr constructs into wild-type mouse fibroblasts, another approach was investigated to compare shedding of the LDLr in a TACE null cell line.

5.2.2 Shedding of LDLr constructs in CHO M2 and CHO A7 cells

The other approach was to investigate shedding in a CHO M2 cell line, which only produced the inactive prodomain of TACE (Borroto et al., 2003). This cell line was chosen so that shedding levels of the LDLr constructs in this TACE deficient cell line could be compared to LDLr shedding in CHO A7 cells (Begg et al., 2004). CHO A7 cells do not express endogenous LDLr. CHO M2 cells have endogenous LDLr expression but the levels are low that the LDLr cannot be detected by Western blotting, using the conditions used in this study.

The TACE-/- mouse fibroblasts are able to produce both the prodomain as well as mature TACE which remains inactive due to the mutation in the zinc-binding catalytic site (Black et al., 1997; Peschon et al., 1998). The CHO M2 cell line is different to the TACE-/- mouse fibroblasts in that the CHO M2 cell line is a chemically mutated cell line that is deficient in the shedding of the TGF-α (Arribas and Massague, 1995). The shedding of APP, pro-HB-EGF and L-selectin was also defective in CHO M2. In a later publication, it was revealed that the cell line was defective in producing active TACE, since only the prodomain is made in these cells as a result of aberrant transport of TACE out of the secretory pathway (Borroto et al., 2003). Trafficking of other ADAMs such as ADAM 9, ADAM 10 or MT1-MMP appear to be normal in these cells, since all the furins are present in these cells, making the defect specific for TACE. In addition, CHO M2 cells were shown to produce two TACE variants that have mutations in the catalytic domain as well as the cysteine-rich disintegrin domain (Li and Fan, 2004). The mutation present in the cysteine-rich disintegrin domain was shown to be important with respect to the loss of TACE activity.

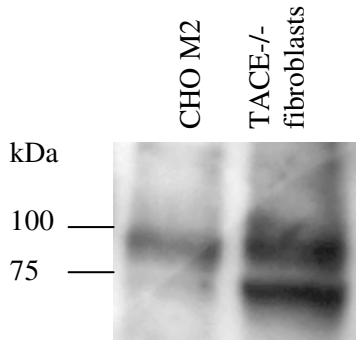

Figure 5.5: Western blot showing expression of TACE in CHO M2 cells and TACE-/- mouse fibroblasts.
40 µg of cell lysates of CHO M2 cells and TACE-/- mouse fibroblasts were loaded on SDS-PAGE (7 % gel) under non-reducing conditions and analysed by Western blotting, using the rabbit polyclonal antibody to TACE.

A comparison of TACE expression in TACE-/- mouse fibroblasts and CHO M2 cells is seen in Figure 5.5. The TACE antibody detected two bands in the TACE-/- mouse fibroblasts, a higher molecular weight component of ~100 kDa, representing the unprocessed inactive prodomain of TACE, and a lower molecular weight component of 75 kDa, corresponding to the processed, mature form of TACE (Fig. 5.5). However, the mature, processed form seen here is inactive due to the lack of the zinc binding motif in the catalytic site (Black et al., 1997; Peschon et al., 1998). The molecular weights detected here corresponded to the values provided in the literature (Borroto et al., 2003). In the CHO M2 cell line, the TACE antibody mainly detects the prodomain and a faint lower molecular weight band can just be seen. This may be due to some minor processing of TACE in these cells.

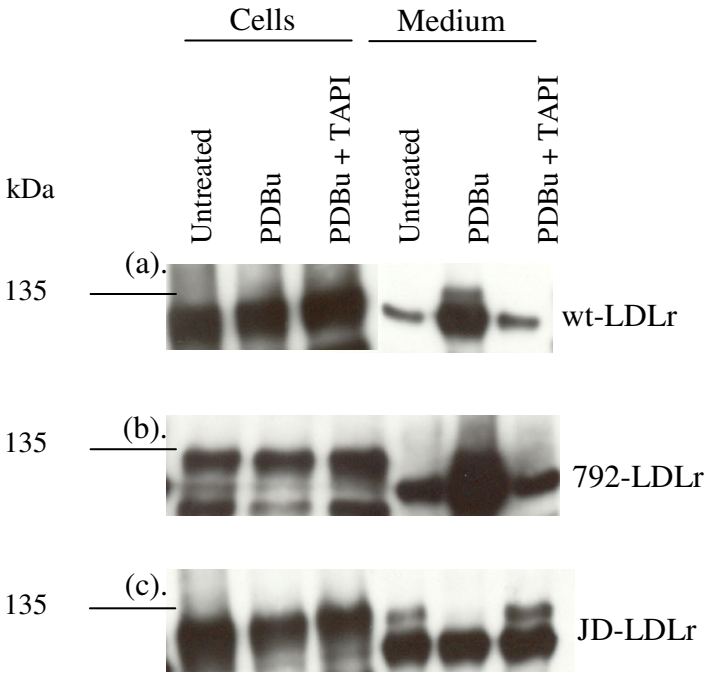

Figure 5.6: Western blots showing LDLr shedding in CHO A7 cells
CHO A7 cells expressing wt-LDLr (a), 792-LDLr (b) or JD-LDLr (c), were incubated for 4 hours with Optimem at 37°C, in the presence or absence of 1 μM PDBu or 1 μM PDBu + 10 μM TAPI. Cell lysate and medium proteins were analysed under non-reducing conditions by Western blot. The Western blots shown here are representative blots.

Stable cell lines of CHO A7 and CHO M2 cells expressing LDLr constructs were made by the calcium phosphate method of transfection. Shedding of the LDLr constructs was assessed in the CHO A7 cell line (Fig. 5.6). Cellular and soluble forms of the LDLr were detected in the cell lysates and medium samples of CHO A7 cells. In the presence of PDBu an increase in the soluble forms of wt-LDLr and 792-LDLr were seen over unstimulated conditions. Here the increase in cellular levels due to PDBu is not that evident from the Western [as seen in TACE-/- mouse fibroblasts (Fig 5.1)], since in CHO cells, the presence of TACE converts the membrane form to the soluble form at a higher rate.

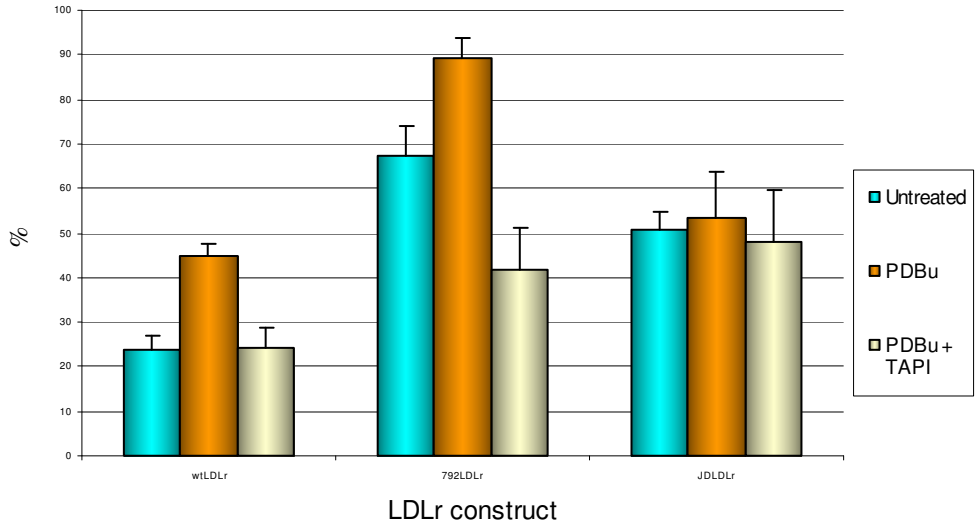

Figure 5.7: Soluble LDLr production in CHO A7 cells.
X-ray films of Western blots were scanned and analysed by densitometry using the GeneSnap and GeneTools, respectively. % soluble LDLr is expressed as a % of total LDLr (cell associated and medium) to normalise for variations in experession levels between cell lines. Results are the average of 2 independent experiments. The error bars indicate the range.

Levels of LDLr shedding were quantified in CHO A7 cells (Fig. 5.7). Soluble LDLr was observed under all conditions assayed. Constitutive levels of ectodomain release of 792-LDLr, and JD-LDLr in CHO A7 cells were higher than wt-LDLr as reported (Begg et al., 2004). Cells incubated with phorbol enhanced the ectodomain release of wt-LDLr ~2-fold, while the shedding of the 792-LDLr increased ~1.3 fold. In the presence of TAPI, the phorbol stimulated shedding of wt-LDLr and 792-LDLr constructs released into the medium was decreased to constitutive levels. Shedding of the JD-LDLr was not increased by stimulation by phorbol and not inhibited by TAPI in the presence of phorbol.

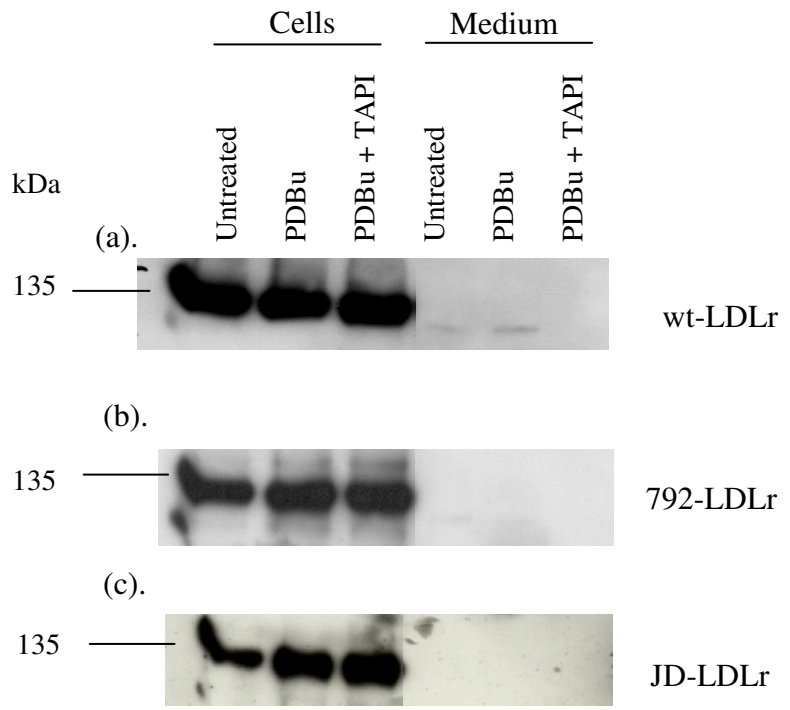

Figure 5.8: Western blots showing LDLr shedding in CHO M2 cells.
CHO M2 cells expressing wt-LDLr (a), 792-LDLr (b) or JD-LDLr (c), were incubated for 4 hours with Optimem at 37°C, in the presence or absence of 1 μM PDBu or 1 μM PDBu + 10 μM TAPI. Cell lysate and medium proteins were analysed under non-reducing conditions by Western blotting. The Westerns presented here are representative blots.

Shedding of the LDLr constructs was assessed in the CHO M2 cell line (Fig. 5.8). Cellular and soluble forms of the LDLr were detected in the cell lysates and medium samples of CHO M2 cells expressing LDLr constructs. Medium levels of the LDLr were low or hardly detectable. Soluble LDLr levels in the CHO M2 cell line were lower than in the CHO A7 cell line and TACE-/- mouse fibroblasts. There was a slight increase in the cellular LDLr expression in the presence of PDBu, but no associated increase in soluble LDLr ectodomain was observed.

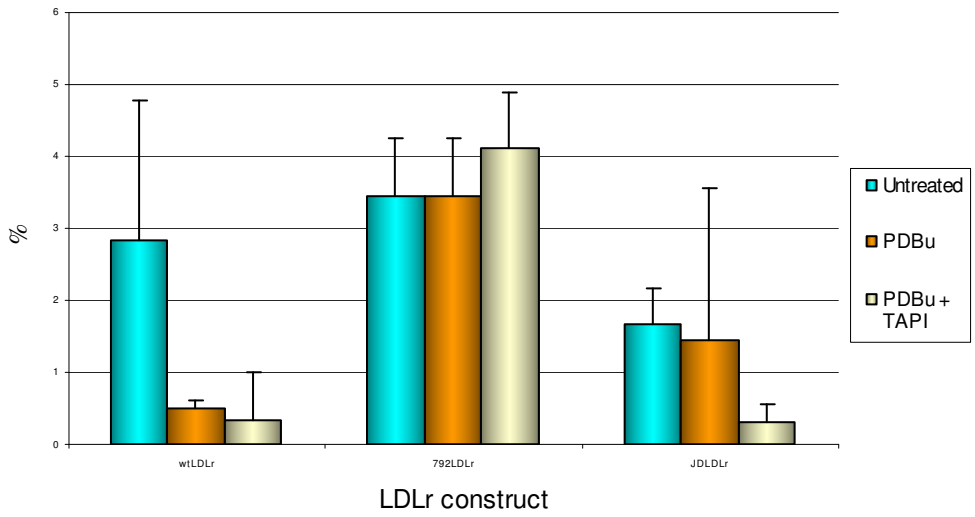

Figure 5.9: Soluble LDLr production in CHO M2 cells.
X-ray films of Western blots were scanned and analysed by densitometry using the GeneSnap and GeneTools, respectively. % soluble LDLr is expressed as a % of total LDLr (cell associated and medium). Results are the average of 2 independent experiments. The error bars indicate the range.

Shedding of the LDLr constructs in CHO M2 cells were quantified by densitometry (Fig. 5.9). The programme used for densitometry could detect low levels of soluble LDLr, which was slightly above background. Levels of LDLr shedding were low in CHO M2 cells, and all the LDLr constructs showed a similar shedding pattern, i.e., no increase in soluble LDLr was seen in the presence of PDBu (Fig. 5.9) The presence of phorbol increased cellular expression, but no associated increase in soluble LDLr was seen (Fig. 5.8, and Fig. 5.9). In addition, TAPI in the presence of phorbol seemed to decrease wt-LDLr and JD-LDLr shedding to lower than constitutive levels. TAPI did not have an effect on the levels of 792-LDLr shedding.

When shedding levels of LDLr was compared between the CHOM2 cells and the TACE-/- mouse fibroblasts, constitutive shedding of the LDLr was calculated to be at least 5-

fold lower in the CHO M2 cells than the TACE-/- mouse fibroblasts (Figures 5.1 and 5.2, compared to Figures 5.8 and 5.9).

Constitutive levels of the wt-LDLr, 792-LDLr, and JD-LDLr in the CHO M2 cells were approximately 6-fold, 19-fold and 33-fold less, respectively, than in the CHO A7 cells (compare Figures 5.7 and 5.9). In the presence of phorbol, shedding of the wt-LDLr, 792-LDLr, and JD-LDLr were approximately 22-fold, 25-fold and 26-fold less, respectively, in the CHO M2 cells compared to the CHO A7 cells. Thus, in CHO M2 cells, constitutive and phorbol stimulated shedding of the wt-LDLr, 792-LDLr and JD-LDLr was TACE dependent.

5.2.3 Comparison of TACE-/- mouse fibroblasts to CHO M2 cells

From the Western blot and shedding results, it appeared that the production of the soluble LDLr was more than 5-fold higher in the TACE-/- mouse fibroblasts when compared to the CHO M2 cells (Figures 5.2 and 5.8). Initially, it was thought that this could be due to higher expression of the LDLr in TACE-/- mouse fibroblasts than in the CHO M2 cells.

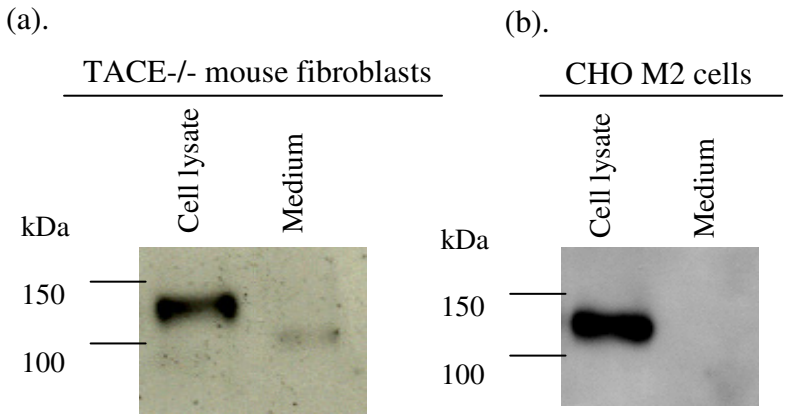

Figure 5.10: Western blots showing a comparison of soluble LDLr production in TACE KO cell lines.
Cells were incubated with Optimem for 4 hours. 40 ug of cell lysate and an equal volume of medium of TACE-/- mouse fibroblasts and CHO M2 cells were separated under non-reducing conditions on a SDS-PAGE (7 % gel) and detected with the antibody to the LDLr.

A TACE-/- mouse fibroblast cell line expressing LDLr at a slightly lower level than a CHO M2 cell line was assessed for shedding (Fig. 5.10). The results indicated that higher shedding levels of LDLr were produced in the TACE-/- mouse fibroblasts than in the CHO M2 cell line, and was not due to higher LDLr expression levels.

This finding led the author to consider the fact that the TACE-/- mouse fibroblasts might have higher non-TACE sheddase activity than in the CHO M2 cell line. To investigate the possibility, a fluorogenic peptide substrate that spans the TNF-α stalk region, was utilised as it was possible to assess TACE, or other sheddase activity, in mammalian cells by a fluorescence resonance energy transfer (FRET) assay (Jin et al., 2002).

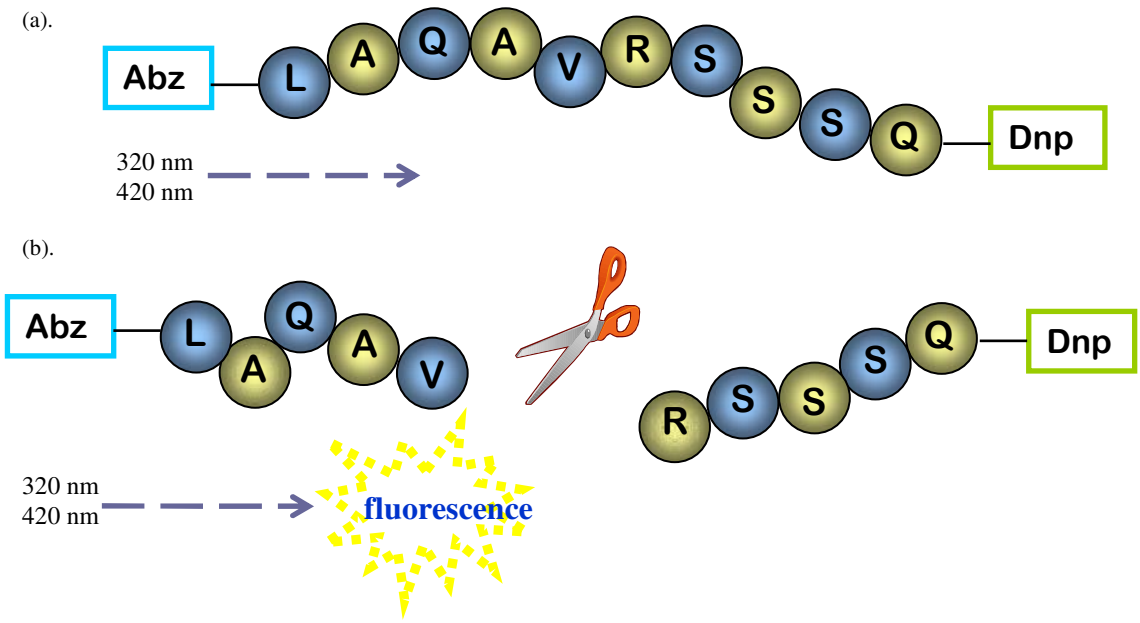

Figure 5.11: Schematic representation of the mechanism of the fluorogenic peptide assay
(a). Intact peptide when excited at 320 nm did not emit fluorescence, as the acceptor (Dnp) quenched the fluorescence emitted by the donor (Abz).
(b). When the peptide was cleaved, the fluorescence emitted by the donor (Abz) was not quenched when excited at 320 nm, and there was an increase in fluorescence.

The TNF-α stalk is flanked by a fluorescent donor (*ortho*-aminobenzoic acid; Abz) and a fluorescent acceptor (2, 4 dinitrophenol; Dnp) (Fig. 5.11). When the intact peptide is excited at 320 nm, the acceptor quenches the fluorescence emitted by the donor. When the peptide is cleaved, the fluorescence emitted by the donor is not quenched when excited, and there is an increase in fluorescence that can be measured continuously.

Peptides spanning the TNF-α stalk peptide were cleaved by recombinant TACE, as well as purified ADAM 9, ADAM 10, MMP-7 and ADAM 19 (Rosendahl et al., 1997;

Roghani et al., 1999; Chesneau et al., 2003; Zheng et al., 2004). Other MMPs like MMP-1, MMP-9 and MMP-13 were also able to cleave this peptide (Jin et al., 2002).

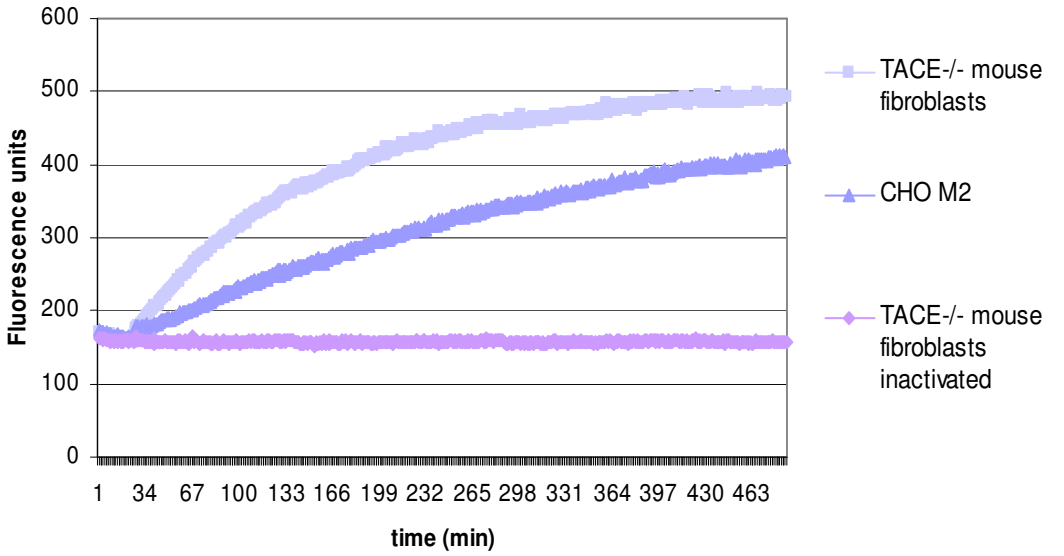

Figure 5.12: Cleavage of TNF-α stalk peptide by TACE-/- mouse fibroblasts and CHO M2 cell lines.
100 µg of cell lysates of TACE-/- mouse fibroblasts, heat inactivated TACE-/- mouse fibroblasts and CHO M2 were assayed for cleavage of the TNF-α stalk peptide at 37℃, measured continuously at an excitation wavelength of 320 nm and emission wavelength of 420 nm.

To assess and compare shedding activies in the two TACE deficient cell lines, equal amounts of total protein from cell lysates of TACE-/- mouse fibroblasts and CHO M2 cells were used. The fluorescence intensity over the experimental time period was higher in TACE-/- mouse fibroblasts compared to CHO M2 cells (Fig. 5.12). At initial rates (within 10 % peptide hydrolysis), the rates of cleavage by TACE-/- and CHO M2 cell lysate were calculated to be 0.43 pmol/min/µg and 0.176 pmol/min/µg, respectively. The rate of the cleavage of the fluorogenic TNF-α stalk peptide was ~2.4-fold higher in the TACE -/- mouse fibroblasts than in the CHO M2 cells. This indicated that non-TACE

sheddase activity was higher in TACE-/- mouse fibroblasts than in CHO M2 cells, which implicated other ADAMs that cleaved the TNF-α stalk peptide to be present at a higher level in the TACE-/- mouse fibroblasts, or that there were other sheddases present in the mouse fibroblasts that were not found in the CHO M2 cells. The possible candidates that could play a role are ADAM 9 and/or ADAM 10, as these ADAMs also cleave the TNF-α stalk peptide. In addition, these ADAMs play a role in the shedding of some other TACE substrates such as APP and HB-EGF (Izumi et al., 1998; Lammich et al., 1999). Thus there might be increased levels of ADAM 9 and/or ADAM 10 expression in the TACE-/- mouse fibroblasts compared to the CHO M2 cells. The increased soluble LDLr production in these cells could be attributed to this phenomenon, as these ADAMs may also play a role in the shedding of the LDLr.

To investigate the possibility that ADAM 9 and/or ADAM 10 expression was higher in TACE-/- mouse fibroblasts compared to that of CHO M2, equal amounts of cell lysates of both the cell lines were assessed by Western blot.

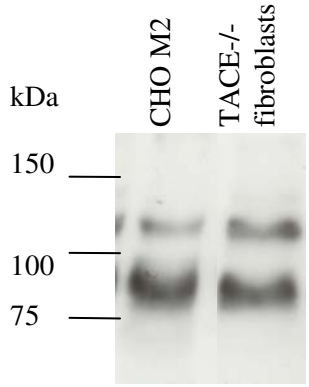

Figure 5.13: Western blot showing ADAM 9 expression in CHO M2 cells and TACE-/- mouse fibroblasts.
40 μg of non-reduced cell lysates of the CHO M2 cells and TACE-/- mouse fibroblasts were loaded onto 7% SDS-PAGE and analysed by Western blotting for ADAM 9 expression, using the polyclonal antibody to ADAM 9.

The antibody to ADAM 9 detected two bands in the cell lysate of CHO M2 and TACE-/- mouse fibroblasts (Fig.5.13). The unprocessed, intact prodomain form was seen at ~120 kDa and the processed mature form of ADAM 9 was seen at ~90 kDa (Borroto et al., 2003). In CHO M2 and TACE-/- mouse fibroblasts, both the prodomain and mature forms of ADAM 9 were detected. Expression levels for both the prodomain and the mature forms of ADAM 9 were similar in TACE-/- mouse fibroblasts and CHO M2 cells. This excludes the possibility that ADAM 9 was responsible for the increased cleavage of the TNF-α stalk in TACE-/- mouse fibroblasts.

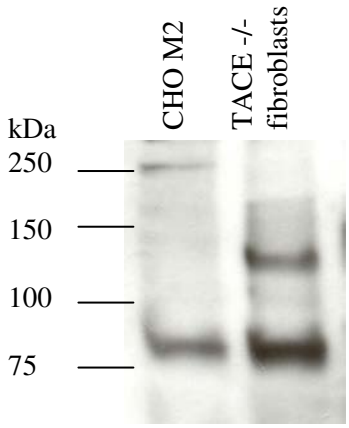

Figure 5.14: Western blot showing ADAM 10 expression in CHO M2 cells and TACE-/- mouse fibroblasts.
40 μg of non-reduced cell lysates of the CHO M2 cells and TACE-/- mouse fibroblasts were loaded onto 7% SDS-PAGE and analysed by Western blotting for ADAM 10 expression, using the polyclonal antibody to ADAM 10.

The antibody to ADAM 10 detected the unprocessed inactive prodomain with a molecular weight of ~130 kDa and the processed mature active form of ADAM 10 with a molecular weight of 85 kDa in TACE-/- mouse fibroblasts (Fig. 5.14). Very low levels of the prodomain form of ADAM 10 levels were seen in the CHO M2 cells. ADAM 10 expression was found to be higher in TACE-/- mouse fibroblasts than in the CHO M2 cells, as indicated by the higher levels of both the prodomain and the mature ADAM 10 forms (Fig. 5.14). When the blot was quantified by densitometry, mature ADAM 10 levels in TACE-/- mouse fibroblasts were ~2.7-fold higher than in CHO M2 cells.

From these data, we can conclude that both forms of ADAM 10 were expressed at higher levels, which could account for higher fluorescence activity seen in the TNF-α peptide assay as well as the increase in production of soluble LDLr seen in TACE-/- mouse

fibroblasts. This ADAM 10 could play a role in the shedding of the LDLr, since this ADAM is the most closely related to TACE and has similar substrate requirements (Killar et al., 1999; Rosendahl et al., 1997; Huovila et al., 2005; Reiss and Saftig, 2008; Reddy et al., 2000).

5.2.4 ADAM 10 as a potential sheddase

Since an increase in ADAM 10 expression was seen in the TACE-/- mouse fibroblasts, it is possible that this ADAM could be responsible for the shedding of LDLr in these cells. To determine if an association between ADAM 10 and the LDLr could be established, cell lysates of TACE-/- cells were co-immunoprecipitated using the C7 monoclonal LDLr antibody to immunoprecipitate the lysate, and the immunoprecipitate was further probed in a Western blot with the ADAM 10 antibody. In addition, cells were cross-linked prior to cell lysis, and these were also immunoprecipitated as outlined in Figure 5.15.

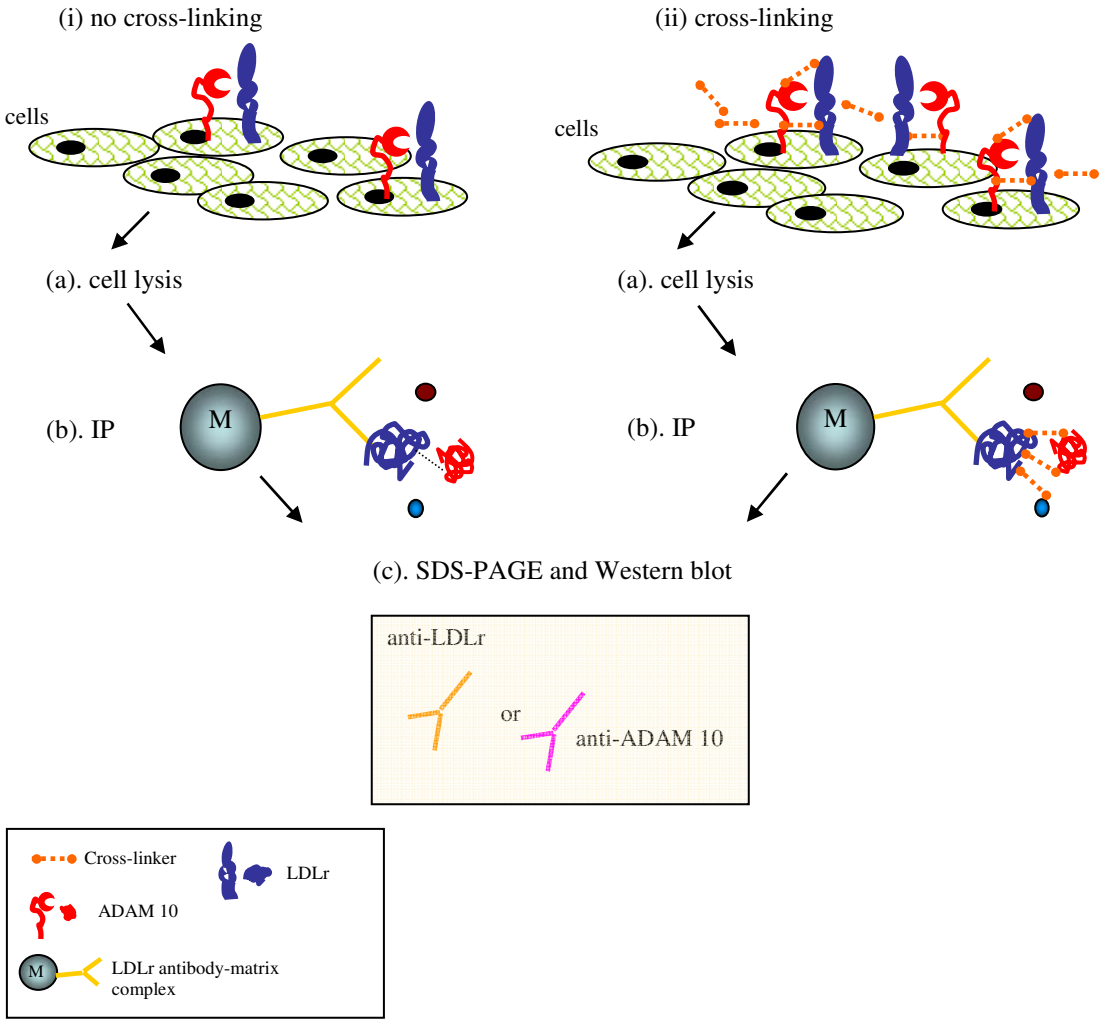

Figure 5.15: Schematic representation of the identification of LDLr cell surface associated proteins by Western blot with cross-linking and IP.
(i). Cells are lysed (a) and subjected to IP (b). Complexes are separated by SDS-PAGE and probed with the LDLr antibody or the ADAM 10 antibody.
(ii). Surface proteins are cross-linked prior to lysis (a), to increase the probability of complex formation, since proteins in close proximity will be cross-linked. The cross-linked cells are subjected to IP and complexes are analysed by western blot with the LDLr antibody or the ADAM 10 antibody.

As a control for the experiment, the Western blots were probed with the rabbit polyclonal antibody to the LDLr. Samples were separated on SDS-PAGE (7 % gel) and Western blots were analysed for LDLr or ADAM 10 expression, using the rabbit polyclonal

antibody to the LDLr or the rabbit polyclonal antibody to ADAM 10, respectively. Detection using the LDLr antibody served as a control for the experiment, to show that the IP and/or cross-linking were successful.

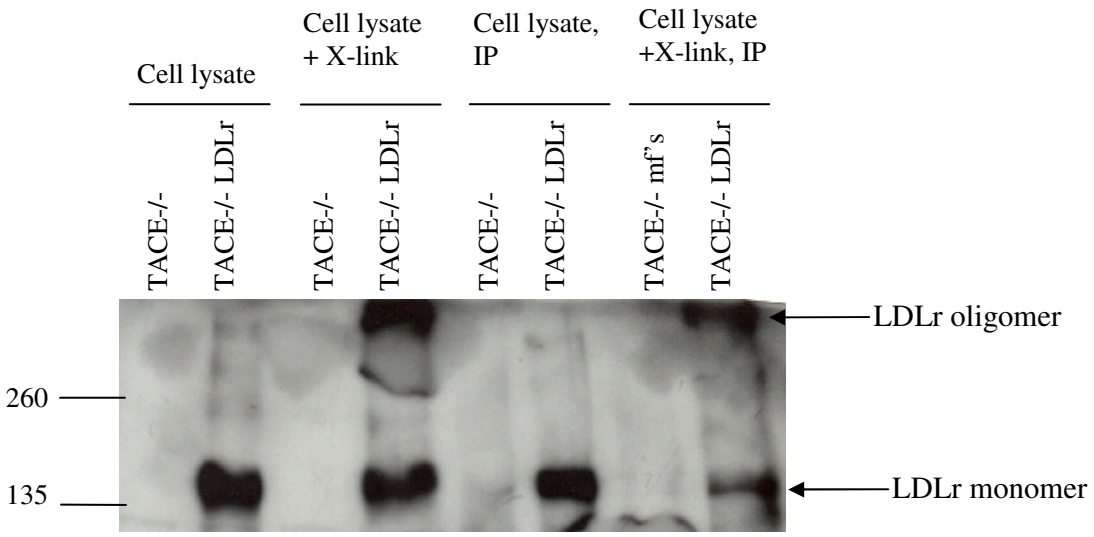

Figure 5.16: Cross-linking and IP of wt-LDLr in TACE-/- mouse fibroblasts. Untransfected and wt-LDLr expressing cells were lysed, or cross-linked prior to cell lysis or cross-linked prior to cell lysis and IP. Non-cross-linked cell lysate was IP as a control. The monoclonal antibody the LDLr (IgG-C7) was used for the IP, while the LDLr was detected in the western blot with the rabbit polyclonal antibody to the LDLr.

In Fig 5.16, the LDLr was detected in LDLr expressing cells only. Here all the samples were reduced, and the LDLr migrated with a relative mobility (Rf) value that corresponded to ~160 kDa. When the cells were cross-linked, an LDLr oligomer was detected, in addition to the monomer, as reported previously (van Driel et al., 1987). The immunoprecipitated sample showed comparable LDLr levels, indicating that the IP was successful. The controls for the experiment were untransfected, non-cross-linked TACE-/- cells. No LDLr was detected in all of the untransfected TACE-/- cell lysate samples.

When the cells were cross-linked prior to lysis followed by IP, the monomer and oligomer were detected with the pull down, indicating that the band seen in those cross-linked samples were specific to the LDLr antibody. Thus, the IP of wt-LDLr as well as the cross-linking were successful in TACE-/- mouse fibroblasts.

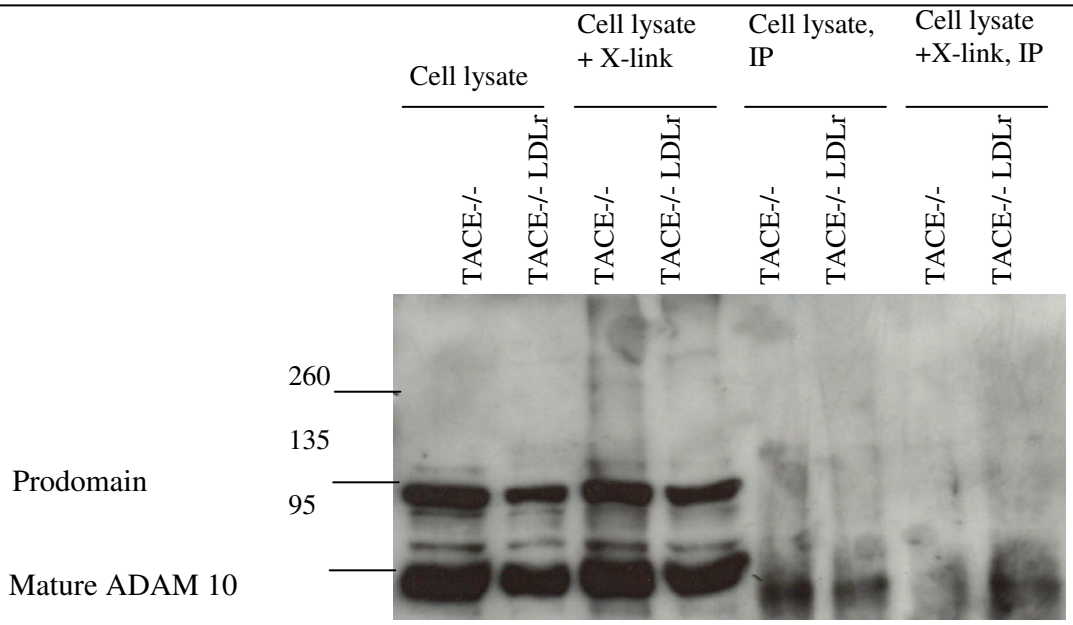

Figure 5.17: Cross-linking and co-immunoprecipitation of wt-LDLr and ADAM 10 in TACE-/- mouse fibroblasts.
Untransfected and wt-LDLr expressing cells were lysed, or cross-linked prior to cell lysis or cross-linked (X-link) prior to cell lysis and immunoprecipitated. Non-cross-linked cell lysate was immunoprecipitated as a control. The monoclonal antibody the LDLr (IgG-C7) was used for the IP, while the ADAM 10 was detected in the Western blot with the rabbit polyclonal antibody to the ADAM 10. All the samples contained β-ME.

To determine if ADAM 10 co-immunoprecipitated with the LDLr, the same samples were probed with the ADAM 10 antibody (Fig. 5.17). The prodomain and mature forms of ADAM 10 were seen in untransfected as well as LDLr-transfected TACE-/- cells. Cross-linking prior to cell lysis had no effect on the ADAM 10 forms, that is, no dimer formation was seen. No ADAM 10 was seen from the IP with IgG-C7, in the

untransfected and LDLr-transfected cells. Cross-linking prior to cell lysis, followed by IP showed no ADAM 10 in the untransfected and LDLr-transfected cells.

From Figure 5.16, it was shown that the IP as well as cross-linking were successful, indicating that in Figure 5.17, the IP with the anti-LDLr did not show any association with ADAM 10 when the samples were probed with the ADAM 10 antibody. Furthermore, cross-linking prior to IP showed no enhancement of an interaction. Apart from the LDLr band and an LDLr oligomer band in Figure 5.16, no other bands were detected that could be attributed to an ADAM 10-LDLr complex. Similarly, when the ADAM 10 antibody was used there were no higher molecular weight bands in the cross-linked sample that could be attributed to an ADAM 10-LDLr complex (Fig. 5.17).

5.3 Discussion

One of the main findings of this chapter indicated that in mouse fibroblasts there were constitutive levels of soluble LDLr production in the absence of TACE. Soluble levels of the wt-LDLr and 792-LDLr were not stimulated by phorbol, suggesting dependence on TACE activity. In CHO cells, constitutive and phorbol-stimulated shedding of wt-LDLr, 792-LDLr and JD-LDLr were dependent on TACE activity.

Using different transfection methods to obtain LDLr expression in TACE+/+ mouse fibroblasts produced antibiotic resistant clones that failed to express LDLr. In addition, GFP expression also failed in TACE+/+ mouse fibroblasts (Fig. 5.4). Transfection and expression of ACE in TACE+/+ mouse fibroblasts was also unsuccessful (unpublished results, Schwager). Since the GFP construct is not dependent on shedding, it served as a

control for determining transfection efficiencies between the two cell lines. The transfection efficiencies between TACE+/+ and TACE-/- mouse fibroblasts have been reported to be different and therefore a reporter gene was used as a correction factor (Tsakadze et al., 2006). In another study, TACE+/+ mouse fibroblasts have been reported to have a lower transfection efficiency than the TACE-/- counterparts (Zhao et al., 2003). As yet, no other explanation why the TACE+/+ mouse fibroblasts have lower transfection efficiencies than the TACE-/- mouse fibroblasts has been found.

Efficient transfection of mammalian cells depends on adequate uptake of foreign DNA into the nucleus (Byrnes et al., 2002). In most cell types DNA uptake into the cytoplasm is efficient, but not enough enters the nucleus. The presence of a nuclear targeting peptide during lipid-mediated transfection enhances protein expression in wild-type mouse fibroblasts. Perhaps wild-type mouse fibroblasts have a lower nuclear uptake of foreign DNA compared to other cells.

Shedding of the LDLr constructs in TACE deficient mouse fibroblasts showed that constitutive levels of LDLr release occurred in the absence of TACE activity (Figures 5.1 and 5.2). However, without knowing the constitutive levels of LDLr shedding in TACE+/+ mouse fibroblasts it could not be concluded that the constitutive shedding was not dependent on TACE, since if constitutive levels were the same in both cell types, then the ectodomain release of the LDLr was not TACE dependent. Constitutive levels of soluble wt-LDLr and 792-LDLr were not stimulated by PDBu. This suggested that the sheddases that were responsible for the shedding of wt-LDLr and 792-LDLr in TACE-/- mouse fibroblasts do not increase soluble LDLr in the presence of phorbol. TAPI in the presence of PDBu decreased soluble LDLr levels to less than that of constitutive levels.

This suggested that TAPI was inhibiting constitutive metalloprotease activity that contributed to the cleavage of wt-LDLr and 792-LDLr. The internalisation mutants did not undergo increased constitutive shedding as expected when compared to the wt-LDLr, as shown previously in CHO cells. This suggested that internalisation of the LDLr does not have an effect on the shedding of the receptor in TACE-/- mouse fibroblasts. These data indicate that phorbol-stimulated shedding was dependent on TACE activity in mouse fibroblasts, but levels needed to be compared to those found in TACE+/+ mouse fibroblasts to confirm this event. The JD-LDLr showed ~3-fold sensitivity to phorbol, and TAPI decreased the phorbol-stimulated release to that of constitutive levels. This indicated that another sheddase(s) might be involved in the shedding of the JD-LDLr. However, there was no shedding data available from TACE+/+ mouse fibroblasts to compare levels to validate this claim.

Higher levels of both the cell associated and soluble TNF-α were seen in TACE-/- mouse fibroblasts compared to TACE+/+ mouse fibroblasts (Zhao et al., 2003). However when % shedding was determined, the normalised values for TACE+/+ fibroblasts indicated higher soluble TNF-α levels. The same phenomenon could apply to the data seen in Figures 5.1 and 5.2., where if levels were to be compared to TACE+/+ fibroblasts, a dependence of TACE activity could be implicated in both the constitutive and stimulated shedding of the LDLr. Therefore, shedding levels of the LDLr was assessed in another TACE null cell line to determine the role of TACE in the ectodomain release of the LDLr.

In CHO cells, shedding of the wt-LDLr, 792-LDLr and JD-LDLr has been previously shown to be increased significantly by phorbol stimulation (Begg et al., 2004). The

experiments here indicated that there was a ~2-fold increase in soluble wt-LDLr and a ~1.3-fold increase in soluble 792-LDLr levels compared to constitutive levels when stimulated with phorbol (Fig. 5.7). Levels of soluble JD-LDLr did not increase in the presence of phorbol. It was possible that the differences in the ectodomain shedding here compared to Begg et al., could be due to the use of a different vector (pLDLr2), a different transfection method (co-transfection with pSV3Neo), a different method of detecting LDLr ([^{35}S] methionine labelled cells and IP with IgG-C7) and a different quantification programme used for densitomtery (Begg et al., 2004). Begg et al. (2004), detected LDLr expression was detected by labelling cells with [^{35}S] methionine, which resulted in the synthesis of radioactively labelled protein. When cell and medium samples were immunoprecipitated with the C7 monoclonal antibody, it bound to the LDLr present in that sample. IgG-C7-LDLr complexes were reduced and separated by SDS-PAGE. Proteins were transferred to nitrocellulose membranes and bands were detected by autoradiography. The affinity of the rabbit polyclonal antibody could possibly have a different affinity for the soluble LDLr compared to the monoclonal C7 antibody used previously. The expression vector used by Begg et al. (2004) was driven by the SV40 promoter, whereas the vector used here was driven by a CMV promoter. The CMV promoter was more sensitive to phorbol stimulation (Clesham et al., 1996; Maass et al., 2003; Mehta et al., 2009) hence an increase in cellular LDLr levels was seen (Figures 5.1, 5.6 and 5.8). In addition, the cellular pool of LDLr was decreased with the concomitant increase of soluble LDLr in response to PMA (Begg et al., 2004). However, the author did not observe this effect in CHO cells, as an increase in the LDLr cellular levels together with increased LDLr release occurred (Fig. 5.8).

Shedding of the LDLr constructs was at least 5-fold lower in the CHO M2 cells compared to the TACE-/- mouse fibroblasts (Fig 5.9 and Fig. 5.2). In addition, constitutive shedding of the LDLr constructs in the CHO M2 cells was more than 6-fold lower than in the CHO A7 cells, while stimulated shedding was more than 20-fold lower (Fig. 5.7 and Fig. 5.9). Levels of 792- and JD-LDLr release were not higher than wt-LDLr in the CHO M2 cells. The same was seen in the TACE-/- mouse fibroblasts, indicating that internalisation does not influence the shedding in TACE deficient cells. It was expected that the constitutive shedding levels of the mutants would be higher, but it could be different here due to the different methods used as explained before. Levels of soluble LDLr in the two CHO cell lines indicate that both the constitutive and phorbol-stimulated shedding of LDLr constructs were dependent on TACE activity.

A number of proteins that undergo proteolytic cleavage to release ectodomains have also been suggested to release the ICD of the C-terminal membrane embedded fragment, similar to Notch-1 and APP processing (Beel and Sanders, 2008). In addition, members of the LDLr family such as the LRP-1, ApoE R2 and vLDLr have been shown to undergo release of the ICD following ectodomain cleavage (May et al., 2002; Rebeck et al., 2006). Recently, a few proteins, in addition to the LDLr were identified by stable isotope labelling with amino acids in cell culture (SILAC) and proteomic profiling, to be novel substrates of the γ-secretase (Hemming et al., 2008). Cells in the presence of DAPT (an inhibitor of the γ-secretase) were labelled with the light isotope label while DMSO-treated cells were labelled with the heavy isotope. In the presence of DAPT, an increase in the C-terminal fragment was seen since it was not cleaved to release the ICD, and this difference could be seen when relative abundance of peptides between the two conditions were measured by liquid chromatography mass spectrometry (LC-MS).

However, only one peptide corresponding to the LDLr was identified in this way. In addition, the LDLr was not studied further by over-expression in mammalian cells like the other proteins identified by the authors of that publication. As a result, the LDLr was not confirmed as a γ-secretase substrate. In another study, the LDLr was also investigated in addition to LRP-1 for the release of ICD, except that the release of an ICD fragment of the LDLr was shown not to occur (May et al., 2002; May et al., 2003). Therefore, more experiments need to be performed to investigate whether the LDLr also undergoes sequential cleavage like Notch-1 processing and like other LDLr family members. It would be of interest to test if the C-terminal fragment of the LDLr undergoes intramembrane proteolysis. The accumulation of the C-terminal fragment of the LDLr could be investigated in the presence of DAPT for future work, to confirm the LDLr as a γ-secretase substrate.

When soluble LDLr levels were compared between the two TACE deficient cells lines, the TACE-/- mouse fibroblasts showed higher soluble LDLr production than the CHO M2 cells. It was thought that there might be more sheddase activity in the TACE-/- mouse fibroblasts than the CHO M2 cells. To investigate sheddase activity in the TACE deficient cell lines, cell lysates were tested for the cleavage of the TNF-α stalk peptide. From the TNF-α stalk peptide cleavage assays, TACE-/- mouse fibroblasts were shown to be ~2.4-fold more efficient than the CHO M2 cells at cleavage (Fig. 5.12). This suggested that there were other non-TACE sheddases present in mouse fibroblasts that were not in the CHO M2 cells, or that there were different levels of expression of different sheddases. Of the sheddases that cleave the TNF-α stalk peptide, ADAM 9 and ADAM 10 were chosen as candidate sheddases for further investigation, as these

ADAMs were also studied as alternative sheddases for TACE substrates (Rosendahl et al., 1997; Roghani et al., 1999; Vincent et al., 2001; Deuss et al., 2008).

ADAM 9 expression levels were the same in TACE-/- mouse fibroblasts and CHO M2 cells (Fig. 5.13), suggesting that this sheddase might not contribute to increased cleavage of the TNF-α stalk peptide in these cells. ADAM 10 expression levels were ~2.7-fold higher in TACE-/- mouse fibroblasts than in the CHO M2 cells (Fig. 5.14), implicating ADAM 10 as a candidate sheddase responsible for TNF-α cleavage in TACE-/- mouse fibroblasts. Since ADAM 10 is the most closely related to TACE in terms of sequence and substrate specificities (Killar et al., 1999; Rosendahl et al., 1997; Edwards et al., 2008), it was thought that ADAM 10 might play a role in the shedding of the LDLr in TACE-/- mouse fibroblasts.

To investigate whether ADAM 10 was associated with or interacted with the LDLr in TACE-/- mouse fibroblasts, co-immunoprecipitation studies were performed. Co-immunoprecipitation was used previously to provide evidence of ADAM 10 and ADAM 10 substrate association (Hattori et al., 2000; Gavert et al., 2007; Lemieux et al., 2007). In Fig. 5.16, the LDLr was detected in the LDLr expressing cells and in the presence of a cross-linker, an oligomer was formed. Both the cross-linking and IP were successful as shown by the LDLr band and the oligomer band (Fig. 5.16). No ADAM 10 was detected in the LDLr immunoprecipitated samples when the ADAM 10 antibody was used to detect ADAM 10 interactions (Fig. 5.17). These results suggested that either ADAM 10 was not involved in the shedding of the LDLr, at least in the case of the wt-LDLr in the absence of TACE, or that the association between the ADAM 10 and the LDLr was not long enough for the detection thereof. With respect to the cross-linking, it could also

possibly be that the cross-linker preferentially allowed LDLr-LDLr formation rather than the LDLr-sheddase formation, since the on-off rate between the enzyme and receptor could be too fast.

Researchers that have used co-immunoprecipitation to illustrate interactions between ADAM 10 and ADAM 10 substrate have used transfected ADAM 10 constructs in their experiments (Hattori et al., 2000; Gavert et al., 2007; Lemieux et al., 2007). Co-immunoprecipitation confirmed that ADAM 10 associated with ephrin-A2, a glycosyl-phospatidylinositol (GPI)-bound membrane protein shed by ADAM 10 (Hattori et al., 2000). For the co-immunoprecipitation, cells were co-transfected with differently tagged constructs, and probed with antibodies specific to the tags. As a control a GPI-anchored protein that was not shed by ADAM 10, did not form a complex. Co-transfection of tagged CD 23 and tagged ADAM 10 also indicated an association between the two proteins using antibodies against the tagged proteins (Lemieux et al., 2007). The association between a GFP-tagged L1-CAM and a tagged ADAM 10 was also shown (Gavert et al., 2007). It is also possible that a different co-localisation between the ADAM 10 and LDLr exists, compared to the proteins in the above-mentioned studies, which may have affected the IP.

ADAM 10 is a likely candidate to investigate further. In addition, the expression of ADAM 19 or other MMPs could be investigated in mouse fibroblasts and could be a possible target for down-regulation, to determine if other sheddases have a role in the shedding of the LDLr. Future work that could be explored would be to assay soluble LDLr shedding levels in TACE-/- mouse fibroblasts in the presence of ADAM 10

siRNA, for the specific down-regulation of ADAM 10 to determine the role ADAM 10 has in LDLr shedding.

In conclusion, the constitutive level of LDLr shedding was not totally dependent on TACE activity in mouse fibroblasts, while in CHO cells the shedding data showed that the constitutive and phorbol-stimulated production of soluble LDLr was almost completely dependent on TACE activity. This phenomenon was mostly due to the higher sheddase activity present in TACE-/- mouse fibroblasts. ADAM 10 expression was confirmed to be higher in TACE-/- mouse fibroblasts and is a likely candidate to investigate further in the shedding of the LDLr.

Chapter 6:

Detection of soluble LDLr in human plasma

6.1 Introduction

A number of unrelated membrane-bound proteins have been found to be released by cleavage secretion into the medium of cultured mammalian cells (Peschon et al., 1998; Arribas and Borroto, 2002; Mezyk et al., 2003). Studies on the ectodomain shedding of proteins have provided some insight into the functions of the soluble proteins (Arribas and Borroto, 2002; Rebeck et al., 2006; Edwards et al., 2008). The formation of soluble LDLr was observed in cultured human skin fibroblasts as well as LDLr transfected CHO cells (Begg et al., 2004). Some soluble protein ectodomains have been found in human plasma, such as TNF-α, TNF-α receptors (Aderka, 1996) and other cytokines and receptors (Novick et al., 1992). Studying the plasma proteome is very useful for the evaluation of soluble proteins as biomarkers in cancers and other diseases (Aderka, 1996; Gattorno et al., 1996; Cavusoglu et al., 2007). The plasma proteome however is a complex system, as its dynamic range extends over several orders of magnitude, making the detection of low abundance proteins extremely difficult. A further complication is the small volumes of plasma used for analysis.

The aim of this section of the project was to identify and characterise soluble LDLr in human plasma. The identification of other members of the LDLr family in plasma (Quinn et al., 1997) as well as the presence of a urinary LDLr (Molina et al., 2007) increased the possibility of finding soluble LDLr in plasma. The urinary LDLr corresponded to residues 4-166 of the ligand binding domain. To ascertain whether the formation of

soluble LDLr occured in humans *in vivo,* the following approaches were used: lectin affinity chromatography, immunoprecipitation and enrichment of plasma.

6.2 Results

6.2.1 Detection of soluble LDLr in plasma using lentil lectin affinity chromatography

The rationale for using lectin affinity was that glycosylated proteins, including the soluble LDLr (as it is O-glycosylated), would bind to the lentil lectin Sepharose beads. This should result in an enrichment of the plasma glycosylated protein fraction.

Human plasma was incubated with lentil lectin Sepharose beads and after washing, the glycoproteins were eluted. The buffer was exchanged to remove sugars, and protein sample was concentrated. Proteins were separated on SDS-PAGE (7 % gel) and proteins were analysed by Coomassie staining and Western blotting.

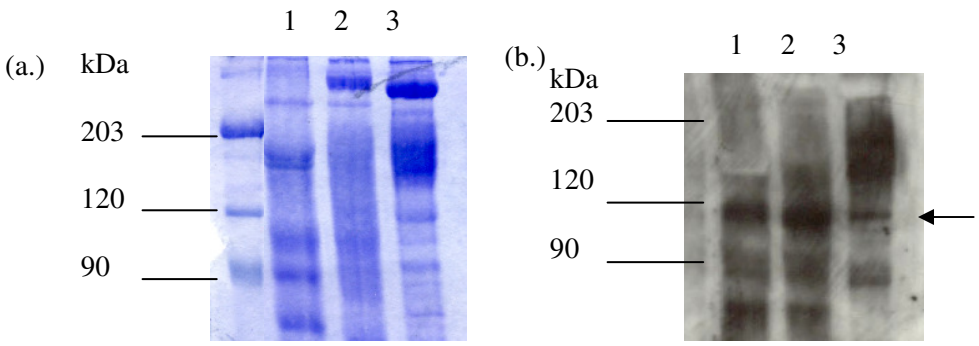

Figure 6.1: Detection of soluble LDLr from plasma glycoproteins by SDS-PAGE (a) and Western blot (b).
Plasma was incubated with lentil lectin Sepharose beads. After washing, the glycoproteins were eluted in 0.2 M α-D-mannopyranoside, and concentrated. Samples were separated by SDS PAGE (7 % gel) and stained with Coomassie or analysed with the rabbit polyclonal antibody to the LDLr.
Lane 1: lentil lectin Sepharose with bound glycoproteins, reduced with β-ME. Lane 2: 3 µl eluted glycoproteins, reduced with β-ME. Lane 3: 3 µl eluted glycoproteins, non-reduced. The arrow indicates a 120 kDa protein detected by the antibody to the LDLr

The Coomassie stained polyacrylamide gel in Figure 6.1 (a.), showed a number of proteins that were bound to (lane 1) and eluted from lentil lectin Sepharose beads (lanes 2 and 3). A protein at ~120 kDa was observed, indicated by the arrow [Fig. 6.1 (b), lane 3]. This is in agreement with the expected molecular weight of soluble LDLr that was released into the medium of cultured cells. When the sample was reduced, the higher molecular weight bands dissociated into the 120 kDa band, as more of this component was seen, migrating just above 120 kDa marker [Fig. 6.1 (b.)]. Other bands were also observed which could be due to degradation products (~85 kDa band) or aggregation of soluble LDLr (high molecular weight bands in lane 3), or non-specific binding to other proteins. Detection using only the secondary antibody as a control showed no interaction

with the bands of interest, indicating that the bands seen here were specific for the LDLr antibody (data not shown).

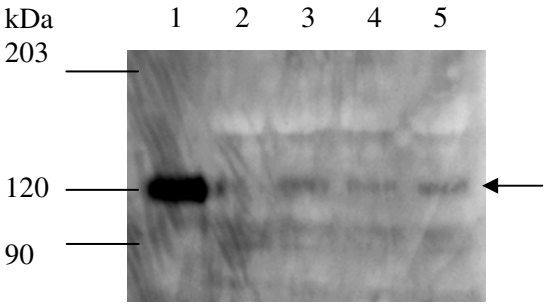

Figure 6.2: Detection of soluble LDLr from plasma glycoproteins by western blot.
Plasma was incubated with lentil lectin Ssepharose beads. After washing, the glycoproteins were eluted in 0.2 M α-D-mannopyranoside, and concentrated. Samples (3 µl) were loaded on 7% SDS PAGE and analysed with the rabbit polyclonal antibody to the LDLr.
Lane 1: 20 µl Mmedium (harvested from CHO LDLr expressing cells). Lanes 2-5: A range of plasma glycoprotein samples. All the samples contained β-ME. The arrow indicates the 120 kDa protein detected by the LDLr antibody.

The experiment was repeated using the same conditions as before with different plasma samples. As a control, a medium sample containing recombinant soluble LDLr (Fig. 6.2, lane 1) was loaded onto the SDS-PAGE. A protein that migrated with the same Rf value (indicated by the arrow) as the recombinant soluble LDLr control was seen. The protein detected here in all the plasma glycoprotein samples (lanes 2-5) was the same size as the protein seen in Figure 6.1. This time there was a fainter signal compared to Figure 6.1, as a longer exposure was needed to detect this signal. The faint signal that was seen could have been due to less glyocoproteins in the eluted sample, and therefore less non-specific binding was also seen.

From Figures 6.1 and 6.2, it seemed likely that the protein which immuno-reacted with the LDLr antibody was soluble LDLr. However, the elution and further characterisation of the plasma glycoproteins proved problematic due to the tight interaction between the sugar moieties of proteins and the lentil lectin Sepharose beads resulting in elution of glycoproteins in the range of ~0.2 % -0.8 %. For this reason, this approach was not used in an attempt to purify soluble LDLr from plasma.

6.2.2 Detection of soluble LDLr from plasma using IP

IP was used to determine if soluble LDLr existed in plasma. Some plasma proteins have previously been isolated using antibody affinity chromatography (Sutcliffe et al., 1980; Cawston et al., 1986; Tseng et al., 2004). The ExactaCruz IP methodology was used to identify soluble LDLr. This approach enables one to immunoprecipitate with a mouse monoclonal antibody and to detect with a rabbit polyclonal antibody for the Western blot. Furthermore, the use of a HRP-linked secondary antibody that is specific for the rabbit polyclonal antibody avoids the detection of the light and heavy chains of the IP antibody. Pre-cleared plasma was used for the IP with the C7 monoclonal antibody, while the rabbit polyclonal antibody to the LDLr was used for the Western blot.

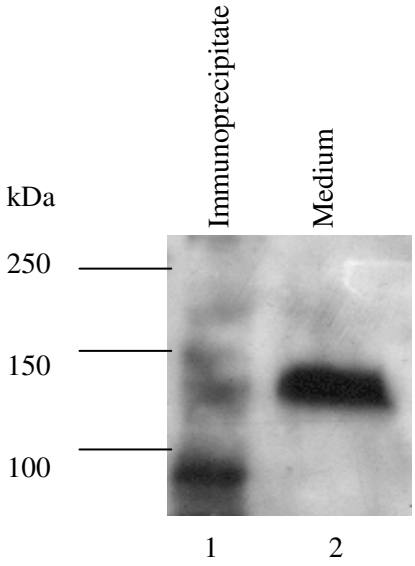

Figure 6.3: Detection of soluble LDLr from plasma by IP and western blot
Precleared plasma was immunoprecipitated with a C7 monoclonal antibody to the LDLr and loaded on 7% SDS-PAGE and for western blot analysis it was probed with the rabbit polyclonal antibody to the LDLr.
Lane 1: Imunnoprecipitate of plasma. Lane 2: Medium (harvested from CHO LDLr expressing cells). The samples contained β-ME.

From the Western blot (Fig. 6.3), the immunoprecipitated plasma sample showed two bands in the region of interest (in comparison to the soluble LDLr control), as well as a smaller component migrating at ~95 kDa. However, it is not certain if the ~140 kDa band is the only fragment released into plasma as a result of ectodomain shedding, as it is possible that the lower band is a differently shed form of soluble LDLr or a degradation product. Even though plasma was precleared using protein G, it did not completely remove all the IgG present in the sample. In addition, IgG and other high abundant proteins present in the plasma sample could have interfered with the IP, and therefore a more definitive signal was not seen. For IP, IgG and albumin removal is important to be able to obtain a more prominent signal.

6.2.3 Detection of soluble LDLr from enriched plasma

The plasma proteome is a complex mixture of proteins and a major obstacle in finding small abundant proteins within the human plasma proteome is that the high abundant proteins mask those present in very low concentrations. This limitation is somewhat overcome with the emergence of albumin, IgG, albumin/IgG or other high abundance protein removal kits. However, these approaches are antibody based and use very small volumes, ranging from 50-100 µl.

The Proteominer protein enrichment kit (Bio-Rad) uses the principle of a bead-based library of combinatorial peptide ligands to deplete high abundant proteins from plasma (Guerrier et al., 2006). When plasma is applied to the beads, the proteins bind to the ligands. When peptides become saturated by the high abundant proteins, excess proteins pass through the column. The complexity of the sample is reduced, while all representative proteins are maintained. After the plasma sample was applied, the beads were washed and the plasma proteins were eluted. After elution, plasma proteins were separated by SDS-PAGE. Following the enrichment of low abundance plasma proteins and separation by SDS-PAGE, a One-Step Western™ system was used, in which only the primary antibody was used for detection to minimise non-specific interactions.

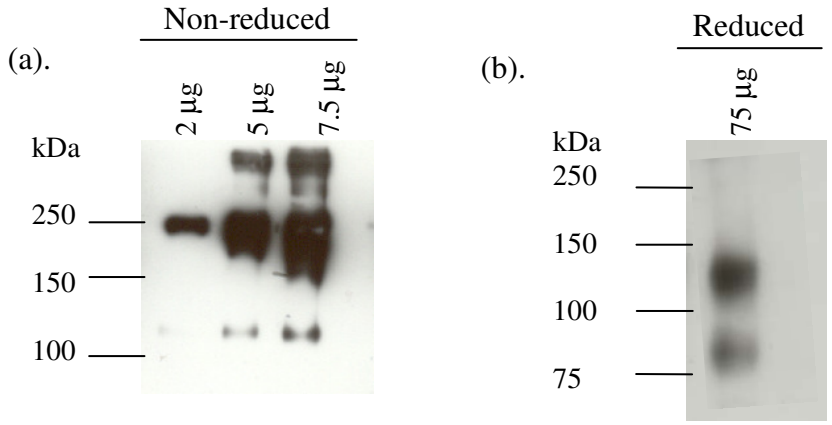

Figure 6.4: Detection of soluble LDLr from enriched plasma using a One-Step Western system.
(a). Eluted, enriched plasma proteins, non-reduced (b). Eluted, enriched plasma proteins, reduced with β-ME. High abundance plasma proteins were removed from plasma by the enrichment of small abundant proteins by the Proteominer system (Bio-Rad), and separated on 7 % SDS-PAGE. The rabbit polyclonal antibody was used to detect soluble LDLr.

When the One-Step Western™ system was used, the non-reduced samples display a high molecular weight band at ~250 kDa band [Fig. 6.4 (a).] in addition to a band of ~120 kDa. Both component intensities increased when an increasing concentration of proteins was loaded. The 250 kDa component could be a dimer of soluble LDLr that dissociates when reduced [Fig. 6.4 (b).] (van Driel et al., 1987). The amount of reduced sample was increased 10-fold to amplify the chances of seeing soluble LDLr, since the antibody used in this experiment was able to detect reduced LDLr albeit to a lesser extent. Under reduced conditions, the cysteine-rich receptor unfolds and the mobility of the protein is reduced (Daniel et al., 1983). In the reduced sample, two proteins were detected, one at ~140 kDa that was likely the soluble LDLr migrating slower due to the reduction the disulfide binds and subsequent conformational change, and a smaller unknown

component of ~85 kDa, which could be a degradation product. The reduced protein of ~140 kDa corresponded to the size of soluble LDLr from medium, in addition to the bands seen in the plasma sample seen in Figure 6.3, lanes 2 and 1, respectively. The bands do not correspond exactly to the sizes seen in Figures 6.1 and 6.2, which could be due a different marker used in those Western blots.

The presence of an LDLr dimer has been demonstrated before, where both the dimer and monomer were able to bind the LDLr antibody and radio-labelled LDL in ligand blots (van Driel et al., 1987). LDLr incubated with increasing concentrations of LDL followed by separation on native PAGE, showed a decrease in dimer and monomer bands under increasing LDL concentrations (Jeon and Shipley, 2000). A recombinant soluble LDLr fragment also formed a dimer (Marlovits et al., 1998c).

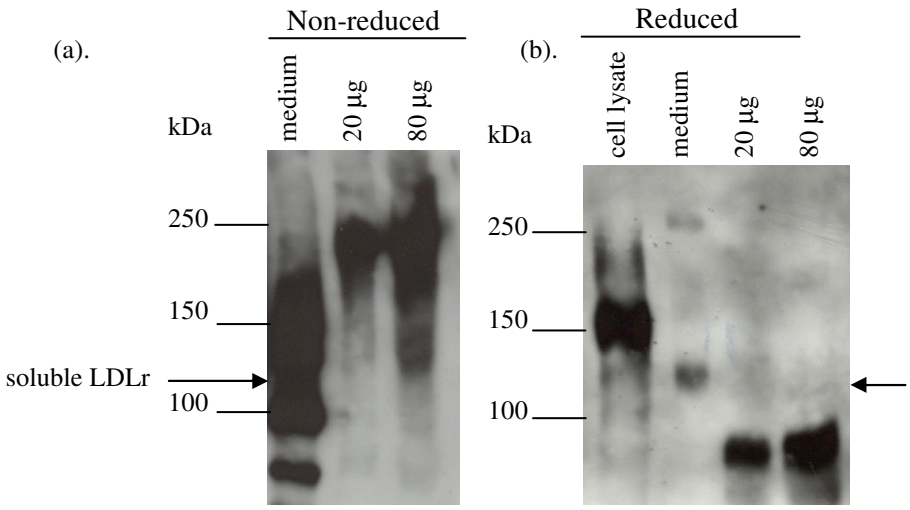

Figure 6.5: Detection of soluble LDLr from enriched plasma using anti-goat LDLr

(a). Medium (harvested from CHO LDLr expressing cells) was loaded as a control. Eluted, enriched plasma proteins, non-reduced (b). Cell lysate and medium (harvested from CHO LDLr expressing cells) were loaded as controls. Eluted, enriched plasma proteins, reduced with β-ME. High abundance plasma proteins were removed from plasma for the enrichment of small abundant proteins by the Proteominer system (Bio-Rad), and separated on 7 % SDS-PAGE.

To achieve an improved signal for the reduced form of the receptor, a different LDLr antibody was used for the following experiment, as according to the suppliers, this antibody was able to bind both the reduced and non-reduced form of the LDLr. In the non-reduced medium sample, the soluble LDLr was detected as indicated by the arrow. The other non-specific bands were due to the antibody binding to proteins present in FCS in the sample as tested as a control before (data not shown). Perhaps some of the non-specific bands were from the antibody binding to bovine soluble LDLr present in FCS. In the non-reduced plasma protein samples, the antibody detected a high molecular weight band [Fig. 6.5 (a).]. This band again disappeared on reduction with β-ME [Fig. 6.5 (b).]. In the reduced samples, a fainter band at ~100 kDa (indicated by the arrow), which was smaller than the recombinant soluble LDLr. There was also a prominent band at 85 kDa,

as seen previously [Fig. 6.4 (b).]. The high molecular weight band could be an oligomer of the 85 kDa band. To eliminate the possibility of non-specific binding of the secondary antibody, the nitrocellulose membrane was stripped and reprobed with the secondary antibody alone. There were no bands detected by the secondary antibody, indicating that the interactions detected were solely due to the primary antibody used in Figure 6.5.

6.2.4 Binding of soluble LDLr to its ligand

Since the soluble LDLr shed from CHO LDLr expressing cells contained the ligand binding domain, it was determined whether soluble LDLr could bind its ligand LDL by using native and SDS-PAGE. Due to the reported molecular weight of LDL to be ~2500-3500 kDa (Fisher et al., 1975), and the molecular weight of the soluble LDLr being ~140 kDa (under non-reducing conditions) (Begg et al., 2004), gradient gel electrophoresis (GGE) was performed. This method is advantageous in that a high resolution is obtained during the separation of a range of high molecular weight and low molecular weight proteins within a particular sample. LDL was incubated with medium containing soluble LDLr and detected for LDLr by Western blotting.

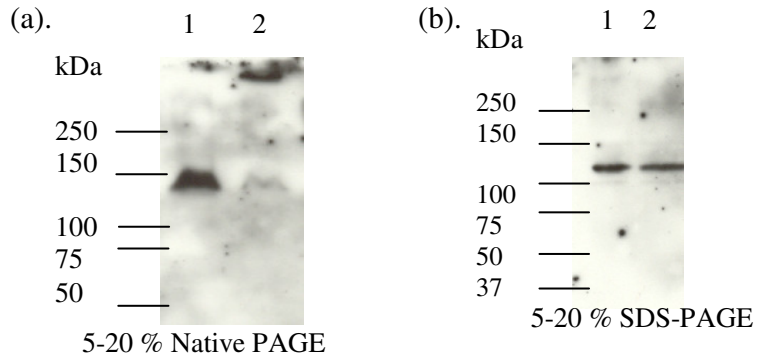

Figure 6.6: Interaction of soluble LDLr from medium and LDL from plasma, shown by GGE and western blot.
Lane 1: 20 µg of medium proteins. Lane 2: 13.8 µg of medium proteins + 7.5 µg LDL. Medium and LDL were incubated on ice for 15 minutes, prior to loading. Samples were loaded on 5-20% gradient gels, under native (a), or denatured conditions (b). The rabbit polyclonal antibody was used to detect soluble LDLr.

Under native conditions, in the absence of LDL, soluble LDLr from conditioned medium was detected at ~140 kDa [Fig. 6.6 (a), lane 1]. When the LDL was added to soluble LDLr in conditioned medium a gel shift was observed with the band now running at a higher molecular weight [Fig. 6.6 (a), lane 2]. In the presence of the ionic detergent SDS, the soluble LDLr was detected at ~120 kDa, [comparing Fig. 6.6 (a) and (b)], the SDS present resulted in the protein becoming more negative, and migrating at a faster rate [Fig. 6.6 (b), lane 1]. When the same LDL-medium mixture was separated by GGE in the presence of SDS, the complex that was formed was disrupted before entering the gel and no gel shift was seen, since the LDLr was not bound to LDL. Hence, the soluble LDLr was detected with a molecular weight of ~120 kDa [Fig. 6.6 (b), lane 2].

6.3 Discussion

Taking the lectin affinity chromatography, IP and protein enrichment experiments into account, it appears that the soluble LDLr does indeed exist in plasma, migrating as a ~120 kDa protein, under non-reducing SDS-PAGE conditions with a similar Rf value as the shed LDLr seen *in vitro*. A factor causing variation between the levels of soluble LDLr for each of the above experiments could be the use of different methods and the use of different plasma samples. In addition to the 120 kDa band, smaller degradation products were also detected, indicating that proteases present in plasma cleaved the soluble LDLr further. This is probable, since the urinary LDLr corresponds to only part of the ligand binding domain (Molina et al., 2007). In all the Western blot experiments except for Figure 6.5, a rabbit polyclonal antibody was used, and a protein of soluble LDLr size as well as a smaller product was seen. However, in Figure 6.5 the ratio between the smaller band to the larger band was higher. A possible explanation could be that the LDLr which was cleaved further resulted in a confirmation that was suited for the goat polyclonal antibody, and therefore a stronger interaction occurred. Another factor in observing a lower amount of the 85 kDa component in Figure 6.4 (b) compared to Figure 6.5 (b), could be attributed to the fact that the eluted plasma proteins that were used in the latter experiment were stored for approximately two weeks at -20℃ before being used. As a result, degradation in the protein sample could have occurred.

Besides identifying the soluble form of the LDLr in plasma, the data also suggested that the soluble LDLr formed a dimer. The dimer formation of the full length membrane LDLr and purified LDLr was shown previously (van Driel et al., 1987). It was also suggested that dimer formation in intact cells occurred via the cytoplasmic tail, as mutants containing a stop codon at position 792 or 807, were unable to form dimers.

Furthermore a mutant containing a cysteine at 807 underwent increased dimerisation compared to wild-type, supporting the theory. On the other hand, it was suggested that the LDLr dimer formation occurred in the extracellular domain, in a confirmation favouring interactions between the EGF repeats (Jeon and Shipley, 2000). Moreover, a recombinant soluble LDLr has been shown to form a dimer, indicating that dimerisation can occur via the ligand binding domain (Marlovits et al., 1998c). It is plausible that dimerisation could occur through the ligand binding domain since this domain is cysteine-rich.

From the ligand binding experiment, soluble LDLr from medium was able to bind LDL in the absence of SDS, since an LDL-LDLr complex was formed and a higher molecular weight was observed [Fig. 6.6 (a), lane 2]. In the presence of SDS this complex was disrupted before entering the gel and LDL did not associate with the LDLr [Fig. 6.6 (b), lane 2]. This was expected since the binding of the ligand to LDLr presumably takes place via the positively charged amino acids on the apo-B-100 protein of the LDL molecule, and the negative charged residues in the ligand binding domain of the LDLr (Brown et al., 1997; Innerarity, 2002).

Binding of detergent solubilised full-length LDLr to LDL was studied in the same way, where the LDLr was incubated with LDL before analysis by native PAGE and Western blotting (Jeon and Shipley, 2000). In the presence of calcium, decreased levels of LDLr were shown with increased levels of LDL in the sample. However, the binding was not studied in the presence of SDS.

A similar experiment was performed previously, where the interaction of LDLr and LDL was investigated and showed by ligand blotting after SDS-PAGE (Daniel et al., 1983). The difference between the experiment performed by Daniel et al., and the one presented in this study was that in their system the SDS was removed after transfer of proteins to nitrocellulose membranes, and the ligand was able to bind. In Figure 6.6 (b), lane 2, the SDS was not removed from the system, and the interaction between LDL and LDLr did not occur. Since the complex could not be formed, it did not enter the gel as a complex and was not seen as one [Fig. 6.6 (b), lane 2]. In the same publication however, they showed by a membrane filter assay that purified LDLr was able to bind LDL, as long as the receptor was not reduced, indicating that the intramolecular chains were intact, since LDLr denatured by guanidine was able to bind the ligand (Daniel et al., 1983). It may be possible though that through a dialysis step before ligand binding removed the guanidine present in the sample, and refolding of the protein occurred (Maxwell et al., 2003; Ma et al., 2008), resulting in binding of the ligand. It was also shown for a recombinant disulphide-rich soluble lectin-like oxidized LDL scavenger (LOX-1) receptor, that binding to oxidized LDL took place after a step-wise removal of guanidine (Vohra et al., 2007).

Possible roles for the ectodomain release of soluble LDLr family members have been proposed. Soluble LRP-1 was purified from plasma by ligand affinity and also shown to bind RAP ligand blots (Quinn et al., 1997; Quinn et al., 1999). The LRP-1 was suggested to modulate Aβ clearance from the brain, as well as in the systemic clearance of Aβ in the liver (Sagare et al., 2007; Deane et al., 2008). In addition the physiological role of soluble LRP-1 in plasma has been implicated to act as an Aβ “sink”, important in the

prevention of the amyloidogenic Aβ peptide in the brain, and prevention of Alzheimer's disease.

LRP-1, ApoER2 and vLDLr were shown to undergo release of the ICD following cleavage by a γ-secretase (May et al., 2002; May et al., 2003; Hoe and Rebeck, 2005). Ectodomain shedding of the LDLr family members such as ApoER2 and vLDLr increased in the presence of ligand (Hoe and Rebeck, 2005). The soluble forms of LDLr family members, vLDLr and ApoER2 were shown to bind some ligands, such as HRV-2 and Reelin, respectively. The function of soluble ApoER2 was determined by showing that it binds to Reelin, acting as a dominant negative receptor and inhibited Reelin signaling in neurons.

Soluble LDLr and vLDLr were suggested to be preventative in common cold infection by binding to HRV-2 *in vitro* (Marlovits et al., 1998a; Marlovits et al., 1998b). Recombinant LDLr comprising of the ligand binding domain was also shown to bind to β-VLDL. In addition a 28-kDa form of soluble LDLr in cultured cells was produced in response to IFN (Fischer et al., 1993). This fragment acts as an antiviral protein in cell culture. It may be possible that such a fragment exists in plasma or that this may be the same fragment that was purified from urine (Molina et al., 2007). A soluble form of the LDLr encompassing the ligand binding domain, proven to bind LDL, was shown to inhibit hepatitis C infection of hepatic cells, while the shorter urinary LDLr fragment could not bind LDL.

Since the LDLr is as yet not known to be involved in signaling, and it is not confirmed whether the ectodomain release initiates the release of an ICD to function as a

downstream signal, the role of soluble LDLr *in vivo* is not clear. No other physiological function has yet been attributed to the function of soluble LDLr formation. It can only be speculated that since the soluble LDLr binds to LDL, it can prevent uptake of LDL into cells. However, we do not know what the half-life of soluble LDLr in plasma is for it to cause an effect. Cleavage of LDLr family members could affect protein turnover, reducing the half-life in cells and preventing lipoprotein uptake (Rebeck et al., 2006). In addition to post-translational regulation by PCSK9, the LDLr appears to be targeted for down-regulation through ectodomain release, and subsequent binding of the released ectodomain to LDL and preventing uptake.

In conclusion, the presence of a ~120 kDa soluble LDLr was shown to be present in plasma, which corresponded to the size of soluble LDLr formed *in vitro*, and probably undergoes further degradation. The soluble LDLr forms a dimer which dissociates when reduced. In addition, it was confirmed by native GGE that recombinant soluble LDLr bound to plasma LDL and in the presence of SDS the interaction was lost, which further confirmed that the charge of the receptor and ligand was important for binding.

Conclusions

The aim of this thesis was to investigate the ectodomain cleavage of the LDLr, with respect to the role of TACE toward soluble LDLr formation *in vitro* and to establish if the existence of soluble LDLr is physiologically relevant.

The production of soluble LDLr was previously shown to be a product of ectodomain shedding, and TACE was implicated in the ectodomain release of membrane-bound LDLr. Since there was no antibody available (during the initial stages of the project) that could detect soluble LDLr from medium by Western blot, the LDLr was tagged with GFP on the extracellular N-terminus in an attempt to study the localisation of the LDLr, allowing shed constructs to be assayed by fluorimetry to characterise the ectodomain shedding. However, stable transfection of GFP constructs was not successful. Also, the use of GFP as a tag for the LDLr to assess shedding levels was not feasible as the stability of the construct was compromised in mammalian cells. This was probably due to incorrect folding and subsequent degradation of the GFP. Therefore the use of the GFP to investigate the shedding of the LDLr could not be pursued any further. Moreover, an antibody that could detect soluble LDLr from medium was sourced during the course of this thesis and immuno-blotting with this antibody to the LDLr was used in assessing LDLr shedding levels.

Neither GFP(s) nor the LDLr could be expressed in TACE+/+ mouse fibroblasts. The results from the GFP transfections indicated that there was a general problem of expressing constructs in these cells. In addition, cell lysates and medium of TACE+/+

mouse fibroblasts that were transfected with the LDLr showed no presence of full-length LDLr or soluble LDLr, respectively.

Knock-out cell lines were utilised to investigate whether TACE was involved in the shedding of the LDLr and thus its ectodomain release was assessed in TACE-/- mouse fibroblasts. Under constitutive conditions, TACE independent shedding of the LDLr occurred in TACE-/- mouse fibroblasts. This indicated that under constitutive conditions in the absence of TACE, other sheddase(s) take over the role of ectodomain cleavage, as was found with TNF-α and APP (Zheng et al., 2004; Deuss et al., 2008). Phorbol-stimulated shedding of the LDLr in TACE-/- mouse fibroblasts did not increase over un-stimulated conditions, indicating that TACE was a major sheddase of stimulated shedding, at least for the wt-LDLr and the 792-LDLr. The JD-LDLr mutant was possibly shed by a different secretase but this was not confirmed as levels could not be compared to levels in TACE+/+ mouse fibroblasts.

In addition, shedding of the LDLr was assessed in CHO M2 cells, an alternative TACE deficient cell line, so that it could be compared to shedding in CHO A7 cells. By the evaluation and comparison of the ectodomain release of the LDLr in CHO M2 to that of CHO A7 cells, it was shown that the LDLr was a substrate almost completely dependent on cleavage by TACE both in the absence and presence of phorbol stimulation. The internalisation mutants did not undergo increased ectodomain release compared to wt-LDLr in the absence or presence of phorbol in CHO M2 cells, which indicated that in the absence of TACE the lack of internalisation did not increase the ectodomain release of the LDLr.

Constitutive levels of soluble LDLr were 5-fold higher in the TACE-/- mouse fibroblasts than in the CHO M2 cells. From the fluorogenic TNF-α cleavage assays, the increased production of soluble LDLr could be attributed to the ~2.4-fold higher sheddase activity. Western blot analysis of ADAM 10 expression supported the results seen for the TNF-α cleavage assays, with a concomitant ~2.7-fold increase in ADAM 10 expression in the TACE-/- mouse fibroblasts compared to the CHO M2 cells. This suggested that ADAM 10 was the major sheddase contributing to the elevated sheddase activity in TACE-/- mouse fibroblasts.

Due to this finding, it was thought that ADAM 10 was a possible candidate sheddase involved in the constitutive shedding of the LDLr in TACE-/- mouse fibroblasts. Even though the co-immunoprecipitation experiments only revealed a self-association between the LDLr protein and not an association between LDLr and ADAM 10, this does not exclude the possibility of the involvement of ADAM 10 in the shedding of the LDLr.

Results from the two TACE deficient cell lines indicated that in mouse fibroblasts: (i) soluble LDLr production was higher, (ii) TNF-α sheddase activity was higher and (iii) ADAM 10 expression was elevated. These data support previous findings which suggested that depending on the cell type and conditions investigated, different sheddases can be substituted in the absence of a particular sheddase, thus leading to the redundancy or compensatory mechanisms which exist between ADAMs (Chow and Fernandez-Patron, 2007).

In the absence of SDS a recombinant soluble LDLr bound plasma LDL, confirming that the ligand binding domain of the soluble LDLr was still able to bind ligand. However, in

the presence of SDS the interaction was lost, which highlighted the importance of the role of non-covalent interactions between the LDLr and ligand for binding.

The detection of soluble LDLr in human plasma as determined by Western blot analysis suggests a physiological relevance for soluble LDLr formation *in vivo*. A smaller degradation fragment was also detected by these methods, which suggested that soluble LDLr released into plasma was cleaved by proteases at other sites within the ectodomain. The generation of a smaller LDLr fragment was also detected in human urine previously (Molina et al., 2007).

The putative physiological function of soluble LDLr formation in human plasma could be the down-regulation of cell surface receptor, ectodomain release and concomitant binding to plasma LDL (or other ligands such as HRV-2), thus reducing LDL (or HRV-2) uptake into cells (Marlovits et al., 1998a; Marlovits et al., 1998c). In addition, it was suggested previously that soluble LDLr could function as an LDL trap, if the LDLr were to become deposited in atherosclerotic plaques, potentially accelerating the harmful effects of atherosclerosis (Begg et al., 2004). Further studies on the *in vivo* production of soluble LDLr with respect to binding of ligands could elucidate the role of the LDLr in the prevention of the common cold, VSV, and hepatitis C infection.

Further studies through the investigation of ADAM 10 inhibition/down-regulation in TACE-/- mouse fibroblasts could clarify the role of ADAM 10 in LDLr shedding. Additionally, since the JD-LDLr shedding was up-regulated by phorbol in the absence of TACE, ADAM 10 could possibly play a bigger role in the shedding of this construct. The

purification of soluble LDLr from plasma could be addressed as well, which needs extra optimisation methods, important for the determination of the cleavage site.

PCSK9-mediated degradation and ectodomain release are two mechanisms of post-translational regulation that the LDLr undergoes. Therefore future questions related to LDLr regulation to answer are, whether the increase of LDLr expression by statins impact LDLr shedding physiologically and what the implications are of TACE-mediated ectodomain release of the LDLr for cholesterol metabolism.

This thesis has provided a characterisation of the ectodomain release of the LDLr and the implications of a soluble LDLr in plasma provide the foundation for the further investigation of soluble LDLr formation *in vivo* to understand its role in cholesterol metabolism.

Appendix I

Primer sequences for the GFP constructs are shown in Fig. I.

Forward primer signal peptide:

Xba I
5'~TGCTCTAGAATGGGGCCCTGGGGC~3'

Reverse primer signal peptide:

5'~CTGCTTGCTCACCATAGTTCCTGCTGCTGC~3'

Forward primer GFP:

5'~GCAGCAGCAGGAACTATGGTGAGCAAGCAG~3'

Reverse primer GFP(s):

Hind III
5'~CCCAAGCTTTTACACCCACTCGTGCAG~3'

Reverse primer GFP(MCS):

Hind *Not* I *Cla* I *Kpn* I *Bam* HI
5'~CCCAAGCTTTGCGGCCGCATCGATGGTACCGGATCCCACCCACTCGTGCA~3'

Forward primer LDLr:

5'~CGGGGTACCGCAGTGGGCGACAGATGTGAAAGAAAG~3'

Reverse primer LDLr:

Hind III
5'~CCCAAGCTTTCACGCCACGTCATCCTC~3'

Figure I: Primers used in the construction of GFP vectors and GFP-LDLr fusion protein.
The underlined sequence indicates incorporated restriction enzyme site sequences.

Primer sequences for mutagenesis are shown in Fig. II.

Forward primer 792-LDLr:

Aat II

5'~CCTTCTATGGAAGAACTGACGTCTTAAGAACATCAACAGC~3'

Reverse primer 792-LDLr:

Aat II

5'~GCTGTTGATGTTCTTAAGACGTCAGTTCTTCCATAGAAGG~3

Forward primer JD-LDLr:

Bfi I

5'~CCCAGTCTGTCAGAAGACCACAG~3'

Reverse primer JD-LDLr:

Bfi I

5'~CTGTGGTCTTCTGACAGACTGGG~3'

Figure II: Primers used in the site-directed mutagenesis of the LDLr.

Complementary mutagenic primers were designed containing the mutation of interest (shown in red), as well as a silent mutation (shown in bold) introducing a unique restriction enzyme site to facilitate screening. WatCut was used in the design of mutagenic primers (http://watcut.uwaterloo.ca/watcut/watcut/template.php Michael Palmer, University of Waterloo, Canada). Underlined sequences indicate novel restriction enzyme site sequences.

Appendix II

Reagents and Buffers

Ampicillin (100 mg/ml)

100 mg Ampicillin in 1 ml water

10 % AMPS

0.1 g AMPS in 1 ml water

40 % acrylamide stock

40 % acrylamide

1.06 % bis-acrylamide

6 X DNA loading dye (5 ml)

0.025 g Bromophenol Blue

0.025 g Xylene Cyanol

6 ml 50 % glycerol

4 ml water

Luria Agar (400 ml)

4 g Tryptone

2 g Yeast extract

4 g NaCl

5 g Agar

Luria Broth (400 ml)

4 g Tryptone

2 g Yeast extract

4 g NaCl

PBS

8 g NaCl

1.15 g Na_2HPO_4

0.23 g KH_2PO_4

0.23g KCl

Water to litre pH 7.2-7.4

References

Aderka,D. (1996). The potential biological and clinical significance of the soluble tumor necrosis factor receptors. Cytokine Growth Factor Rev. *7*, 231-240.

Allinson,T.M., Parkin,E.T., Condon,T.P., Schwager,S.L., Sturrock,E.D., Turner,A.J., and Hooper,N.M. (2004). The role of ADAM10 and ADAM17 in the ectodomain shedding of angiotensin converting enzyme and the amyloid precursor protein. Eur. J. Biochem. *271*, 2539-2547.

Amour,A., Knight,C.G., English,W.R., Webster,A., Slocombe,P.M., Knauper,V., Docherty,A.J., Becherer,J.D., Blobel,C.P., and Murphy,G. (2002). The enzymatic activity of ADAM8 and ADAM9 is not regulated by TIMPs. FEBS Lett. *524*, 154-158.

Arribas,J. and Borroto,A. (2002). Protein ectodomain shedding. Chem. Rev. *102*, 4627-4638.

Arribas,J., Coodly,L., Vollmer,P., Kishimoto,T.K., Rose-John,S., and Massague,J. (1996). Diverse cell surface protein ectodomains are shed by a system sensitive to metalloprotease inhibitors. J. Biol. Chem. *271*, 11376-11382.

Arribas,J. and Massague,J. (1995). Transforming Growth-Factor-Alpha and Beta-Amyloid Precursor Protein Share A Secretory Mechanism. Journal of Cell Biology *128*, 433-441.

Asai,M., Hattori,C., Szabo,B., Sasagawa,N., Maruyama,K., Tanuma,S., and Ishiura,S. (2003). Putative function of ADAM9, ADAM10, and ADAM17 as APP alpha-secretase. Biochem. Biophys. Res. Commun. *301*, 231-235.

Asakura,M., Kitakaze,M., Takashima,S., Liao,Y., Ishikura,F., Yoshinaka,T., Ohmoto,H., Node,K., Yoshino,K., Ishiguro,H., Asanuma,H., Sanada,S., Matsumura,Y., Takeda,H., Beppu,S., Tada,M., Hori,M., and Higashiyama,S. (2002). Cardiac hypertrophy is inhibited by antagonism of ADAM12 processing of HB-EGF: metalloproteinase inhibitors as a new therapy. Nat. Med. *8*, 35-40.

Bax,D.V., Messent,A.J., Tart,J., van Hoang,M., Kott,J., Maciewicz,R.A., and Humphries,M.J. (2004). Integrin alpha5beta1 and ADAM-17 interact *in vitro* and co-localize in migrating HeLa cells. J. Biol. Chem. *279*, 22377-22386.

Bech-Serra,J.J., Santiago-Josefat,B., Esselens,C., Saftig,P., Baselga,J., Arribas,J., and Canals,F. (2006). Proteomic identification of desmoglein 2 and activated leukocyte cell adhesion molecule as substrates of ADAM17 and ADAM10 by difference gel electrophoresis. Mol. Cell Biol. *26*, 5086-5095.

Beel,A.J. and Sanders,C.R. (2008). Substrate specificity of gamma-secretase and other intramembrane proteases. Cell Mol. Life Sci. *65*, 1311-1334.

Begg,M.J., Sturrock,E.D., and van der Westhuyzen,D.R. (2004). Soluble LDL-R are formed by cell surface cleavage in response to phorbol esters. Eur. J. Biochem. *271*, 524-533.

Benjannet,S., Rhainds,D., Essalmani,R., Mayne,J., Wickham,L., Jin,W., Asselin,M.C., Hamelin,J., Varret,M., Allard,D., Trillard,M., Abifadel,M., Tebon,A., Attie,A.D., Rader,D.J., Boileau,C., Brissette,L., Chretien,M., Prat,A., and Seidah,N.G. (2004). NARC-1/PCSK9 and its

natural mutants: zymogen cleavage and effects on the low density lipoprotein (LDL) receptor and LDL cholesterol. J. Biol. Chem. *279*, 48865-48875.

Benjannet,S., Rhainds,D., Hamelin,J., Nassoury,N., and Seidah,N.G. (2006). The proprotein convertase (PC) PCSK9 is inactivated by furin and/or PC5/6A: functional consequences of natural mutations and post-translational modifications. J. Biol. Chem. *281*, 30561-30572.

Biemesderfer,D. (2006). Regulated intramembrane proteolysis of megalin: Linking urinary protein and gene regulation in proximal tubule? Kidney International *69*, 1717-1721.

Bieri,S., Atkins,A.R., Lee,H.T., Winzor,D.J., Smith,R., and Kroon,P.A. (1998). Folding, calcium binding, and structural characterization of a concatemer of the first and second ligand-binding modules of the low-density lipoprotein receptor. Biochemistry *37*, 10994-11002.

Black,R.A. (2002). Tumor necrosis factor-alpha converting enzyme. Int. J. Biochem. Cell Biol. *34*, 1-5.

Black,R.A., Doedens,J.R., Mahimkar,R., Johnson,R., Guo,L., Wallace,A., Virca,D., Eisenman,J., Slack,J., Castner,B., Sunnarborg,S.W., Lee,D.C., Cowling,R., Jin,G., Charrier,K., Peschon,J.J., and Paxton,R. (2003). Substrate specificity and inducibility of TACE (tumour necrosis factor alpha-converting enzyme) revisited: the Ala-Val preference, and induced intrinsic activity. Biochem. Soc. Symp. 39-52.

Black,R.A., Rauch,C.T., Kozlosky,C.J., Peschon,J.J., Slack,J.L., Wolfson,M.F., Castner,B.J., Stocking,K.L., Reddy,P., Srinivasan,S., Nelson,N., Boiani,N., Schooley,K.A., Gerhart,M., Davis,R., Fitzner,J.N., Johnson,R.S., Paxton,R.J., March,C.J., and Cerretti,D.P. (1997). A metalloproteinase disintegrin that releases tumour-necrosis factor-alpha from cells. Nature *385*, 729-733.

Borroto,A., Ruiz-Paz,S., de la Torre,T.V., Borrell-Pages,M., Merlos-Suarez,A., Pandiella,A., Blobel,C.P., Baselga,J., and Arribas,J. (2003). Impaired trafficking and activation of tumor necrosis factor-alpha-converting enzyme in cell mutants defective in protein ectodomain shedding. J. Biol. Chem. *278*, 25933-25939.

Bradford,M.M. (1976). A rapid and sensitive method for the quantitation of microgram quantities of protein utilizing the principle of protein-dye binding. Anal. Biochem. *72*, 248-254.

Brou,C., Logeat,F., Gupta,N., Bessia,C., LeBail,O., Doedens,J.R., Cumano,A., Roux,P., Black,R.A., and Israel,A. (2000). A novel proteolytic cleavage involved in Notch signaling: The role of the disintegrin-metalloprotease TACE. Molecular Cell *5*, 207-216.

Brown,M.S. and Goldstein,J.L. (1986). A receptor-mediated pathway for cholesterol homeostasis. Science *232*, 34-47.

Brown,M.S., Herz,J., and Goldstein,J.L. (1997). LDL-receptor structure. Calcium cages, acid baths and recycling receptors. Nature *388*, 629-630.

Buckley,C.A., Rouhani,F.N., Kaler,M., Adamik,B., Hawari,F.I., and Levine,S.J. (2005). Amino-terminal TACE prodomain attenuates TNFR2 cleavage independently of the cysteine switch. Am. J. Physiol Lung Cell Mol. Physiol *288*, L1132-L1138.

Buxbaum,J.D., Liu,K.N., Luo,Y., Slack,J.L., Stocking,K.L., Peschon,J.J., Johnson,R.S., Castner,B.J., Cerretti,D.P., and Black,R.A. (1998). Evidence that tumor necrosis factor alpha converting enzyme is involved in regulated alpha-secretase cleavage of the Alzheimer amyloid protein precursor. J. Biol. Chem. *273*, 27765-27767.

Byrnes,C.K., Nass,P.H., Duncan,M.D., and Harmon,J.W. (2002). A nuclear targeting peptide, m9, improves transfection efficiency in fibroblasts. Journal of Surgical Research *108*, 85-90.

Cavusoglu,E., Kornecki,E., Sobocka,M.B., Babinska,A., Ehrlich,Y.H., Chopra,V., Yanamadala,S., Ruwende,C., Salifu,M., Clark,L.T., Eng,C., Pinsky,D.J., and Marmur,J.D. (2007). Association of Plasma Levels of F11 Receptor Junctional Adhesion Molecule A (F11R/JAM-A) with Human Atherosclerosis. Journal of the American College of Cardiology *50*, 1768-1776.

Cawston,T.E., Noble,D.N., Murphy,G., Smith,A.J., Woodley,C., and Hazleman,B. (1986). Rapid Purification of Tissue Inhibitor of Metalloproteinases from Human-Plasma and Identification As A Gamma-Serum Protein. Biochemical Journal *238*, 677-682.

Chen,W.J., Goldstein,J.L., and Brown,M.S. (1990). NPXY, a sequence often found in cytoplasmic tails, is required for coated pit-mediated internalization of the low density lipoprotein receptor. J. Biol. Chem. *265*, 3116-3123.

Chesneau,V., Becherer,J.D., Zheng,Y., Erdjument-Bromage,H., Tempst,P., and Blobel,C.P. (2003). Catalytic properties of ADAM19. J. Biol. Chem. *278*, 22331-22340.

Chow,F.L. and Fernandez-Patron,C. (2007). Many membrane proteins undergo ectodomain shedding by proteolytic cleavage. Does one sheddase do the job on all of these proteins? IUBMB. Life *59*, 44-47.

Clesham,G.J., Browne,H., Efstathiou,S., and Weissberg,P.L. (1996). Enhancer stimulation unmasks latent gene transfer after adenovirus-mediated gene delivery into human vascular smooth muscle cells. Circ. Res. *79*, 1188-1195.

Daniel,T.O., Schneider,W.J., Goldstein,J.L., and Brown,M.S. (1983). Visualization of lipoprotein receptors by ligand blotting. J. Biol. Chem. *258*, 4606-4611.

Davis,C.G., Elhammer,A., Russell,D.W., Schneider,W.J., Kornfeld,S., Brown,M.S., and Goldstein,J.L. (1986). Deletion of clustered O-linked carbohydrates does not impair function of low density lipoprotein receptor in transfected fibroblasts. J. Biol. Chem. *261*, 2828-2838.

Davis,C.G., Goldstein,J.L., Sudhof,T.C., Anderson,R.G., Russell,D.W., and Brown,M.S. (1987). Acid-dependent ligand dissociation and recycling of LDL receptor mediated by growth factor homology region. Nature *326*, 760-765.

Deane,R., Sagare,A., and Zlokovic,B.V. (2008). The role of the cell surface LRP and soluble LRP in blood-brain barrier a clearance in Alzheimer's Disease. Current Pharmaceutical Design *14*, 1601-1605.

Delwig,A. and Rand,M.D. (2008). Kuz and TACE can activate Notch independent of ligand. Cellular and Molecular Life Sciences *65*, 2232-2243.

Deuss,M., Reiss,K., and Hartmann,D. (2008). Part-time alpha-secretases: the functional biology of ADAM 9, 10 and 17. Curr. Alzheimer Res. *5*, 187-201.

Doedens,J.R. and Black,R.A. (2000). Stimulation-induced down-regulation of tumor necrosis factor-alpha converting enzyme. J. Biol. Chem. *275*, 14598-14607.

Doedens,J.R., Mahimkar,R.M., and Black,R.A. (2003). TACE/ADAM-17 enzymatic activity is increased in response to cellular stimulation. Biochem. Biophys. Res. Commun. *308*, 331-338.

Dubuc,G., Chamberland,A., Wassef,H., Davignon,J., Seidah,N.G., Bernier,L., and Prat,A. (2004). Statins upregulate PCSK9, the gene encoding the proprotein convertase neural apoptosis-regulated convertase-1 implicated in familial hypercholesterolemia. Arterioscler. Thromb. Vasc. Biol. *24*, 1454-1459.

Edwards,D.R., Handsley,M.M., and Pennington,C.J. (2008). The ADAM metalloproteinases. Molecular Aspects of Medicine *29*, 258-289.

Ehlers,M.R. and Riordan,J.F. (1991). Membrane proteins with soluble counterparts: role of proteolysis in the release of transmembrane proteins. Biochemistry *30*, 10065-10074.

Endres,K., Anders,A., Kojro,E., Gilbert,S., Fahrenholz,F., and Postina,R. (2003). Tumor necrosis factor-alpha converting enzyme is processed by proprotein-convertases to its mature form which is degraded upon phorbol ester stimulation. Eur. J. Biochem. *270*, 2386-2393.

Fan,H. and Derynck,R. (1999). Ectodomain shedding of TGF-alpha and other transmembrane proteins is induced by receptor tyrosine kinase activation and MAP kinase signaling cascades. EMBO J. *18*, 6962-6972.

Fan,H., Turck,C.W., and Derynck,R. (2003). Characterization of growth factor-induced serine phosphorylation of tumor necrosis factor-alpha converting enzyme and of an alternatively translated polypeptide. J. Biol. Chem. *278*, 18617-18627.

Fischer,D.G., Tal,N., Novick,D., Barak,S., and Rubinstein,M. (1993). An antiviral soluble form of the LDL receptor induced by interferon. Science *262*, 250-253.

Fisher,T.S., Lo,S.P., Pandit,S., Mattu,M., Santoro,J.C., Wisniewski,D., Cummings,R.T., Calzetta,A., Cubbon,R.M., Fischer,P.A., Tarachandani,A., De Francesco,R., Wright,S.D., Sparrow,C.P., Carfi,A., and Sitlani,A. (2007). Effects of pH and low density lipoprotein (LDL) on PCSK9-dependent LDL receptor regulation. J. Biol. Chem. *282*, 20502-20512.

Fisher,W.R., Hammond,M.G., Mengel,M.C., and Warmke,G.L. (1975). Genetic Determinant of Phenotypic Variance of Molecular-Weight of Low-Density Lipoprotein. Proceedings of the National Academy of Sciences of the United States of America *72*, 2347-2351.

Gattorno,M., Picco,P., Buoncompagni,A., Stalla,F., Facchetti,P., Sormani,M.P., and Pistoia,V. (1996). Serum p55 and p75 tumour necrosis factor receptors as markers of disease activity in juvenile chronic arthritis**.** Annals of the Rheumatic Diseases *55*, 243-247.

Gavert,N., Sheffer,M., Raveh,S., Spaderna,S., Shtutman,M., Brabletz,T., Barany,F., Paty,P., Notterman,D., Domany,E., and Ben Ze'ev,A. (2007). Expression of L1-CAM and ADAM10 in human colon cancer cells induces metastasis. Cancer Research *67*, 7703-7712.

Gent,J. and Braakman,I. (2004). Low-density lipoprotein receptor structure and folding. Cellular and Molecular Life Sciences *61*, 2461-2470.

Glass,C.K. and Witztum,J.L. (2001). Atherosclerosis: The road ahead. Cell *104*, 503-516.

Goldstein,J.L., Brown,M.S., Anderson,R.G., Russell,D.W., and Schneider,W.J. (1985). Receptor-mediated endocytosis: concepts emerging from the LDL receptor system. Annu. Rev. Cell Biol. *1*, 1-39.

Gonzales,P.E., Solomon,A., Miller,A.B., Leesnitzer,M.A., Sagi,I., and Milla,M.E. (2004). Inhibition of the tumor necrosis factor-alpha-converting enzyme by its pro domain. J. Biol. Chem. *279*, 31638-31645.

Guerrier,L., Thulasiraman,V., Castagna,A., Fortis,F., Lin,S.H., Lomas,L., Righetti,P.G., and Boschetti,E. (2006). Reducing protein concentration range of biological samples using solid-phase ligand libraries. Journal of Chromatography B-Analytical Technologies in the Biomedical and Life Sciences *833*, 33-40.

Guo,L., Eisenman,J.R., Mahimkar,R.M., Peschon,J.J., Paxton,R.J., Black,R.A., and Johnson,R.S. (2002). A proteomic approach for the identification of cell-surface proteins shed by metalloproteases. Mol. Cell Proteomics. *1*, 30-36.

Haddad,L., Day,I.N., Hunt,S., Williams,R.R., Humphries,S.E., and Hopkins,P.N. (1999). Evidence for a third genetic locus causing familial hypercholesterolemia. A non-LDLR, non-APOB kindred. J. Lipid Res. *40*, 1113-1122.

Haga,S., Yamamoto,N., Nakai-Murakami,C., Osawa,Y., Tokunaga,K., Sata,T., Yamamoto,N., Sasazuki,T., and Ishizaka,Y. (2008). Modulation of TNF-alpha-converting enzyme by the spike protein of SARS-CoV and ACE2 induces TNF-alpha production and facilitates viral entry. Proc. Natl. Acad. Sci. U. S. A *105*, 7809-7814.

Haro,H., Crawford,H.C., Fingleton,B., Shinomiya,K., Spengler,D.M., and Matrisian,L.M. (2000). Matrix metalloproteinase-7-dependent release of tumor necrosis factor-alpha in a model of herniated disc resorption. Journal of Clinical Investigation *105*, 143-150.

Hattori,M., Osterfield,M., and Flanagan,J.G. (2000). Regulated cleavage of a contact-mediated axon repellent. Science *289*, 1360-1365.

Hemming,M.L., Elias,J.E., Gygi,S.P., and Selkoe,D.J. (2008). Proteomic Profiling of gamma-Secretase Substrates and Mapping of Substrate Requirements. Plos Biology *6*, 2314-2328.

Herz,J. (2001). Deconstructing the LDL receptor--a rhapsody in pieces. Nat. Struct. Biol. *8*, 476-478.

Hinkle,C.L., Mohan,M.J., Lin,P., Yeung,N., Rasmussen,F., Milla,M.E., and Moss,M.L. (2003). Multiple metalloproteinases process protransforming growth factor-alpha (proTGF-alpha). Biochemistry *42*, 2127-2136.

Hiraoka,Y., Yoshida,K., Ohno,M., Matsuoka,T., Kita,T., and Nishi,E. (2008). Ectodomain shedding of TNF-alpha is enhanced by nardilysin via activation of ADAM proteases. Biochem. Biophys. Res. Commun. *370*, 154-158.

Hoe,H.S. and Rebeck,G.W. (2005). Regulation of ApoE receptor proteolysis by ligand binding. Molecular Brain Research *137*, 31-39.

Hofer,F., Berger,B., Gruenberger,M., Machat,H., Dernick,R., Tessmer,U., Kuechler,E., and Blaas,D. (1992). Shedding of a rhinovirus minor group binding protein: evidence for a Ca(2+)-dependent process. J. Gen. Virol. *73 (Pt 3)*, 627-632.

Hofer,F., Gruenberger,M., Kowalski,H., Machat,H., Huettinger,M., Kuechler,E., and Blaas,D. (1994). Members of the low density lipoprotein receptor family mediate cell entry of a minor-group common cold virus. Proc. Natl. Acad. Sci. U. S. A *91*, 1839-1842.

Holla,O.L., Cameron,J., Berge,K.E., Ranheim,T., and Leren,T.P. (2007). Degradation of the LDL receptors by PCSK9 is not mediated by a secreted protein acted upon by PCSK9 extracellularly. BMC. Cell Biol. *8*, 9.

Holst,H.U., Dagnaes-Hansen,F., Corydon,T.J., Andreasen,P.H., Jorgensen,M.M., Kolvraa,S., Bolund,L., and Jensen,T.G. (2001). LDL receptor-GFP fusion proteins: new tools for the characterisation of disease-causing mutations in the LDL receptor gene. Eur. J. Hum. Genet. *9*, 815-822.

Homer,V.M., Marais,A.D., Charlton,F., Laurie,A.D., Hurndell,N., Scott,R., Mangili,F., Sullivan,D.R., Barter,P.J., Rye,K.A., George,P.M., and Lambert,G. (2008). Identification and characterization of two non-secreted PCSK9 mutants associated with familial hypercholesterolemia in cohorts from New Zealand and South Africa. Atherosclerosis *196*, 659-666.

Hooper,N.M., Karran,E.H., and Turner,A.J. (1997). Membrane protein secretases. Biochem. J. *321 (Pt 2)*, 265-279.

Horton,J.D., Cohen,J.C., and Hobbs,H.H. (2007). Molecular biology of PCSK9: its role in LDL metabolism. Trends Biochem. Sci. *32*, 71-77.

Huovila,A.P., Turner,A.J., Pelto-Huikko,M., Karkkainen,I., and Ortiz,R.M. (2005). Shedding light on ADAM metalloproteinases. Trends Biochem. Sci. *30*, 413-422.

Hussain,M.M., Strickland,D.K., and Bakillah,A. (1999). The mammalian low-density lipoprotein receptor family. Annu. Rev. Nutr. *19*, 141-172.

Innerarity,T.L. (2002). LDL receptor's beta-propeller displaces LDL. Science *298*, 2337-2339.

Izumi,Y., Hirata,M., Hasuwa,H., Iwamoto,R., Umata,T., Miyado,K., Tamai,Y., Kurisaki,T., Sehara-Fujisawa,A., Ohno,S., and Mekada,E. (1998). A metalloprotease-disintegrin, MDC9/meltrin-gamma/ADAM9 and PKCdelta are involved in TPA-induced ectodomain shedding of membrane-anchored heparin-binding EGF-like growth factor. EMBO J. *17*, 7260-7272.

Jeon,H. and Blacklow,S.C. (2005). Structure and physiologic function of the low-density lipoprotein receptor. Annu. Rev. Biochem. *74*, 535-562.

Jeon,H. and Shipley,G.G. (2000). Localization of the N-terminal domain of the low density lipoprotein receptor. J. Biol. Chem. *275*, 30465-30470.

Jin,G., Huang,X., Black,R., Wolfson,M., Rauch,C., McGregor,H., Ellestad,G., and Cowling,R. (2002). A continuous fluorimetric assay for tumor necrosis factor-alpha converting enzyme. Anal. Biochem. *302*, 269-275.

Kaether,C. and Gerdes,H.H. (1995). Visualization of protein transport along the secretory pathway using green fluorescent protein. FEBS Lett. *369*, 267-271.

Karasuyama,H., Kudo,A., and Melchers,F. (1990). The proteins encoded by the VpreB and lambda 5 pre-B cell-specific genes can associate with each other and with mu heavy chain. J. Exp. Med. *172*, 969-972.

Killar,L., White,J., Black,R., and Peschon,J. (1999). Adamalysins. A family of metzincins including TNF-alpha converting enzyme (TACE). Ann. N. Y. Acad. Sci. *878*, 442-452.

Kim,M.L., Zhang,B., Mills,I.P., Milla,M.E., Brunden,K.R., and Lee,V.M. (2008). Effects of TNFalpha-converting enzyme inhibition on amyloid beta production and APP processing in vitro and in vivo. J. Neurosci. *28*, 12052-12061.

Kirsch,P., Hafner,M., Zentgraf,H., and Schilling,L. (2003). Time course of fluorescence intensity and protein expression in HeLa cells stably transfected with hrGFP. Mol. Cells *15*, 341-348.

Kong,W.J., Liu,J., and Jiang,J.D. (2006). Human low-density lipoprotein receptor gene and its regulation. J. Mol. Med. *84*, 29-36.

Kounnas,M.Z., Chappell,D.A., Strickland,D.K., and Argraves,W.S. (1993). Glycoprotein 330, a member of the low density lipoprotein receptor family, binds lipoprotein lipase in vitro. J. Biol. Chem. *268*, 14176-14181.

Kozarsky,K., Kingsley,D., and Krieger,M. (1988). Use of A Mutant-Cell Line to Study the Kinetics and Function of O-Linked Glycosylation of Low-Density Lipoprotein Receptors. Proceedings of the National Academy of Sciences of the United States of America *85*, 4335-4339.

Kwon,H.J., Lagace,T.A., McNutt,M.C., Horton,J.D., and Deisenhofer,J. (2008). Molecular basis for LDL receptor recognition by PCSK9. Proc. Natl. Acad. Sci. U. S. A *105*, 1820-1825.

Laemmli,U.K. (1970). Cleavage of structural proteins during the assembly of the head of bacteriophage T4. Nature *227*, 680-685.

Lagace,T.A., Curtis,D.E., Garuti,R., McNutt,M.C., Park,S.W., Prather,H.B., Anderson,N.N., Ho,Y.K., Hammer,R.E., and Horton,J.D. (2006). Secreted PCSK9 decreases the number of LDL receptors in hepatocytes and in livers of parabiotic mice. J. Clin. Invest *116*, 2995-3005.

Lambert,D.W., Yarski,M., Warner,F.J., Thornhill,P., Parkin,E.T., Smith,A.I., Hooper,N.M., and Turner,A.J. (2005). Tumor necrosis factor-alpha convertase (ADAM17) mediates regulated ectodomain shedding of the severe-acute respiratory syndrome-coronavirus (SARS-CoV) receptor, angiotensin-converting enzyme-2 (ACE2). J. Biol. Chem. *280*, 30113-30119.

Lambert,G., Charlton,F., Rye,K.A., and Piper,D.E. (2008). Molecular basis of PCSK9 function. Atherosclerosis.

Lammich,S., Kojro,E., Postina,R., Gilbert,S., Pfeiffer,R., Jasionowski,M., Haass,C., and Fahrenholz,F. (1999). Constitutive and regulated alpha-secretase cleavage of Alzheimer's amyloid precursor protein by a disintegrin metalloprotease. Proc. Natl. Acad. Sci. U. S. A *96*, 3922-3927.

Lehrman,M.A., Russell,D.W., Goldstein,J.L., and Brown,M.S. (1987). Alu-Alu recombination deletes splice acceptor sites and produces secreted low density lipoprotein receptor in a subject with familial hypercholesterolemia. J. Biol. Chem. *262*, 3354-3361.

Lehrman,M.A., Schneider,W.J., Sudhof,T.C., Brown,M.S., Goldstein,J.L., and Russell,D.W. (1985). Mutation in LDL receptor: Alu-Alu recombination deletes exons encoding transmembrane and cytoplasmic domains. Science *227*, 140-146.

Lemieux,G.A., Blumenkron,F., Yeung,N., Zhou,P., Williams,J., Grammer,A.C., Petrovich,R., Lipsky,P.E., Moss,M.L., and Werb,Z. (2007). The low affinity IgE receptor (CD23) is cleaved by the metalloproteinase ADAM10. J. Biol. Chem. *282*, 14836-14844.

Lemjabbar,H. and Basbaum,C. (2002). Platelet-activating factor receptor and ADAM10 mediate responses to *Staphylococcus aureus* in epithelial cells. Nature Medicine *8*, 41-46.

Li,J., Tumanut,C., Gavigan,J.A., Huang,W.J., Hampton,E.N., Tumanut,R., Suen,K.F., Trauger,J.W., Spraggon,G., Lesley,S.A., Liau,G., Yowe,D., and Harris,J.L. (2007a). Secreted

PCSK9 promotes LDL receptor degradation independently of proteolytic activity. Biochem. J. *406*, 203-207.

Li,X. and Fan,H. (2004). Loss of ectodomain shedding due to mutations in the metalloprotease and cysteine-rich/disintegrin domains of the tumor necrosis factor-alpha converting enzyme (TACE). J. Biol. Chem. *279*, 27365-27375.

Li,X., Perez,L., Pan,Z., and Fan,H. (2007b). The transmembrane domain of TACE regulates protein ectodomain shedding. Cell Res. *17*, 985-998.

Li,Y., Lu,W., Schwartz,A.L., and Bu,G. (2004). Degradation of the LDL receptor class 2 mutants is mediated by a proteasome-dependent pathway. J. Lipid Res. *45*, 1084-1091.

Lum,L., Wong,B.R., Josien,R., Becherer,J.D., Erdjument-Bromage,H., Schlondorff,J., Tempst,P., Choi,Y., and Blobel,C.P. (1999). Evidence for a role of a tumor necrosis factor-alpha (TNF-alpha)-converting enzyme-like protease in shedding of TRANCE, a TNF family member involved in osteoclastogenesis and dendritic cell survival. J. Biol. Chem. *274*, 13613-13618.

Ma,J.K., Lee,S., Choi,M., Bishop,G.R., Hosler,J.P., and Davidson,V.L. (2008). The axial ligand and extent of protein folding determine whether Zn or Cu binds to amicyanin. Journal of Inorganic Biochemistry *102*, 342-346.

Maass,A., Langer,S.J., Oberdorf-Maass,S., Bauer,S., Neyses,L., and Leinwand,L.A. (2003). Rational promoter selection for gene transfer into cardiac cells. J. Mol. Cell Cardiol. *35*, 823-831.

Magrane,J., Casaroli-Marano,R.P., Reina,M., Gafvels,M., and Vilaro,S. (1999). The role of O-linked sugars in determining the very low density lipoprotein receptor stability or release from the cell. FEBS Lett. *451*, 56-62.

Marlovits,T.C., Abrahamsberg,C., and Blaas,D. (1998a). Soluble LDL minireceptors. Minimal structure requirements for recognition of minor group human rhinovirus. J. Biol. Chem. *273*, 33835-33840.

Marlovits,T.C., Abrahamsberg,C., and Blaas,D. (1998b). Very-low-density lipoprotein receptor fragment shed from HeLa cells inhibits human rhinovirus infection. J. Virol. *72*, 10246-10250.

Marlovits,T.C., Zechmeister,T., Gruenberger,M., Ronacher,B., Schwihla,H., and Blaas,D. (1998c). Recombinant soluble low density lipoprotein receptor fragment inhibits minor group rhinovirus infection *in vitro*. FASEB J. *12*, 695-703.

Martini,C. and Pallottini,V. (2007). Cholesterol: from feeding to gene regulation. Genes & Nutrition *2*, 181-193.

Maxwell,K.L., Bona,D., Liu,C.S., Arrowsmith,C.H., and Edwards,A.M. (2003). Refolding out of guanidine hydrochloride is an effective approach for high-throughput structural studies of small proteins. Protein Science *12*, 2073-2080.

Maxwell,K.N. and Breslow,J.L. (2004). Adenoviral-mediated expression of Pcsk9 in mice results in a low-density lipoprotein receptor knockout phenotype. Proc. Natl. Acad. Sci. U. S. A *101*, 7100-7105.

Maxwell,K.N., Fisher,E.A., and Breslow,J.L. (2005). Overexpression of PCSK9 accelerates the degradation of the LDLR in a post-endoplasmic reticulum compartment. Proc. Natl. Acad. Sci. U. S. A *102*, 2069-2074.

May,P., Bock,H.H., Nimpf,J., and Herz,J. (2003). Differential glycosylation regulates processing of lipoprotein receptors by gamma-secretase. J. Biol. Chem. *278*, 37386-37392.

May,P., Reddy,Y.K., and Herz,J. (2002). Proteolytic processing of low density lipoprotein receptor-related protein mediates regulated release of its intracellular domain. Journal of Biological Chemistry *277*, 18736-18743.

McNutt,M.C., Lagace,T.A., and Horton,J.D. (2007). Catalytic activity is not required for secreted PCSK9 to reduce low density lipoprotein receptors in HepG2 cells. J. Biol. Chem. *282*, 20799-20803.

Mehta,A.K., Majumdar,S.S., Alam,P., Gulati,N., and Brahmachari,V. (2009). Epigenetic regulation of cytomegalovirus major immediate-early promoter activity in transgenic mice. Gene *428*, 20-24.

Mehta,K.D., Radominska-Pandya,A., Kapoor,G.S., Dave,B., and Atkins,B.A. (2002). Critical role of diacylglycerol- and phospholipid-regulated protein kinase C epsilon in induction of low-density lipoprotein receptor transcription in response to depletion of cholesterol. Mol. Cell Biol. *22*, 3783-3793.

Mezyk,R., Bzowska,M., and Bereta,J. (2003). Structure and functions of tumor necrosis factor-alpha converting enzyme. Acta Biochim. Pol. *50*, 625-645.

Milla,M.E., Leesnitzer,M.A., Moss,M.L., Clay,W.C., Carter,H.L., Miller,A.B., Su,J.L., Lambert,M.H., Willard,D.H., Sheeley,D.M., Kost,T.A., Burkhart,W., Moyer,M., Blackburn,R.K., Pahel,G.L., Mitchell,J.L., Hoffman,C.R., and Becherer,J.D. (1999). Specific sequence elements are required for the expression of functional tumor necrosis factor-alpha-converting enzyme (TACE). J. Biol. Chem. *274*, 30563-30570.

Miyake,Y., Tajima,S., Funahashi,T., and Yamamoto,A. (1989). Analysis of a recycling-impaired mutant of low density lipoprotein receptor in familial hypercholesterolemia. J. Biol. Chem. *264*, 16584-16590.

Mohan,M.J., Seaton,T., Mitchell,J., Howe,A., Blackburn,K., Burkhart,W., Moyer,M., Patel,I., Waitt,G.M., Becherer,J.D., Moss,M.L., and Milla,M.E. (2002). The tumor necrosis factor-alpha converting enzyme (TACE): a unique metalloproteinase with highly defined substrate selectivity. Biochemistry *41*, 9462-9469.

Molina,S., Castet,V., Fournier-Wirth,C., Pichard-Garcia,L., Avner,R., Harats,D., Roitelman,J., Barbaras,R., Graber,P., Ghersa,P., Smolarsky,M., Funaro,A., Malavasi,F., Larrey,D., Coste,J., Fabre,J.M., Sa-Cunha,A., and Maurel,P. (2007). The low-density lipoprotein receptor plays a role in the infection of primary human hepatocytes by hepatitis C virus. J. Hepatol. *46*, 411-419.

Moss,M.L., Jin,S.L., Milla,M.E., Bickett,D.M., Burkhart,W., Carter,H.L., Chen,W.J., Clay,W.C., Didsbury,J.R., Hassler,D., Hoffman,C.R., Kost,T.A., Lambert,M.H., Leesnitzer,M.A., McCauley,P., McGeehan,G., Mitchell,J., Moyer,M., Pahel,G., Rocque,W., Overton,L.K., Schoenen,F., Seaton,T., Su,J.L., Becherer,J.D., and . (1997). Cloning of a disintegrin metalloproteinase that processes precursor tumour-necrosis factor-alpha. Nature *385*, 733-736.

Naus,S., Reipschlager,S., Wildeboer,D., Lichtenthaler,S.F., Mitterreiter,S., Guan,Z., Moss,M.L., and Bartsch,J.W. (2006). Identification of candidate substrates for ectodomain shedding by the metalloprotease-disintegrin ADAM8. Biol. Chem. *387*, 337-346.

Nicodemou,A., Petsch,M., Konecsni,T., Kremser,L., Kenndler,E., Casasnovas,J.M., and Blaas,D. (2005). Rhinovirus-stabilizing activity of artificial VLDL-receptor variants defines a new mechanism for virus neutralization by soluble receptors. FEBS Lett. *579*, 5507-5511.

Novick,D., Cohen,B., and Rubinstein,M. (1992). Soluble interferon-a receptor molecules are present in body fluids. Federation of Europeun Biochemical Societies *314*, 445-448.

Nykjaer,A. and Willnow,T.E. (2002). The low-density lipoprotein receptor gene family: a cellular Swiss army knife? Trends Cell Biol. *12*, 273-280.

Ogawa,H., Inouye,S., Tsuji,F.I., Yasuda,K., and Umesono,K. (1995). Localization, trafficking, and temperature-dependence of the Aequorea green fluorescent protein in cultured vertebrate cells. Proc. Natl. Acad. Sci. U. S. A *92*, 11899-11903.

Park,S.W., Moon,Y.A., and Horton,J.D. (2004). Post-transcriptional regulation of low density lipoprotein receptor protein by proprotein convertase subtilisin/kexin type 9a in mouse liver. J. Biol. Chem. *279*, 50630-50638.

Persson,S., Love,J., Tsou,P.L., Robertson,D., Thompson,W.F., and Boss,W.F. (2002). When a day makes a difference. Interpreting data from endoplasmic reticulum-targeted green fluorescent protein fusions in cells grown in suspension culture. Plant Physiol *128*, 341-344.

Peschon,J.J., Slack,J.L., Reddy,P., Stocking,K.L., Sunnarborg,S.W., Lee,D.C., Russell,W.E., Castner,B.J., Johnson,R.S., Fitzner,J.N., Boyce,R.W., Nelson,N., Kozlosky,C.J., Wolfson,M.F., Rauch,C.T., Cerretti,D.P., Paxton,R.J., March,C.J., and Black,R.A. (1998). An essential role for ectodomain shedding in mammalian development. Science *282*, 1281-1284.

Pollok,B.A. and Heim,R. (1999). Using GFP in FRET-based applications. Trends Cell Biol. *9*, 57-60.

Qian,Y.W., Schmidt,R.J., Zhang,Y., Chu,S., Lin,A., Wang,H., Wang,X., Beyer,T.P., Bensch,W.R., Li,W., Ehsani,M.E., Lu,D., Konrad,R.J., Eacho,P.I., Moller,D.E., Karathanasis,S.K., and Cao,G. (2007). Secreted PCSK9 downregulates low density lipoprotein receptor through receptor-mediated endocytosis. J. Lipid Res. *48*, 1488-1498.

Quinn,K.A., Grimsley,P.G., Dai,Y.P., Tapner,M., Chesterman,C.N., and Owensby,D.A. (1997). Soluble low density lipoprotein receptor-related protein (LRP) circulates in human plasma. J. Biol. Chem. *272*, 23946-23951.

Quinn,K.A., Pye,V.J., Dai,Y.P., Chesterman,C.N., and Owensby,D.A. (1999). Characterization of the soluble form of the low density lipoprotein receptor-related protein (LRP). Exp. Cell Res. *251*, 433-441.

Rader,D.J., Cohen,J., and Hobbs,H.H. (2003). Monogenic hypercholesterolemia: new insights in pathogenesis and treatment. Journal of Clinical Investigation *111*, 1795-1803.

Rebeck,G.W., LaDu,M.J., Estus,S., Bu,G., and Weeber,E.J. (2006). The generation and function of soluble apoE receptors in the CNS. Mol. Neurodegener. *1*, 15.

Reddy,P., Slack,J.L., Davis,R., Cerretti,D.P., Kozlosky,C.J., Blanton,R.A., Shows,D., Peschon,J.J., and Black,R.A. (2000). Functional analysis of the domain structure of tumor necrosis factor-alpha converting enzyme. J. Biol. Chem. *275*, 14608-14614.

Reiss,K. and Saftig,P. (2008). The "A Disintegrin And Metalloprotease" (ADAM) family of sheddases: Physiological and cellular functions. Semin. Cell Dev. Biol.

Rio,C., Buxbaum,J.D., Peschon,J.J., and Corfas,G. (2000). Tumor necrosis factor-alpha-converting enzyme is required for cleavage of erbB4/HER4. J. Biol. Chem. *275*, 10379-10387.

Roghani,M., Becherer,J.D., Moss,M.L., Atherton,R.E., Erdjument-Bromage,H., Arribas,J., Blackburn,R.K., Weskamp,G., Tempst,P., and Blobel,C.P. (1999). Metalloprotease-disintegrin MDC9: intracellular maturation and catalytic activity. J. Biol. Chem. *274*, 3531-3540.

Rosendahl,M.S., Ko,S.C., Long,D.L., Brewer,M.T., Rosenzweig,B., Hedl,E., Anderson,L., Pyle,S.M., Moreland,J., Meyers,M.A., Kohno,T., Lyons,D., and Lichenstein,H.S. (1997). Identification and characterization of a pro-tumor necrosis factor-alpha-processing enzyme from the ADAM family of zinc metalloproteases. J. Biol. Chem. *272*, 24588-24593.

Rozanov,D.V., Hahn-Dantona,E., Strickland,D.K., and Strongin,A.Y. (2004). The low density lipoprotein receptor-related protein LRP is regulated by membrane type-1 matrix metalloproteinase (MT1-MMP) proteolysis in malignant cells. Journal of Biological Chemistry *279*, 4260-4268.

Russell,D.W., Brown,M.S., and Goldstein,J.L. (1989). Different combinations of cysteine-rich repeats mediate binding of low density lipoprotein receptor to two different proteins. J. Biol. Chem. *264*, 21682-21688.

Sadhukhan,R., Santhamma,K.R., Reddy,P., Peschon,J.J., Black,R.A., and Sen,I. (1999). Unaltered cleavage and secretion of angiotensin-converting enzyme in tumor necrosis factor-alpha-converting enzyme-deficient mice. J. Biol. Chem. *274*, 10511-10516.

Sagare,A., Deane,R., Bell,R.D., Johnson,B., Hamm,K., Pendu,R., Marky,A., Lenting,P.J., Wu,Z.H., Zarcone,T., Goate,A., Mayo,K., Perlmutter,D., Coma,M., Zhong,Z.H., and Zlokovic,B.V. (2007). Clearance of amyloid-beta by circulating lipoprotein receptors. Nature Medicine *13*, 1029-1031.

Sahin,U., Weskamp,G., Kelly,K., Zhou,H.M., Higashiyama,S., Peschon,J., Hartmann,D., Saftig,P., and Blobel,C.P. (2004). Distinct roles for ADAM10 and ADAM17 in ectodomain shedding of six EGFR ligands. J. Cell Biol. *164*, 769-779.

Sakai,J. and Rawson,R.B. (2001). The sterol regulatory element-binding protein pathway: control of lipid homeostasis through regulated intracellular transport. Current Opinion in Lipidology *12*, 261-266.

Schlondorff,J., Becherer,J.D., and Blobel,C.P. (2000). Intracellular maturation and localization of the tumour necrosis factor alpha convertase (TACE). Biochem. J. *347 Pt 1*, 131-138.

Schmidt,R.J., Beyer,T.P., Bensch,W.R., Qian,Y.W., Lin,A., Kowala,M., Alborn,W.E., Konrad,R.J., and Cao,G. (2008). Secreted proprotein convertase subtilisin/kexin type 9 reduces both hepatic and extrahepatic low-density lipoprotein receptors *in vivo*. Biochem. Biophys. Res. Commun. *370*, 634-640.

Schneider,W.J., Beisiegel,U., Goldstein,J.L., and Brown,M.S. (1982). Purification of the low density lipoprotein receptor, an acidic glycoprotein of 164,000 molecular weight. J. Biol. Chem. *257*, 2664-2673.

Simons,K. and Ikonen,E. (2000). How cells handle cholesterol. Science *290*, 1721-1726.

Smith,P.M., Cowan,A., and White,B.A. (2004). The low-density lipoprotein receptor is regulated by estrogen and forms a functional complex with the estrogen-regulated protein ezrin in pituitary GH3 somatolactotropes. Endocrinology *145*, 3075-3083.

Sudhof,T.C., Goldstein,J.L., Brown,M.S., and Russell,D.W. (1985). The Ldl Receptor Gene - A Mosaic of Exons Shared with Different Proteins. Science *228*, 815-822.

Sutcliffe,R.G., Kukulskalanglands,B.M., Coggins,J.R., Hunter,J.B., and Gore,C.H. (1980). Studies on Human Pregnancy-Associated Plasma Protein-A - Purification by Affinity Chromatography and Structural Comparisons with Alpha-2-Macroglobulin. Biochemical Journal *191*, 799-809.

Suzuki,E., Terada,S., Ueda,H., Fujita,T., Komatsu,T., Takayama,S., and Reed,J.C. (1997a). Establishing apoptosis resistant cell lines for improving protein productivity of cell culture. Cytotechnology *23*, 55-59.

Suzuki,M., Raab,G., Moses,M.A., Fernandez,C.A., and Klagsbrun,M. (1997b). Matrix metalloproteinase-3 releases active heparin-binding EGF-like growth factor by cleavage at a specific juxtamembrane site. J. Biol. Chem. *272*, 31730-31737.

Timms,K.M., Wagner,S., Samuels,M.E., Forbey,K., Goldfine,H., Jammulapati,S., Skolnick,M.H., Hopkins,P.N., Hunt,S.C., and Shattuck,D.M. (2004). A mutation in PCSK9 causing autosomal-dominant hypercholesterolemia in a Utah pedigree. Hum. Genet. *114*, 349-353.

Tsakadze,N.L., Sithu,S.D., Sen,U., English,W.R., Murphy,G., and D'Souza,S.E. (2006). Tumor necrosis factor-alpha-converting enzyme (TACE/ADAM-17) mediates the ectodomain cleavage of intercellular adhesion molecule-1 (ICAM-1). Journal of Biological Chemistry *281*, 3157-3164.

Tseng,C.F., Huang,H.Y., Yang,Y.T., and Mao,S.J.T. (2004). Purification of human haptoglobin 1-1, 2-1, and 2-2 using monoclonal antibody affinity chromatography. Faseb Journal *18*, A1150.

Tsien,R.Y. (1998). The green fluorescent protein. Annu. Rev. Biochem. *67*, 509-544.

van Driel,I.R., Davis,C.G., Goldstein,J.L., and Brown,M.S. (1987). Self-association of the low density lipoprotein receptor mediated by the cytoplasmic domain. J. Biol. Chem. *262*, 16127-16134.

Vincent,B., Paitel,E., Saftig,P., Frobert,Y., Hartmann,D., De Strooper,B., Grassi,J., Lopez-Perez,E., and Checler,F. (2001). The disintegrins ADAM10 and TACE contribute to the constitutive and phorbol ester-regulated normal cleavage of the cellular prion protein. J. Biol. Chem. *276*, 37743-37746.

Vohra,R.S., Murphy,J.E., Walker,J.H., Homer-Vanniasinkam,S., and Ponnambalam,S. (2007). Functional refolding of a recombinant C-type lectin-like domain containing intramolecular disulfide bonds. Protein Expression and Purification *52*, 415-421.

von Arnim,C.A., Kinoshita,A., Peltan,I.D., Tangredi,M.M., Herl,L., Lee,B.M., Spoelgen,R., Hshieh,T.T., Ranganathan,S., Battey,F.D., Liu,C.X., Bacskai,B.J., Sever,S., Irizarry,M.C., Strickland,D.K., and Hyman,B.T. (2005). The low density lipoprotein receptor-related protein (LRP) is a novel beta-secretase (BACE1) substrate. J. Biol. Chem. *280*, 17777-17785.

Vrablik,M., Ceska,R., and Horinek,A. (2001). Major apolipoprotein B-100 mutations in lipoprotein metabolism and atherosclerosis. Physiol Res. *50*, 337-343.

Wacker,I., Kaether,C., Kromer,A., Migala,A., Almers,W., and Gerdes,H.H. (1997). Microtubule-dependent transport of secretory vesicles visualized in real time with a GFP-tagged secretory protein. J. Cell Sci. *110 (Pt 13)*, 1453-1463.

Yamamoto,T., Davis,C.G., Brown,M.S., Schneider,W.J., Casey,M.L., Goldstein,J.L., and Russell,D.W. (1984). The human LDL receptor: a cysteine-rich protein with multiple Alu sequences in its mRNA. Cell *39*, 27-38.

Yokoyama,C., Wang,X., Briggs,M.R., Admon,A., Wu,J., Hua,X., Goldstein,J.L., and Brown,M.S. (1993). SREBP-1, a basic-helix-loop-helix-leucine zipper protein that controls transcription of the low density lipoprotein receptor gene. Cell *75*, 187-197.

Yu,W.H., Woessner,J.F., McNeish,J.D., and Stamenkovic,I. (2002). CD44 anchors the assembly of matrilysin/MMP-7 with heparin-binding epidermal growth factor precursor and ErbB4 and regulates female reproductive organ remodeling. Genes & Development *16*, 307-323.

Zeng,X., Chen,J., Sanchez,J.F., Coggiano,M., Dillon-Carter,O., Petersen,J., and Freed,W.J. (2003). Stable expression of hrGFP by mouse embryonic stem cells: promoter activity in the undifferentiated state and during dopaminergic neural differentiation. Stem Cells *21*, 647-653.

Zeyda,M., Borth,N., Kunert,R., and Katinger,H. (1999). Optimization of sorting conditions for the selection of stable, high-producing mammalian cell lines. Biotechnol. Prog. *15*, 953-957.

Zhang,D.W., Lagace,T.A., Garuti,R., Zhao,Z., McDonald,M., Horton,J.D., Cohen,J.C., and Hobbs,H.H. (2007). Binding of proprotein convertase subtilisin/kexin type 9 to epidermal growth factor-like repeat A of low density lipoprotein receptor decreases receptor recycling and increases degradation. J. Biol. Chem. *282*, 18602-18612.

Zhang,Q., Thomas,S.M., Lui,V.W., Xi,S., Siegfried,J.M., Fan,H., Smithgall,T.E., Mills,G.B., and Grandis,J.R. (2006). Phosphorylation of TNF-alpha converting enzyme by gastrin-releasing peptide induces amphiregulin release and EGF receptor activation. Proc. Natl. Acad. Sci. U. S. A *103*, 6901-6906.

Zhang,Y., Jiang,J., Black,R.A., Baumann,G., and Frank,S.J. (2000). Tumor necrosis factor-alpha converting enzyme (TACE) is a growth hormone binding protein (GHBP) sheddase: the metalloprotease TACE/ADAM-17 is critical for (PMA-induced) GH receptor proteolysis and GHBP generation. Endocrinology *141*, 4342-4348.

Zhang,Z., Oliver,P., Lancaster,J.R., Jr., Schwarzenberger,P.O., Joshi,M.S., Cork,J., and Kolls,J.K. (2001). Reactive oxygen species mediate tumor necrosis factor alpha-converting, enzyme-dependent ectodomain shedding induced by phorbol myristate acetate. FASEB J. *15*, 303-305.

Zhao,X.J., Marrero,L., Song,K., Oliver,P., Chin,S.Y., Simon,H., Schurr,J.R., Zhang,Z., Thoppil,D., Lee,S., Nelson,S., and Kolls,J.K. (2003). Acute alcohol inhibits TNF-alpha processing in human monocytes by inhibiting TNF/TNF-alpha-converting enzyme interactions in the cell membrane. J. Immunol. *170*, 2923-2931.

Zheng,Y., Saftig,P., Hartmann,D., and Blobel,C. (2004). Evaluation of the contribution of different ADAMs to tumor necrosis factor alpha (TNFalpha) shedding and of the function of the TNFalpha ectodomain in ensuring selective stimulated shedding by the TNFalpha convertase (TACE/ADAM17). J. Biol. Chem. *279*, 42898-42906.

Zou,J., Zhu,F., Liu,J., Wang,W., Zhang,R., Garlisi,C.G., Liu,Y.H., Wang,S., Shah,H., Wan,Y., and Umland,S.P. (2004a). Catalytic activity of human ADAM33. J. Biol. Chem. *279*, 9818-9830.

Zou,Z.Y., Chung,B., Nguyen,T., Mentone,S., Thomson,B., and Biemesderfer,D. (2004b). Linking receptor-mediated endocytosis and cell signaling - Evidence for regulated

intramembrane proteolysis of megalin in proximal tubule. Journal of Biological Chemistry *279*, 34302-34310.